NASA CR-144996

SONIC ENVIRONMENT OF AIRCRAFT STRUCTURE IMMERSED IN A SUPERSONIC JET FLOW STREAM

JUNE 1976

By

WILEY A. GUINN
FRANK J. BALENA
JAAK SOOVERE

Prepared under Contract No. NAS1-13978
Lockheed-California Company
Burbank, California

for

NATIONAL AERONAUTICS AND SPACE ADMINISTRATION
LANGLEY RESEARCH CENTER
HAMPTON, VIRGINIA

1. Report No. NASA CR-144996	2. Government Accession No.	3. Recipient's Catalog No.
4. Title and Subtitle Sonic Environment of Aircraft Structure Immersed in a Supersonic Jet Flow Stream		5. Report Date May 1976
		6. Performing Organization Code
7. Author(s) Wiley A. Guinn, Frank J. Balena and Jaak Soovere		8. Performing Organization Report No. LR 27338
9. Performing Organization Name and Address Lockheed California Company Burbank, California 91502		10. Work Unit No.
		11. Contract or Grant No. NAS1-13978
12. Sponsoring AGency Name and Address National Aeronautics & Space Administration Langley Research Center, Hampton, Virginia		13. Type of Report and Period Covered
		14. Sponsoring Agency Code

15. Supplementary Notes

This study was conducted from June 1975 thru February 1976

16. Abstract

A study was performed to investigate test methods for determining the sonic environment of aircraft structure that is immersed in the flow stream of a high velocity jet or that is subjected to the noise field surrounding the jet.

Test data requirements that are needed to make sonic fatigue, crack growth, interior noise, and equipment vibration analyses are defined. Formats for reporting the data are illustrated and synopses are given to describe how the data is utilized.

Sonic environment test data that were previously measured on a SCAT 15-F model in the flow field of Mach 1.5 and 2.5 jets were processed. Narrow band, lateral cross-correlation and noise contour plots are presented. Data acquisition and reduction methods are depicted. Deficiencies in instrumentation, procedure, or model characteristics that were found to exist in the previous test program are discussed. Methods for obtaining useful data are delineated.

A computer program for scaling the model data is given that accounts for model size, jet velocity, transducer size, and jet density. Comparisons of scaled model data and full size aircraft data are made for the L-1011, S-3A, and a V/STOL lower surface blowing concept. Sonic environment predictions are made for an engine-over-the-wing SST configuration.

17. Key Words (Suggested by Author(s)	18. Distribution Statement
Acoustics, Noise, Sonic Environment, Aircraft Noise, Structure Sonic Environment	

19. Security Classif. (of this report)	20. Security Classif. (of this page)	21. No. of Pages	22. Price
Unclassified		113	

TABLE OF CONTENTS

TABLE OF CONTENTS (Continued)

LIST OF FIGURES

LIST OF FIGURES (Continued)

LIST OF TABLES

LIST OF TABLES (Continued)

LIST OF SYMBOLS

NOTE: All units are metric system units except where the symbols represent input to existing computer programs.

		Units
a	Speed of sound in the jet flow field	m/s
ATM	Atmospheric pressure	---
A_1, A_2	Integration area	m^2
a_1	Amplitude of autocorrelation function	m
$a_{1,2}$	Amplitude of cross-correlation function	m
a_2	Amplitude of autocorrelation function	m
c	Viscous damping coefficient	---
D	Nozzle exit diameter	m
D_a	Diameter of aircraft engine nozzle exit	m
D_m	Diameter of model nozzle exit	m
dA_1, dA_2	Differential of area	---
dB	Decibel	---
dc	Direct current	---
dmi	Model nozzle exit diameter	in.
dz	Differential of dummy variable	---
f	Frequency	Hz
f_a	Aircraft frequency	Hz
f_m	Model frequency	Hz

		Units
f_r	Frequency of mode r	Hz
$f_r(x,y)$	Modal deflection of any point for mode r	---
$f_r(x_1,y_1)$	Modal deflection at point 1 for mode r	---
$f_s(x,y)$	Modal deflection at any point for mode s	---
$f_s(x_2,y_2)$	Modal deflection at point 2 for mode s	---
FM	Frequency modulated	---
FS	Full Scale	---
G	Acceleration of gravity	m/s^2
$G(x,y;\omega)$	Response spectral density at a point (x,y)	$g^2/(rad/s)$
G^2/Hz	Acceleration spectral density	---
$G_p(f_r)$	Excitation spectral density for frequency f_r	$(N/m^2)^2/Hz$
$G_p(\xi,\eta;\omega)$	Excitation spectral for transducer longitudinal and lateral separation distances	$(N/m^2)^2/(rad/s)$
$G_p(\omega)$	Direct Excitation spectral density	$(N/m^2)^2/(rad/s)$
G_{RMS}	Acceleration root-mean-square	m/s^2
Hz	Frequency	
I	Impulse	
i	$\sqrt{-1}$	---
k	Spring constant	N/m
K	Constant (= 80 for V_r < 610 m/s and = 30 for V_r > 610 m/s)	---
KHz	Kilohertz	---
m	Mass of simple spring-mass system	kg

		Units
M_r	Generalized mass for mode r	kg
M_s	Generalized mass for mode s	kg
Mach	Mach number	---
MHz	Megahertz	---
mixa	Fuel/air mixture of aircraft engine exhaust gas	N-fuel/N-air
mixm	Fuel/air mixture of model nozzle exhaust flow	N-fuel/N-air
NASA	National Aeronautics and Space Administration	---
OASPL	Overall sound pressure level	dB
p	Pressure	N/m^2
P_o	Amplitude of harmonic excitation	m
p_r	Reference sound pressure	N/m^2
P(t)	Exciting force at time t	N
$P(t+\tau)$	Exciting force at time $(t+\tau)$	N
p(t)	Value of pressure at time t	N/m^2
$p(t+\tau)$	Value of pressure at time $(t+\tau)$	N/m^2
P(x)	Probability distribution function	---
$P(x_A, t)$	Distributed pressure at x_A	N/m^2
p(x)	Probability density function	---
P_1	Designates pressure measurement location 1	---
$p_1(t)$	Value of pressure at time t for point 1	N/m^2
$p_1(t+\tau)$	Value of pressure at time $t+\tau$ for point 1	N/m^2
P_2	Designates pressure measurement location 2	---

		Units
$p_2(t+\tau)$	Value of pressure at time t+τ for point 2	N/m^2
pra	Engine nozzle pressure ratio	---
ptmi	Total pressure upstream of the nozzle	lb/in^2
q	Dynamic pressure	N/m^2
R	Radius of pressure transducer	m
r	Subscript designating mode	---
R_a	Distance from nozzle exit to transducer on aircraft	m
R_m	Distance from nozzle exit to transducer on model	m
$R_p(\tau)$	Excitation autocorrelation function	---
$R_p(x_A, x_B; \omega)$	Excitation cross-correlation function for points x_A and x_B	---
$R_{P_1}(0)$	Excitation autocorrelation function for point P_1 at delay time zero	---
$R_{P_1}(\tau)$	Excitation autocorrelation function for point P_1 at delay time τ	---
$R_{P_1P_2}(\tau)$	Excitation cross-correlation function for points P_1 and P_2 at delay time τ	---
$R_{P_1P_2}(\tau_{1,2})$	Excitation cross-correlation function for points P_1 and P_2 at delay time $\tau_{1,2}$	---
$R_{P_2}(0)$	Excitation autocorrelation function for point P_2 at delay time zero	---
$R_{P_2}(\tau)$	Excitation autocorrelation function for point P_2 at delay time τ	---
$R_x(\tau)$	Response autocorrelation function for point X at delay time τ	---
$R_{11,11}(\tau)$	Excitation autocorrelation function for SCAT 15-F test transducer 11	---

		Units
$R_{11,12}(\tau)$	Excitation cross-correlation function for SCAT 15-F test transducers 11 and 12	---
$R_{12,12}(\tau)$	Excitation atuocorrelation function for SCAT 15-F test transducer 12	---
rmi	Distance from model nozzle exit to pressure transducer	in.
s	Subscript denoting mode s	---
$S_P(f)$	Direct spectral density at point P for frequency f	---
$S_P(x_A, x_B; \omega)$	Excitation cross-spectral density for points x_A and x_B	$(N/m^2)^2/(rad/s)$
$S_P(\omega)$	Direct excitation spectral density for point P	$(N/m^2)^2/(rad/s)$
$S_\omega(x_1, \omega)$	Response spectral density for point x_1	$m^2/(rad/s)$
$S_x(f)$	Response spectral density at point x for frequency f	$m^2/(rad/s)$
$S_{x_r, X_s}(f)$	Response cross-spectral density between points X_r and X_s	$m^2/(rad/s)$
$S_x(\omega)$	Response spectral density at point x	g^2/Hz
scafac	Modal scale	---
SCAR	Supersonic cruise aircraft research	---
SN	Strouhal number, fD/V_j	---
S/N	Random fatigue curve	---
SPL	Sounc pressure level	dB
SPL_a	Sound pressure level for aircraft noise	dB
SPL_m	Sound pressure level of model noise	dB

		Units
SPL_r	Reference sound pressure level spectrum	dB
splm	Sound pressure levels corresponding to f_m	dB
SST	Supersonic transport	---
t	time	s,sec
tria	Diameter of pressure transducer sensing element (full scale test)	in.
trim	Diameter of pressure transducer sensing element (model test)	in.
ttar	Total temperature of engine jet	deg R
ttmr	Total temperature of model jet	deg R
U_c	Jet convection velocity	m/s
V_a	Aircraft velocity	m/s
V_j	Jet velocity	m/s
$\left(V_j\right)_a$	Aircraft engine jet velocity	m/s
$\left(V_j\right)_m$	Model fully expanded jet velocity	m/s
V_r	Relative jet velocity	m/s
V/STOL	Vertical/Short Takeoff and Landing vehicle	---
W(t)	Response to unit impulse	---
W(x,t)	Displacement at any point	m
$w_r(x)$	Mode r	---
wa	Aircraft engine weight flow	kg/s
x	Coordinate of mass displacement for simple spring-mass system	m

		Units
x_A	Coordinate of point A	m
x_B	Coordinate of point B	m
$<x^2(t)>$	Time average of mean square random signal	---
$y_o(x,y)$	Static displacement due to a unit pressure over the surface of the structure	$m/(N/m^2)$
$<y^2(x,y,t)>$	Time average of the response of a structure	m^2
α_{x_1,x_A}	Receptance at point x_1 for a force applied at x_A	m/N
α_{x_1,x_B}	Receptance at point x_1 for a force applied at x_B	m/N
$\alpha(i\omega)$	Receptance of simple spring-mass system in terms of ω	m/N
δ	Viscous damping factor	---
δ_r	Viscous damping factor for mode r	---
δ_s	Viscous damping factor for mode s	---
$\delta(t)$	Dirac delta function	---
Δf	Band width being considered	Hz
Δf_r	Reference band width	Hz
η	Lateral distance between transducers at (x_1,y_1) and (x_2,y_2)	m
ξ	Longitudinal distance between transducers at (x_1,y_1) and $x_2,y_2)$	m
$\xi_r(t)$	Normal coordinates	m
ρ_a	Fully expanded density of aircraft engine exhaust	kg/m^3
ρ_m	Fully expanded density of model nozzle exhaust	kg/m^3

		Units
$\rho_P(0,\eta,\tau;\omega)$	Normalized lateral cross-correlation coefficient	---
$\rho_P(\xi,0,\tau;\omega)$	Normalized longitudinal cross-correlation coefficient	---
$\rho_P(\xi,\eta,\tau;\omega)$	Normalized cross-correlation coefficient for points (X_1,Y_1) and $X_2,Y_2)$ at delay time	---
$\rho_{P_1P_2}\ \tau$	Normalized cross-correlation coefficient for points P_1 and P_2 at delay time	---
$\rho_{P_1P_2}(\tau_{1,2})$	Normalized cross-correlation coefficient for points P_1 and P_2 at delay time $\tau_{1,2}$	---
$\rho_{11,12}(\tau)$	Cross-correlation coefficient for SCAT 15-F test transducers 11 and 12	---
σ	Standard deviation	m
σ^2	Variance	---
$<\sigma^2(x,y,t)>$	Time average of mean square stress	---
$\sigma_o(x,y)$	Static stress due to a unit pressure over the surface of the structure	N/m^2
τ	Delay time	s,sec
$\tau_{1,2}$	Delay time for signal to travel from point (x_1,y_1) to point (x_2,y_2)	s,sec
ϕ	True value of spectral density for a random pressure loading	$(N/m^2)^2/(rad/s)$
ϕ_m	Spectral density measured by a pressure transducer	$(N/m^2)^2/(rad/s)$
ω	Forcing circular frequency	rad/s
ω_d	Damped circular frequency	rad/s
ω_n	Natural frequency of system	rad/s
ω_r	Circular frequency for mode r	rad/s
ω_s	Circular frequency for mode s	rad/s

SONIC ENVIRONMENT OF AIRCRAFT STRUCTURE IMMERSED IN A SUPERSONIC JET FLOW STREAM

Wiley A. Guinn, Frank J. Balena, and Jaak Soovere
Lockheed-California Company
Burbank, California

SUMMARY

Results of a study that was performed to make an assessment of the technological basis for using a small model to determine the sonic environment on aircraft structure immersed in a supersonic jet flow stream is reported herein.

Background information is given that pertains to noise source considerations, selection of test conditions, and resolution of hydrodynamic and acoustic pressure fields.

Test data requirements that are needed to make sonic fatigue, crack growth, interior noise and equipment analyses are defined. Data reporting formats are illustrated and data applications are discussed.

Instrumentation requirements for data acquisition, storage and reduction are given. Detailed discussions are given that pertain to pressure transducer and tape recorder requirements. Methods are given for computing cross-correlation coefficients from autocorrelation and space-time cross-correlation function plots. Instrumentation used for a SCAT 15-F sonic environment test is discussed and methods used for data reduction are explained. A list of methods for improving data acquisition and reduction for future sonic environment test programs is given.

Methods are given for scaling of model data to full-size aircraft conditions. A literature search failed to provide a set of corresponding model and full-size engine test data associated with supersonic jet flows that was suitable for evaluating the scaling procedure. Therefore, subsonic jet test data for S-3A, L-1011, and a V/STOL configuration are compared. The SCAT 15-F model test data are scaled to dimensions and operating characteristics of a current SST duct burning turbofan engine concept.

Appendixes include a derivation of the response spectral density equation, a synopsis of the literature search, a listing of the computer program used for data scaling and computer program outputs for S-3A, L-1011, V/STOL, and SCAT 15-F test data.

1. INTRODUCTION

A supersonic cruise aircraft research (SCAR) program was initiated by NASA in 1972 to develop technology for an advanced supersonic transport. Prediction of the sonic environment on aircraft surfaces that is caused by high velocity jet flows is one technology area that has been identified where advances are required. The accuracy of analytical prediction methods or scaling of model test data to full size aircraft dimensions has not been established. However, the sonic environment must be known in order to perform analysis of sonic fatigue, crack growth, equipment environment and interior noise.

One of the SCAR program aircraft concepts that requires sonic environment evaluation is an over-the-wing engine configuration that gains lift for slow-speed flight by using Coanda turning of the jet stream. To achieve Coanda turning, the jet flow stream must be attached to the upper wing surface. The resulting thermal-acoustic environment on the parts of the wing surfaces that are immersed in the flow field will reduce the structural life of a typical wing structure. Therefore, special designs are required to withstand the adverse environment. Design methods for skin-stringer-type structures that will withstand the thermal-acoustic environment are given in References 1 through 3. However, more efficient designs may use hat-stiffened skins (Refs. 4 and 5), thermal tiles (Ref. 6) or ceramic composites.

The current study was performed to investigate problems encountered in conducting model tests for supersonic jets and to evaluate accuracy of the test results. Background information leading to the study are given in the following paragraphs.

1.1 Noise Source Considerations

The degree to which model test data is comparable to full-size aircraft dimensions is dependent on several factors. These include the following noise source considerations:

- Shock cell noise
- Crackle
- Internally generated noise
- Aircraft speed

Shock cell noise is generated by supersonic jets when the exhaust flow is not fully expanded (Refs. 7 through 12). In cold jets a pure tone noise called screech is generated, whereas in hot jets the shock noise is broad band (Ref. 13). Because of difficulties associated with designing and manufacturing a practical convergent-divergent nozzle which operates at fully expanded conditions during the entire flight mission, shock noise may occur during some portion of the flight (Refs. 9 through 12). Shock cell noise intensity and frequency are functions of the nozzle pressure ratio. Therefore, as the pressure ratio changes with altitude, shock cell noise may sweep through the frequency range of predominant response. Consequently, premature structural failures may occur as a result of shock cell noise unless it is accounted for in the design phase (Ref. 9). Model tests to investigate true effects of shock cell noise must be conducted with hot jets.

Crackle may be significant in high-velocity jets (Ref. 13). When this phenomenon occurs, the noise signature has a distinctive bias toward high-amplitude, positive, short-duration peaks. This results in increased skewness of the noise probability density distribution with increasing jet velocity. Therefore, when crackle occurs, a substantial number of positive peaks may exceed the 3σ rms peak level.

Internally generated noise associated with rotating machinery, combustion, or high-velocity flows over obstructions is not simulated in a model test. If these noise sources are significant, model test data may be misleading.

The effect of aircraft speed on the sonic environment of a structure immersed in a jet flow stream is dependent on the relative importance of hydrodynamic and acoustic-pressure fluctuations on the structure. If the acoustic pressure field is predominant, the structure environment is likely to decrease with aircraft velocity because noise generated by a jet is a function of the relative jet velocity ($V_r = V_j - V_a$). If the hydrodynamic pressure field is predominant, the aircraft velocity may not significantly alter the sonic environment since the jet velocity relative to the wing surface is virtually unchanged. Wind tunnel, sled, or whirling model tests are required to evaluate the effects of aircraft velocity on sonic environment characteristics.

1.2 Selection of Test Conditions

Before a meaningful test can be conducted, aircraft operating conditions that are likely to establish noise design criteria must be determined. Static takeoff thrust generally produces the highest noise on a structure in and adjacent to a jet flow stream. Thus, structure that is designed to withstand takeoff noise can usually withstand the sonic environment for other operating modes. Reverse thrust also produces high noise levels that may be predominant on some areas of the structure. Although jet noise decreases as aircraft velocity increases, the lower sonic environment may produce significant structural damage because of the relatively long length of exposure time during flight. The relative importance of each test condition must be determined to ensure that test results obtained will provide the correct environment for design of the structure.

1.3 Resolution of Hydrodynamic and Acoustic Pressure Fields

Fluctuating pressures in a supersonic jet are composed of hydrodynamic and acoustic pressures. The impinging and attached jet flow surface pressure fluctuations (Refs. 14 and 15) and separated flow pressures (Refs. 16 through 18) which may occur over the trailing-edge control surfaces due to adverse pressure gradients differ from the acoustic field pressure in convection velocity and correlation signature. Therefore, it may be possible to resolve the two pressure fields by narrowband space-time correlation coefficient analyses if the local flow convection velocity differs from the speed of sound in the jet flow field. Generally, flow pressure fluctuations associated with boundary layers (Refs. 19 through 22) and with separated flow pressure exhibit a reduced coupling with the structure relative to that produced by the acoustic field. Therefore, unless the degree of coupling is considered when making structural design analyses, overdesign of the structure and corresponding weight increases are likely to occur.

2. TASK I - TEST DATA REQUIREMENTS

Predictions for sonic fatigue, crack growth, equipment vibration and interior noise analyses require that response of the structure be determined. Frequency ranges normally investigated are:

- Sonic fatigue and crack growth (50 to 1000 Hz)
- Equipment vibration (50 to 2000 Hz)
- Interior noise (50 to 10,000 Hz)

The following sections define test data parameters, show data presentation formats, and discuss data applications that are required to determine structural response caused by a random pressure loading on an aircraft structure.

2.1 Data Requirements

Noise Contours.-An OASPL distribution over the surface of an aircraft structure provides an indication of potential noise areas. The following guideline (based on rule-of-thumb estimates) can be used for making an assessment of potential problems.

- OASPL > 120 dB: Interior noise and equipment vibration problems may exist
- OASPL > 150 dB: Sonic fatigue and crack-growth problems may exist

Noise Spectra.-Spectral noise contours for the octave-band center frequencies over the range of 63 to 1000 Hz are generally sufficient to allow a designer to evaluate integrity and estimate weight of an aircraft structure. Octave-band, one-third-octave-band, or narrow-band frequencies provide sufficient information that can be used by empirical predictions to predict interior-noise and equipment-vibration environments.

Correlation Functions and Spectral Densities.-Cross-spectral density of the excitation is required to compute response of a structure by the normal mode method. The cross-spectral density can be determined directly from a noise signal. However, when this is done, signal-phase relations are lost. Therefore, autocorrelation and cross-correlation functions are normally determined and Fourier Transforms are used to compute the spectral densities.

Distribution Functions.-The probability density function indicates percentage of time that a random signal dwells between two amplitude limits. Two probability density distributions are commonly used in performing sonic fatigue analyses. They are:

- Gaussian distribution
- Rayleigh distribution

Jet noise is generally considered to have a Gaussian distribution that is defined by Equation (1).

$$p(x) = \frac{1}{\sigma\sqrt{2\pi}} e^{-x^2/2\sigma^2} \tag{1}$$

$p(x)$ = probability density

x = instantaneous value of the noise signal with zero mean

σ^2 = variance = $\langle x^2(t) \rangle$

σ = standard deviation = $\sqrt{\langle x^2(t) \rangle}$

Instantaneous stress peaks of an aircraft structure that is subjected to a narrow-band random signal are generally considered to have a Rayleigh distribution that is defined by Equation (2).

$$p(x) = \frac{x}{\sigma^2} e^{-x^2/2\sigma^2} \tag{2}$$

x = instantaneous value of the envelope of noise peaks

Assumptions are often made that excitation signal and stress response have Gaussian and Rayleigh distributions, respectively. Increased confidence in accuracy of fatigue analyses may be established by analyzing a random signal to show that its distribution compares with the Gaussian and Rayleigh distributions.

Model Data.-Atmospheric conditions, model geometry, flow conditions and pressure transducer characteristics should be reported. Also, flow-field boundaries, convection velocities and boundary-layer thickness may need to be determined. The use of these data will become evident in the subsequent discussions.

2.2 Data Reporting Formats

Table 1 gives a summary of the test data requirements that were defined in Section 2.1 and shows why each type of data is needed. The following paragraphs depict the format for data presentation.

Noise Contours.-Figure 1 is a typical example of takeoff OASPL contours for an arrow wing supersonic transport. The values shown are for engines that are equipped with high-attenuation mechanical suppressors. The spectral level contours for the 63- to 1000-Hz frequency range octave-band center frequencies can be presented in a similar manner.

Noise Spectra.-Figure 2 shows typical octave-band, one-third-octave-band, narrowband (20-Hz) and spectrum (1 Hz) plots. The abscissa of these plots can be changed to Strouhal numbers by application of Equation (3) for noise of a jet flow stream

$$SN = \frac{fD}{V_j} \tag{3}$$

SN = Strouhal number

f = band center frequency

D = diameter of nozzle

V_j = jet velocity

The noise levels of one type of spectrum (e.g., one-third-octave band) can be converted to another type spectrum (e.g., octave bands) by application of Equation (4).

$$SPL = SPL_r + 10 \log_{10} \frac{\Delta f}{\Delta f_r} \tag{4}$$

SPL = sound pressure level for desired bandwidth spectrum

SPL_r = sound pressure level for reference spectrum

Δf = desired frequency bandwidth

Δf_r = reference bandwidth

TABLE 1. UTILIZATION OF SONIC ENVIRONMENT TEST DATA

	Preliminary Structural Design	Sonic Fatigue Analysis	Equipment Vibration Analysis	Interior Noise Analysis
Noise Contours	X		X	
Noise Spectra	X		X	X
Cross Correlation		X		
Distribution Functions		X		

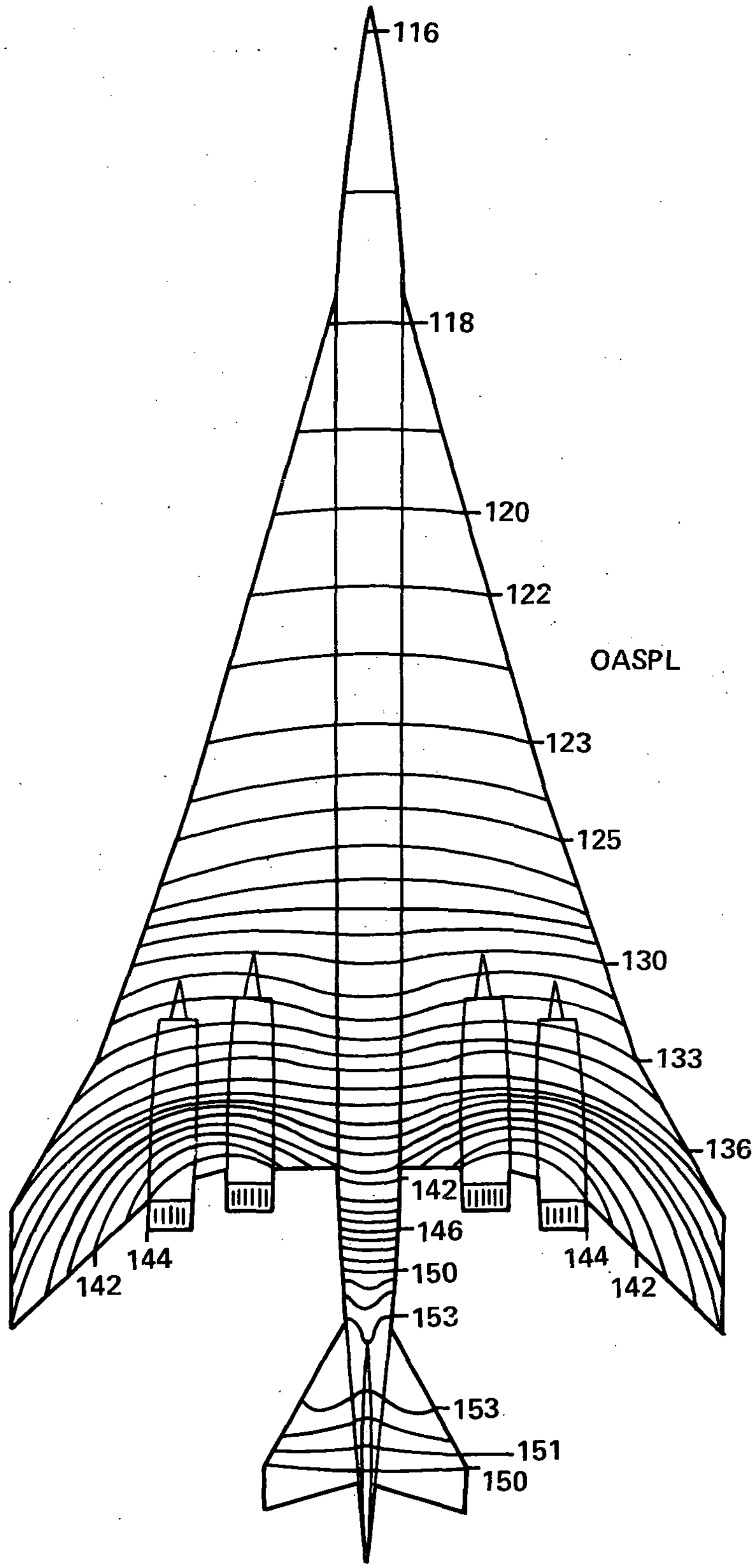

Figure 1 . Typical Engine Noise Contours

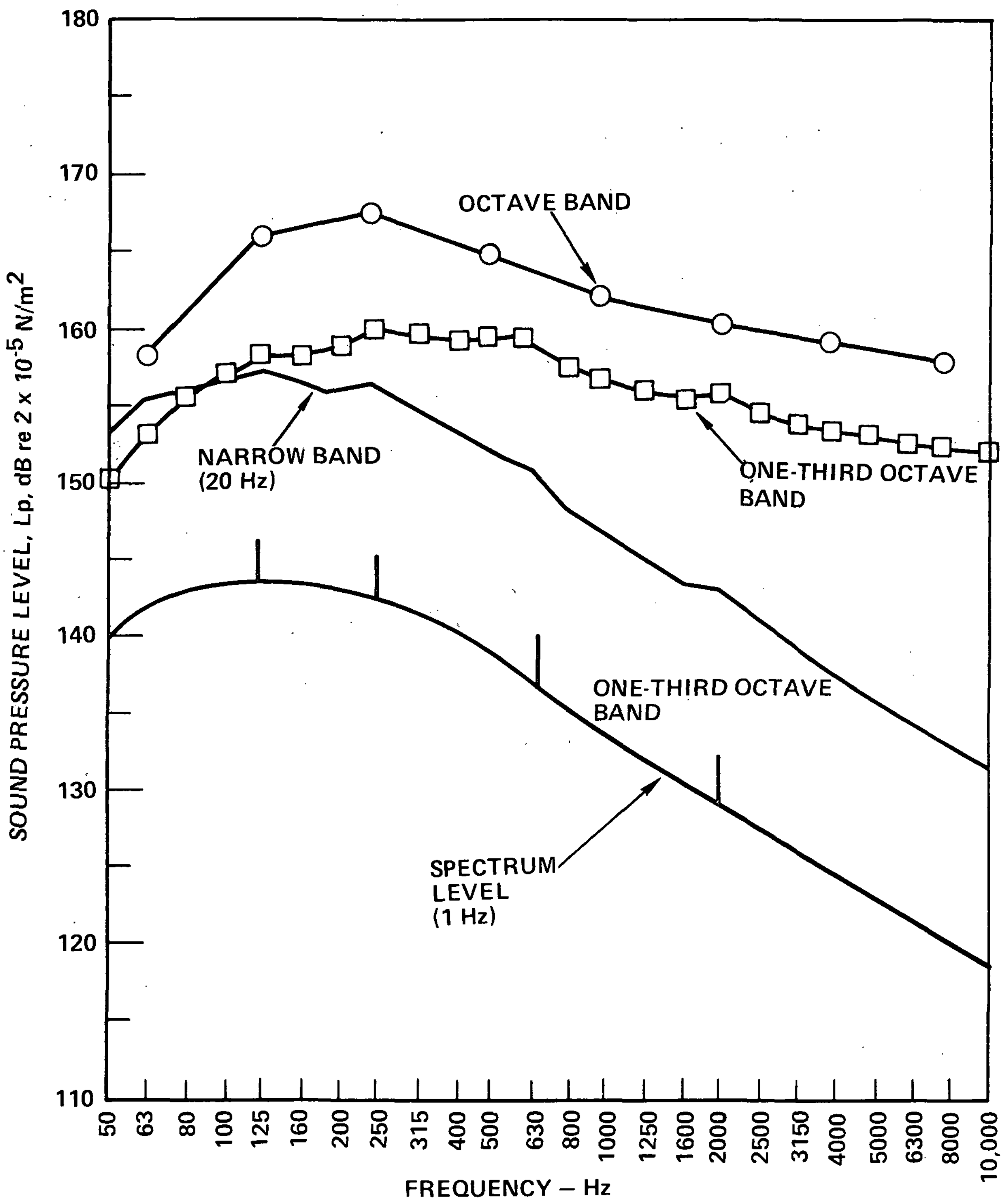

Figure 2. Typical Noise Spectra Plots

Correlation Density Functions and Spectral Densities.-Figure 3 shows a typical power spectral plot. this plot can be converted to sound pressure levels for any bandwidth by Equation (5).

$$SPL = 10 \log_{10} \frac{p^2}{p_r^2} + 10 \log_{10} \Delta f \qquad (5)$$

p^2 = ordinate value of Figure 3

p_r^2 = reference pressure squared

Figure 4 shows typical autocorrelation and cross-correlation plots. Section 3.2 contains equations for computing correlation coefficients from these curves. Section 2.3 describes methods for determining the spectral density by using the correlation coefficient values.

Distribution Functions.-Figure 5 gives plots of the probability density Gaussian and Rayleigh distributions that are defined by Equations (1) and (2), respectively. The curves shown are normalized with respect to the standard deviation.

2.3 Utilization of Data

Sonic Fatigue.-The first step in sonic fatigue analysis is to establish the design life of a structure at the highest noise level. This is achieved by studying the aircraft utilization pattern. Parameters included are takeoff, landing, flight profiles, ground taxi, and static aircraft test noise levels. A general procedure used for sonic fatigue analyses (Ref. 9) is to account for noise-reduction levels during the ground run and flight by computing the equivalent damage duration at static takeoff noise levels. This procedure assumes that the nature of the flight and takeoff acoustic environments remain essentially the same.

It is current practice to require sonic fatigue proof testing of any novel structures, such as those required for high thermal-acoustic environments, because structural details cannot be accounted for by analyses. These tests are usually conducted in an acoustic progressive wave test facility that provides for adjustment of spectrum levels and shapes for a predefined correlation function.

Two basic methods are used for performing sonic fatigue analyses. The first is an empirical method that is based on design charts. The other method is the normal mode approach based on the procedure given in Reference 23. Current sonic fatigue analyses are based on a predominant

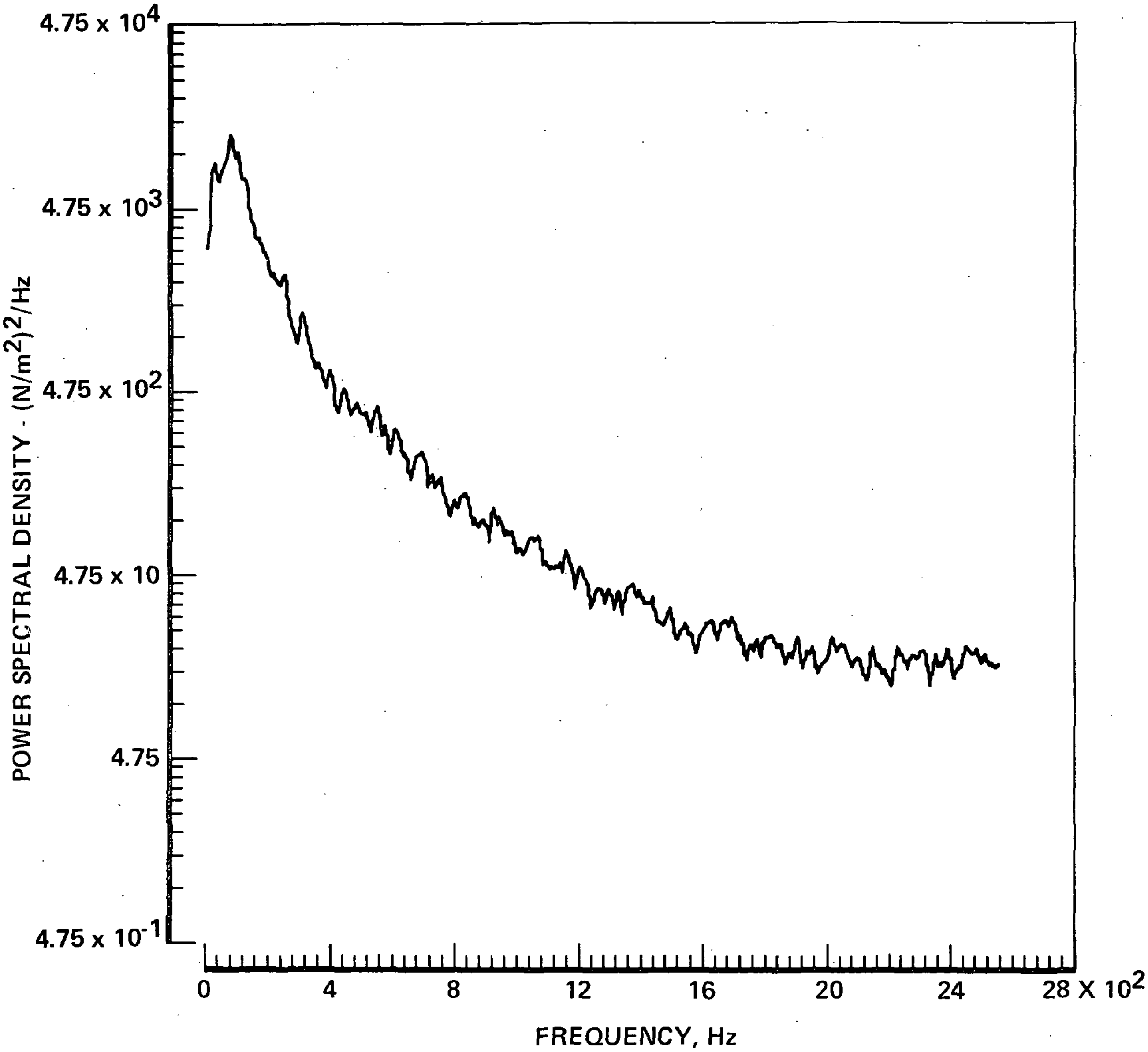

Figure 3. Typical Power Spectral Density Plot

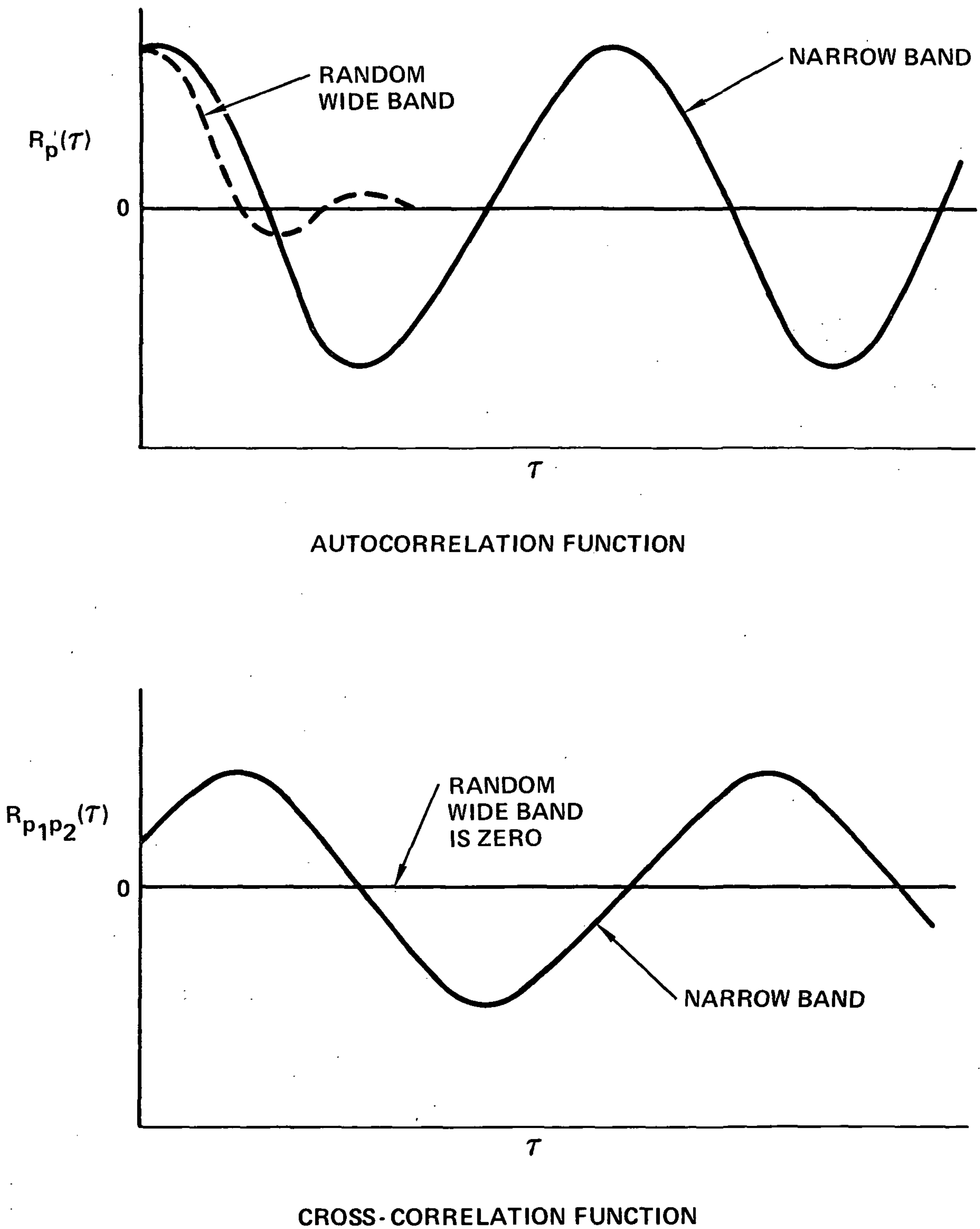

Figure 4. Typical Autocorrelation and Cross-Correlation Plots

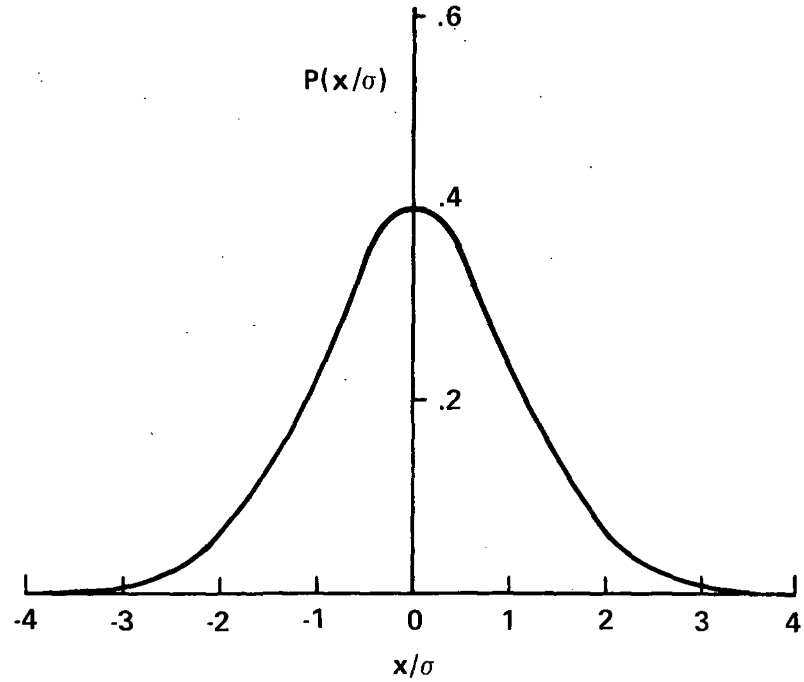

A. NORMALIZED GAUSSIAN DISTRIBUTION

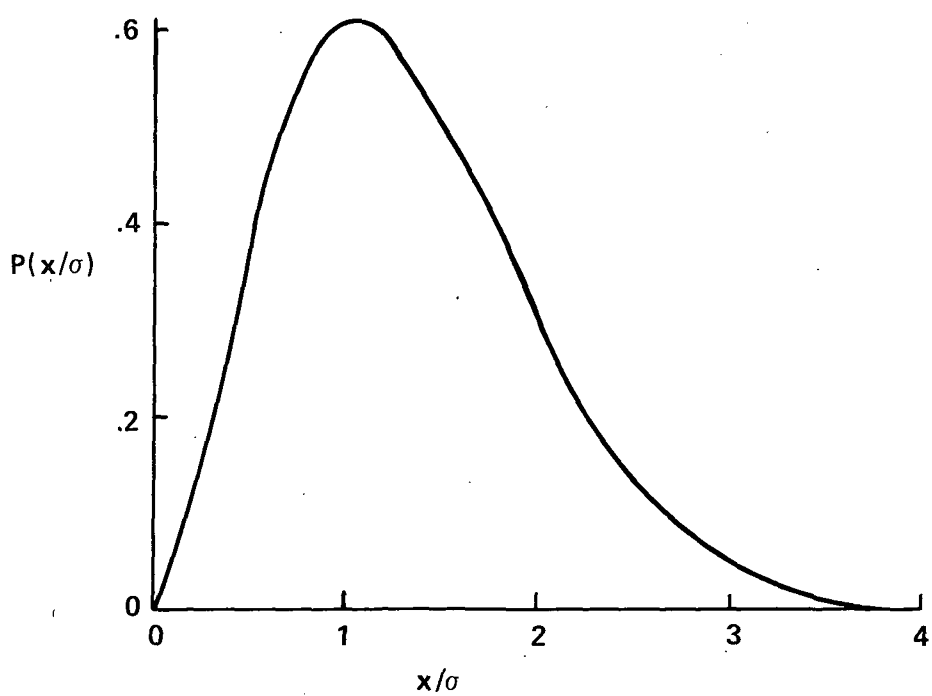

B. NORMALIZED RAYLEIGH DISTRIBUTION

Figure 5. Typical Normalized Probability Density Curves

single-mode response. The analyses are used in conjunction with random fatigue data for critical joints. Most random fatigue data are based on the Rayleigh distribution of stress peaks which is obtained from a single modal response to a broadband Gaussian-type random excitation. A reasonable approximation to the Rayleigh distribution occurs when the multimodal response falls within a frequency band that has an upper limit approximately twice that of the lower limit (Ref. 24). The current trends in generation of random S/N data by coupon testing is to use a broader spectrum of excitation to include the contribution from the higher modes.

The empirical analysis method of obtaining data is expensive and is usually restricted to simple rectangular structures such as skin-stiffener structure, simple honeycomb panels and beaded panels. After the panel dimensions are selected, the panel frequency is computed. The structural life is determined by assuming the single-mode response and using the equivalent damage duration for static takeoff levels. This process is repeated until a suitable design has been achieved.

The basic normal mode approach equation for the response spectral density at a point (x,y) is given by Equation (6).

$$G(x,y;\omega) = \sum_{r=1}^{\infty} \sum_{s=1}^{\infty} \frac{1}{M_r(\omega_r^2-\omega^2+2i\delta_r\omega_r\omega)} \frac{1}{M_s(\omega_s^2-\omega^2+2i\delta_s\omega_s\omega)} \times f_r(x,y) f_s(x,y) \int_{A_1}\int_{A_2} f_r(x_1,y_1) f_s(x_2,y_2) G_P(\xi,\eta;\omega)\,dA_1\,dA_2 \tag{6}$$

$G(x,y;\omega)$ = response spectral density

$f_r(x,y), f_s(x,y)$ = normal mode deflection at point (x,y) for modes r and s

$f(x_1,y_1)$ = normal mode deflection at point (x_1,y_1)

$f(x_2,y_2)$ = normal deflection at point (x_2,y_2)

$G_P(\xi,\eta;\omega)$ = excitation cross-spectral density at separation distances ξ and η between points (x_1,y_1) and $x_2,y_2)$

M_r, M_s = generalized mass corresponding to r and s modes

ω_r, ω_s = natural frequency corresponding to mode shapes r and s, respectively

ω = forced frequency

δ_r, δ_s = viscous damping factor corresponding to modes r and s

Derivation of Equation (6) is given in Appendix A. The first two factors following the summation signs are the receptances of the system for modes r and s, respectively. The double integral term represents the degree of coupling between the excitation and structural response. The equation is applicable to jet noise, turbulent boundary layer excitation (Ref. 20), and separated flow excitation (Ref. 17). For turbulent boundary-layer excitation, the cross-spectral density can be computed by Equation (7).

$$G_P(\xi,\eta;\omega) = G_P(\omega)\left|\rho_P(\xi,0,\tau;\omega)\right|\left|\rho_P(0,\eta,\tau;\omega)\right|e^{-i\omega\xi/U_c} \quad (7)$$

$G_P(\omega)$ = direct spectral density

$\rho_P(\xi,0,\tau;\omega)$ = *longitudinal narrowband space-time correlation coefficient*

$\rho_P(0,\eta,\tau;\omega)$ = lateral narrowband space-time correlation coefficient

P = subscript designating excitation quantities

ξ = longitudinal separation distance between transducers (e.g. transducers 1 and 2)

η = lateral separation distance between transducers

U_c = convection velocity of the flow stream

Narrow-band correlation coefficients for a traveling acoustic wave at grazing incidence can be computed by use of Equation (8) or from test data (Section 3.2).

$$\rho(\xi, \eta, \tau, \omega) = \cos(\tau - \xi/a) \quad (8)$$

a = speed of sound in the flow field

Considerable simplification of Equation (6) is obtained by making assumptions that are commonly used when making sonic fatigue analyses. The assumptions are:

- A predominant single-mode response
- A fully correlated excitation across the panel
- A constant excitation spectrum level.

The double area integral in Equation (6) is reduced to an integral of mode shapes if the pressure field is assumed to be fully correlated over the panel area. This assumption is correct for normal incident acoustic waves and results in very small errors for a fundamental mode progressive wave. Therefore, the mean-square response obtained by integrating Equation (6) with respect to circular frequency (ω) results in Equation (9a).

$$\langle y^2(x,y,t)\rangle = \frac{\pi\ f_r^2(x,y)\ G_p(f_r)}{4M_r^2\omega_r^3\delta} \tag{9a}$$

A similar expression to Equation (9a) was developed by Miles (Ref. 25). The expression (Equation 9b) is based on the static displacement $y_o(x,y)$ at point (x,y) due to a unit pressure on the structure.

$$\langle y^2(\ x,y,t)\rangle = \frac{\pi}{4\delta}\,\omega_r G_p(\omega) y_o^2(x,y) \tag{9b}$$

The corresponding expression for mean-square panel stress is given by Equation (10).

$$\langle \sigma^2(\ x,y,t)\rangle = \frac{\pi}{4\delta}\,\omega_r G_p(\omega)\sigma_o^2(x,y) \tag{10}$$

σ_o = static stress at point (x,y) on the structure due to a unit pressure over the structure

The panel stress is used with random fatigue data for representative structure to determine fatigue life of the structure (Ref. 26).

Crack Growth.-Crack-growth analyses (Ref. 27) are based on a modified Rayleigh Ritz method of assumed cracked-panel modes. Initially the panel response spectral density is computed by Equation (6). Expressions for computing stress spectra are then developed by using the assumed cracked-panel modes. Baseline panel crack-growth data due to a random loading are obtained from electromagnetic shaker-excited coupon specimens. The baseline crack-growth test data are used in conjunction with computed stress spectra to predict crack growth.

Equipment Vibration.-Dynamic characteristics of structural vibration reflects the combined effects of sonic environment and structural response characteristics. Complexity of the aircraft structure makes a theoretical prediction method impractical for making engineering analyses. Therefore, empirical methods are used. These methods are based on the use of correlation curves. The curves are established by correlating acceleration response levels that are measured on primary structure of existing aircraft with the aircraft sonic environment (Refs. 28 and 29). The problem approach is:

- Division of the aircraft into zones of approximately equal-vibration response levels
- Estimation of the octave-band acoustic levels over the aircraft flight conditions of interest
- Use of response correlation curves (Refs. 28 and 29)
- Prediction of frequency-dependent vibration spectra

Typical vibration zones for a jet-powered subsonic airplane are shown in Figure 6. Figure 7 illustrates the procedure for converting the sonic environment of each zone to acceleration spectral density. A typical environment for the outboard wing area is shown in Figure 8 (Ref. 29). The spectral density levels are used as standards for equipment qualification test levels.

Interior Noise.-Interior noise in passenger-occupied areas of an aircraft that is associated with jet noise is maximum at takeoff. It is still present during flight at a level comparable to turbulent boundary-layer noise for the lower-frequency region (Ref. 30). Once the exterior noise levels on the fuselage have been determined, interior noise analysis includes obtaining values for the following quantities.

- Transmission loss of the structure and acoustic treatments
- Interior absorptivity
- Interior equipment noise

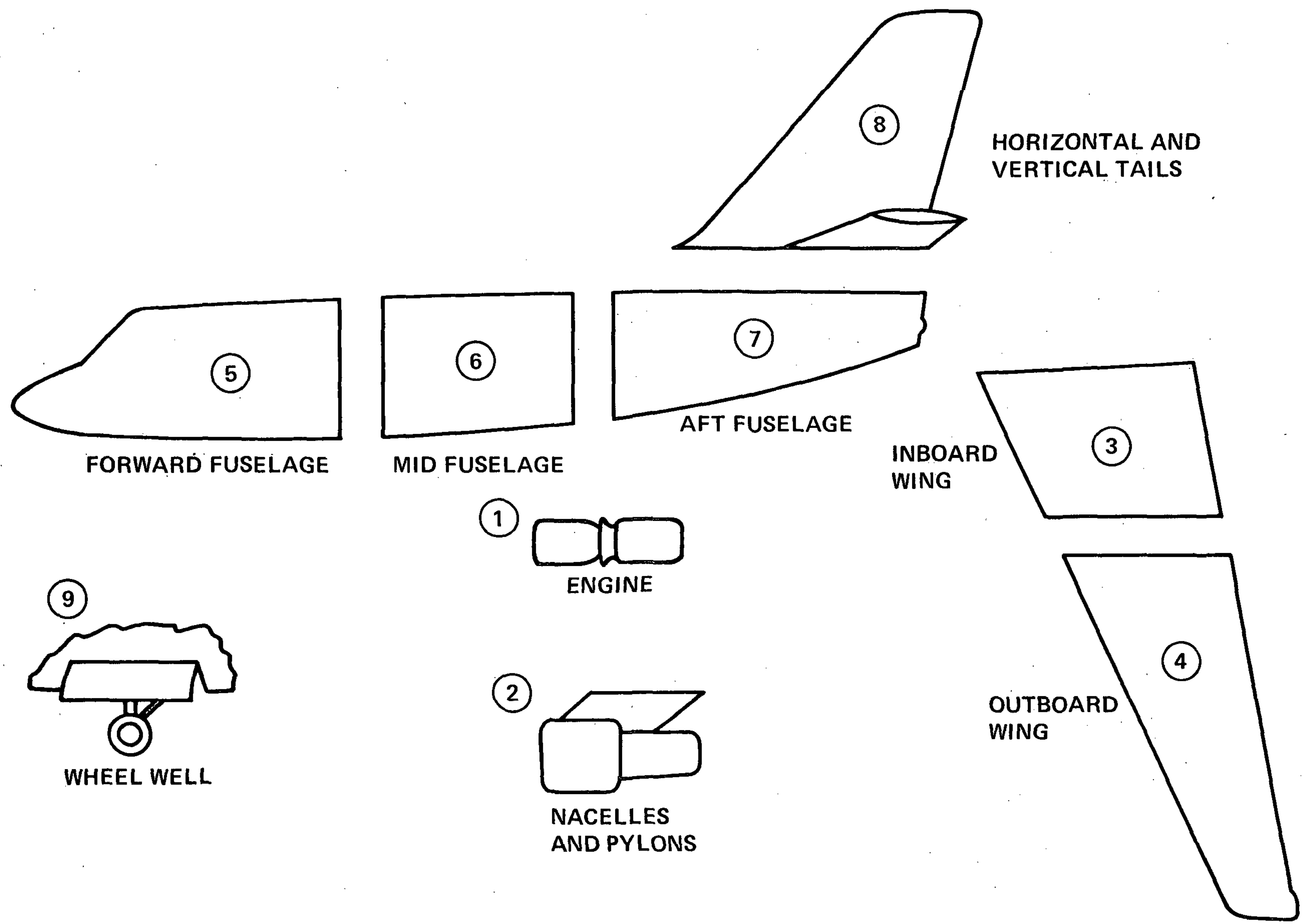

Figure 6. Vibration Zones and Their Location

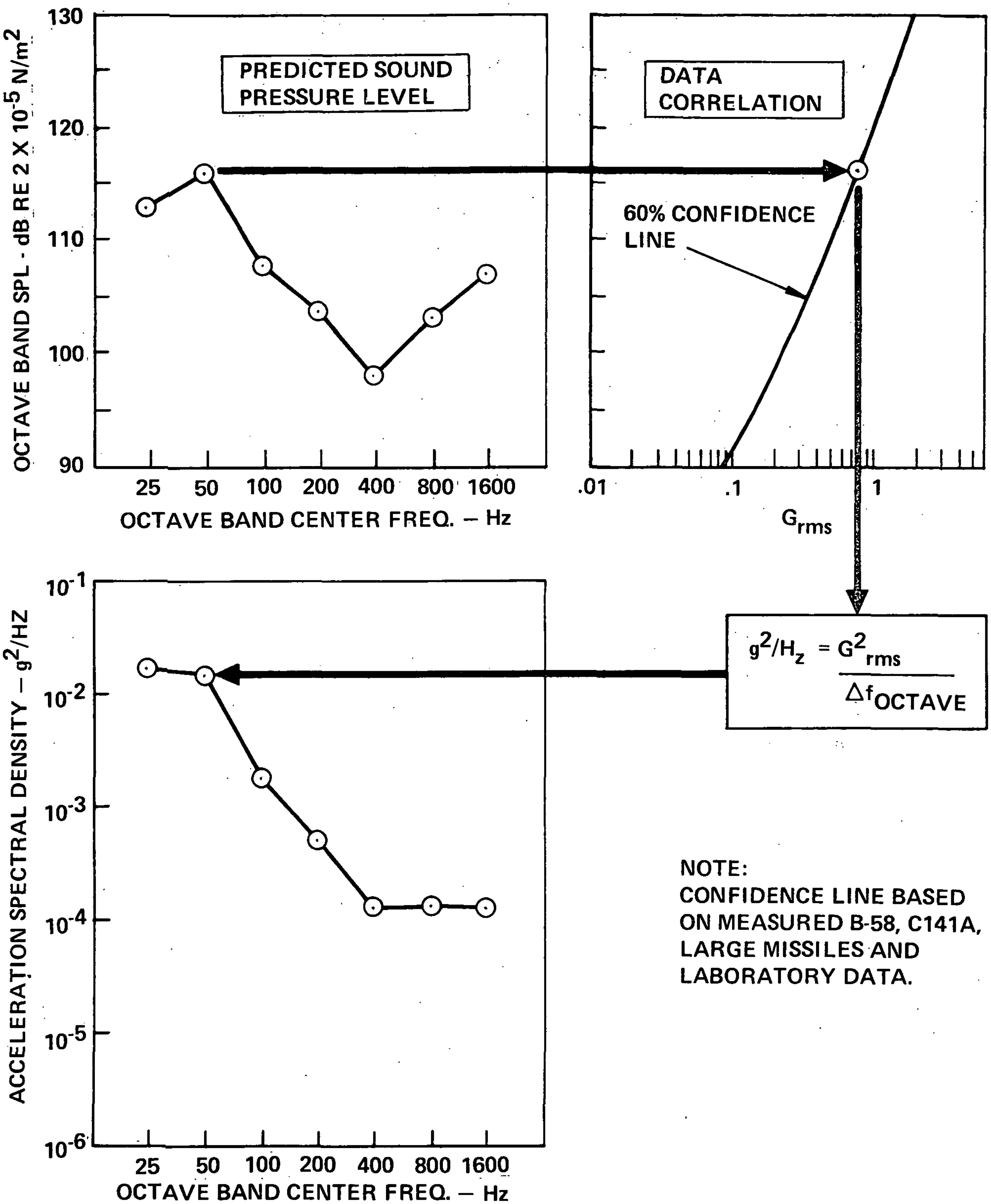

Figure 7. Method of Predicting Random Vibration Environment

- Mechanical vibration noise generation
- Size and shape of interior

Computation of the interior noise is an intricate task. Currently, analytical prediction methods have not been developed that can be used to accurately predict the interior noise. Methods that are representative of the technology are given in References 22 and 31. Empirical methods for interior noise predictions rely heavily on test data banks that have been compiled which give noise levels in existing aircraft along with the corresponding acoustic treatments. The aircraft data are supplemented by mounting a representative section of the aircraft fuselage (e.g., structure plus acoustic treatment plus interior trim) between two reverberation rooms and measuring the transmission loss. Normally, the noise on the exterior side of the panel has approximately the same spectral content as the jet or turbulent boundary-layer noise, but it is a normal incident wave which does not simulate the degree of coupling for a turbulent flow field. Nevertheless, comparison of different acoustically treated panel configurations provides a relative comparison of the panel noise reduction characteristics.

3. TASK II - DATA ACQUISITION AND REDUCTION

3.1 Instrumentation and Procedures

Pressure transducers and tape recorders that are used to record the noise for a jet model test must be carefully selected. Required characteristics for each of these are discussed below.

Pressure Transducers.-Selection of pressure transducers for a sonic environment test must include the following considerations.

- Environmental conditions to which the transducers are exposed (e.g. temperature, humidity, and vibration)
- Size of the sensing element
- Dynamic range
- Frequency response

Temperature Environment: The temperature environment in a hot jet flow stream is a formidable requirement for pressure transducers. Pressure transducer manufacturers have developed several transducers for measuring pressure fluctuations in a high temperature jet flow stream. The suitability of these for use on hot jet model tests remains to be determined. Limitations for various types of the high temperature pressure transducers include the following:

- They cannot be flush mounted
- They require water cooling
- They have insufficient frequency response

The accuracy of these transducers needs to be determined. The rationale for this statement is based on a comparison of measurements made by 12 different low-temperature pressure transducers (Ref. 32) in a wind tunnel. Data recorded by the various transducers for Mach numbers of 1.6 to 2.5 showed significant differences. A similar test has not been conducted for high-temperature transducers, but it is anticipated that a comparison of data recorded by different models would result in large discrepancies.

Size of Sensing Element: Finite size of a transducer sensing element limits its space resolution of a pressure field (Ref. 33). As the value of the quantity $\omega R/U_c$ increases, there is a corresponding increase in measurement error (Figure 9). For a given jet flow stream, the circular frequency (ω) and the convection velocity (U_c) are fixed. Consequently, space resolution can be improved only by making the transducer sensing element radius (R) smaller.

Dynamic Range: The dynamic range of a pressure transducer must be compatible with the magnitude of pressure fluctuations that are to be measured. The lower level of the range is limited by the signal-to-noise ratio and the upper level is limited by clipping of the signal.

Frequency Response: The transducer frequency response required for model testing depends on the model scale (Section 4.1). As the model size is decreased, the frequency range to be measured increases. Transducers that are suitable for measurement of high-frequency noise need small sensing elements to ensure good frequency response. However, frequency response and sensitivity of a transducer vary inversely. Therefore, the most suitable transducer for making sonic environment measurements is the one with the smallest sensing element that has sufficient sensitivity for the intensity levels being measured.

Data Storage.-Test data are generally stored on magnetic tape. This can be accomplished by recording data in the direct or the FM mode. The mode to be used depends on the frequency bandwidth to be measured and the manner in which the data will be analyzed.

Direct Recording Mode: The direct mode permits measurements up to 600 kHz in the intermediate band mode of operation and to 2 MHz in the wideband mode of operation. Disadvantages of the direct mode are poor low-frequency response, complexity of frequency response corrections for time expansion, amplitude instability (commonly referred to as dropout) at very high frequencies and low signal-to-noise ratio. The poor low-frequency response will not be a problem if the model scale is sufficiently small so that measurement of frequencies below approximately 400 Hz are not required. Time expansion is not required if a spectral analyzer is used for data processing that has a sufficiently wide bandwidth so that data can be reproduced at the same speed at which it is recorded. Amplitude instability can be minimized by using high-quality magnetic tape and keeping recorder heads, guides and other parts of the recorder that come in contact with the tape scrupulously clean. The low signal-to-noise ratio is a definite limitation.

FM Recording Mode: The FM mode has good amplitude stability (virtually insensitive to dropouts) and low-frequency measurement capability (down to dc). Wideband Group 2 FM recording permits measurements of frequencies ranging from dc to 500 kHz. Time expansion can be accomplished by recording

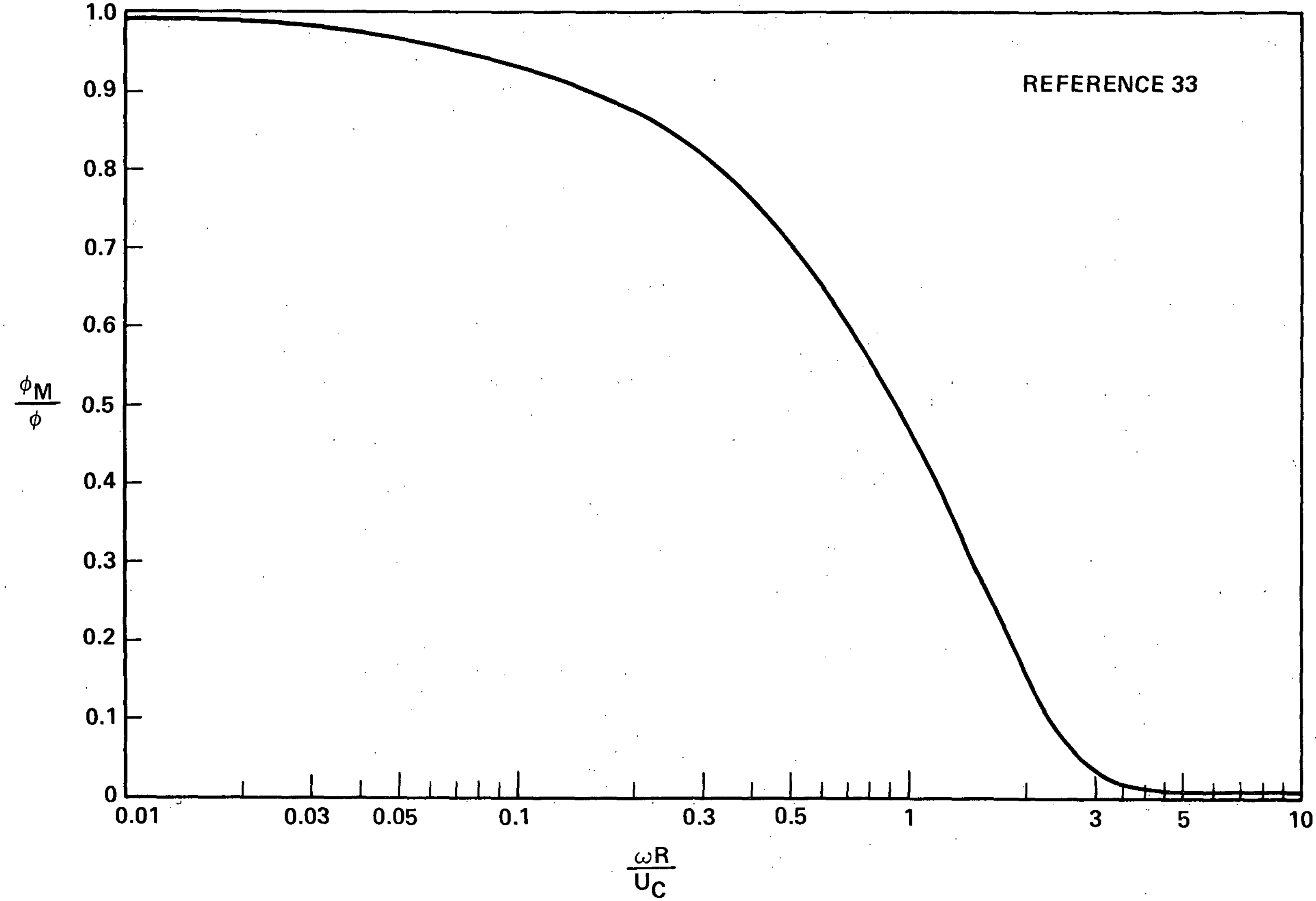

Figure 9. Resolution of Frequency Spectral Density for a Round Transducer

at a high tape speed and playing back at a low tape speed. When this is accomplished in the FM mode, minimal frequency response corrections are required in comparison to those for the direct mode of operation. This time-expansion capability is useful when analyzing transient signals or when the measured data bandwidth is wider than that of the data-reduction analyzer. Group I FM recordings have a singal-to-noise ratio that is approximately 15 dB greater than the direct mode and the Group II signal-to-noise ratio is approximately the same as that of the direct mode. The Group I mode can be used if frequencies of the data to be measured do not exceed approximately 80 kHz.

The FM mode of operation is considered to be most favorable in light of the aforementioned considerations.

Phase Calibration.-When cross-correlation plots are to be made, a phase calibration of all data channels that are to be used for cross correlations is necessary. If this calibration is not performed, the cross-correlation functions will include initial phase differences which result in a time shift of the entire function. It is good practice to record all data to be correlated on either even- or odd-numbered tape recorder channels. This eliminates the possibility of errors caused by differences in the recording head locations for even and odd channels.

Cross-Correlation Coefficient.-Figure 10 illustrates the manner in which narrowband cross correlation coefficients are determined. The autocorrelation functions are determined by taking the time average of the product $p(t)p(t+\tau)$ where τ is the delay time. $R_{p_1}(\tau)$ and $R_{p_2}(\tau)$ are typical narrowband plots for pressure measurements at locations P_1 and P_2, respectively. The cross-correlation plot is determined by taking the time average of the product $p_1(t)p_2(t+\tau)$. This plot is the lower plot in Figure 10. The cross-correlation coefficient is obtained by dividing the peak amplitude of the cross-correlation plot corresponding to the delay time $\tau_{1,2}$ by the square root of the product of the amplitudes of the autocorrelation functions for $\tau=0$. Figure 10 shows the narrowband autocorrelation functions and the cross-correlation function to be slowly decaying periodic functions. However, correlation plots for wide-band random signals decay rapidly to zero as the value of τ increases.

3.2 SCAT 15-F Model Test Data Analyses

A schematic diagram of the data acquisition and data-processing system used for the SCAT 15-F model test (Ref. 34) are shown in Figure 11.

Pressure Transducers.-Three different models of pressure transducers were used for measuring the sonic environment of the upper wing surface during the SCAT 15-F model test. They were Bruel and Kjaer (B&K) 4138 microphones, Kulite VQL-250-25 transducers and Piezatronics 112A02 pressure transducers. Characteristics of these transducers are listed in Table 2.

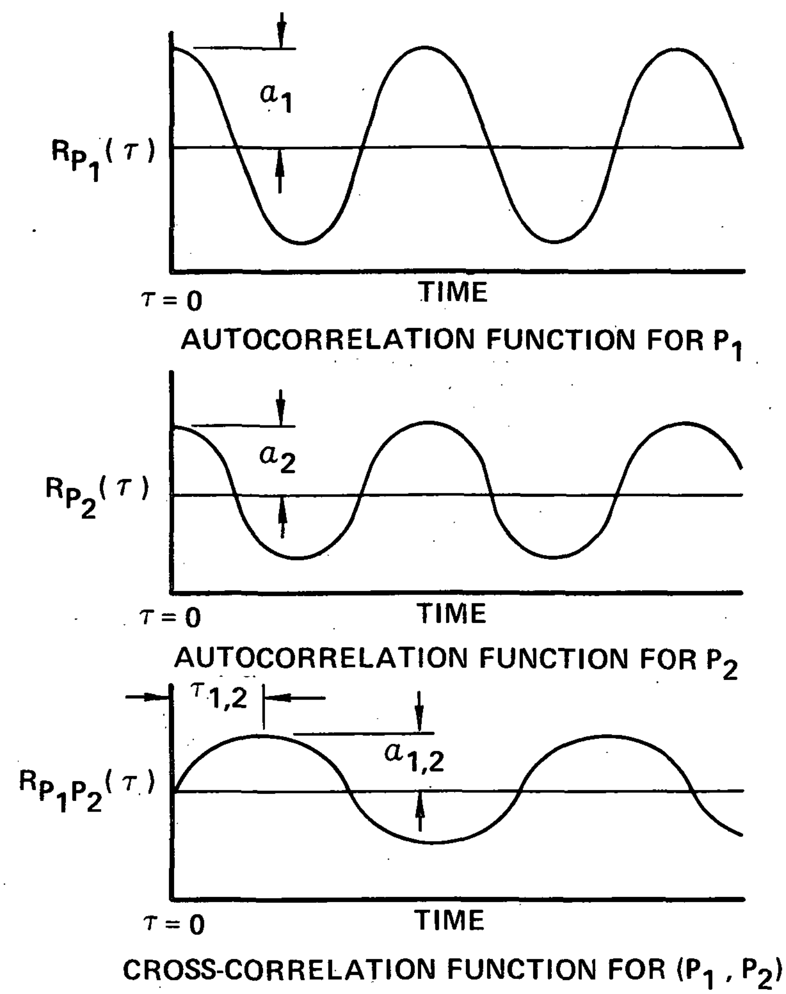

$$\rho_{P_1P_2}(\tau_{1,2}) = \frac{R_{P_1P_2}(\tau_{1,2})}{\sqrt{R_{P_1}(0)\,R_{P_2}(0)}} = \frac{a_{1,2}}{\sqrt{a_1 \; a_2}}$$

$\rho_{P_1P_2}(\tau_{1,2})$ = CROSS CORRELATION COEFFICIENT

Figure 10. Computation of Cross-Correlation Coefficient

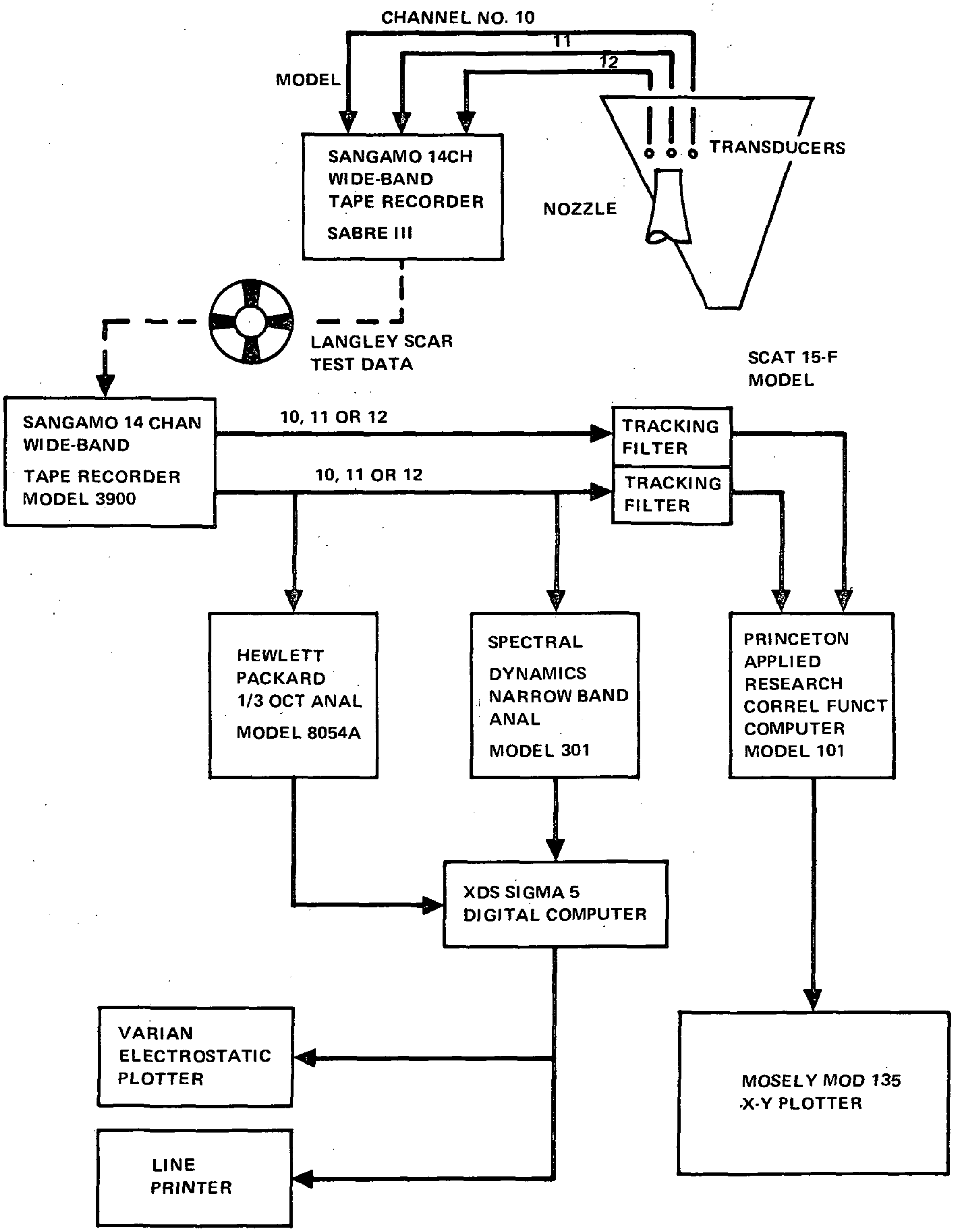

Figure 11. Data Reduction and Analysis System

TABLE 2. SCAT 15-F TEST PRESSURE TRANSDUCER CHARACTERISTICS

	B&K 4138	KULITE VQL-250-25	PIEZATRONICS 112A02
Diameter	3.175×10^{-3}m	6.35×10^{-3}m	5.537×10^{-3}m
Dynamic Range	76-168 dB	--	131 to 211
Frequency Response	7-140 kHz	--	--
Resonant Frequency	--	35 kHz	250 kHz
Vibration Sensitivity	1G = 80 dB	1G = 100 dB	0.002 $N/m^2/G$
Thermal Sensitivity	0.0028 dB/°C	0.011% FS/°C	0.011% FS/°C
Static Pressure Sensit.	-1 dB/ATM	NA	NA

Initially three B&K microphones were flush mounted in the wing surface of the model (Figure 12). However, as the jet velocity was increased during the first test condition when the nozzle was located at position 1, the diaphragm of one of the microphones was destroyed. Since time allotted for conducting the test was two weeks and the primary objective of the test program was to determine far-field noise reductions that can be attained through shielding of a jet noise source by an arrow wing structure, the B&K microphones had to be replaced by transducers that were readily available. Two Piezatronics transducers and one Kulite transducer appeared to be the best that were available. Therefore, they were flush mounted in the wing surface. These transducers are extremely rugged. The Kulite transducer is a solid state sensor that is rated for 1.724×10^5 N/m^2 with a maximum usable pressure of 3.447×10^5 N/m^2 and the Piezatronics pressure transducers can withstand a maximum static pressure of 1.3×10^4 N/m^2.

Environmental Conditions.-Environmental conditions did not appear to have a significant influence on the choice of transducers. Since the test was conducted in an anechoic room, humidity was not considered to be a problem. Model weight and rigidity of the model support were believed to be sufficient to prevent excessive vibration levels that would affect the noise measurements. Air supply to the nozzle was near ambient conditions. Therefore, the jet temperature was not considered to affect the transducer sensitivities. However, the fully expanded jet static temperature was about -157 degrees Celsius and may have been a factor that contributed to failure of the B&K microphone.

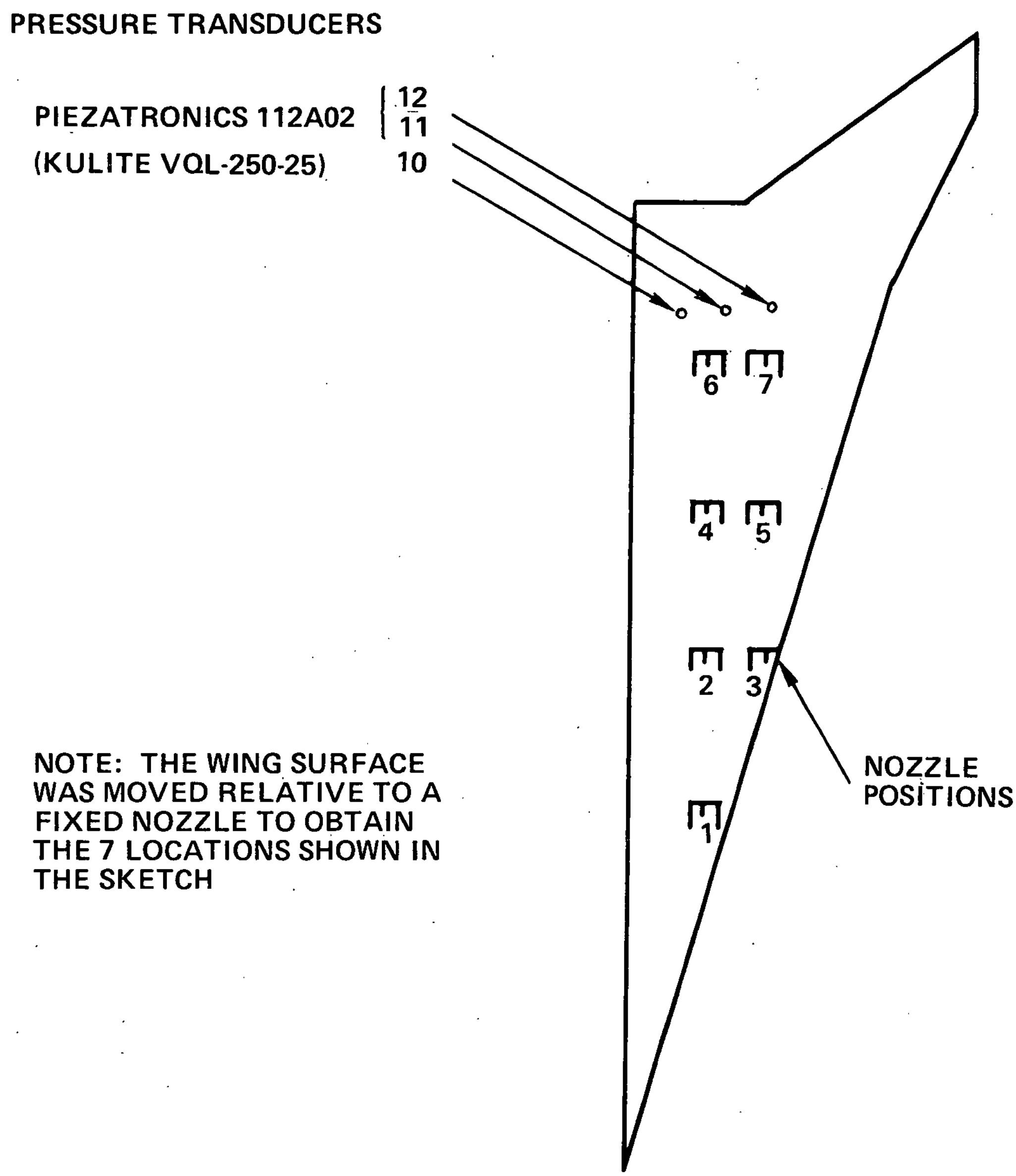

Figure 12. SCAT 15-F Sonic Environment Test Configuration

Finite Size of Sensing Element.-The sensing element for the Kulite and for the Piezatronics transducers was 6.35×10^{-3} and 5.537×10^{-3}m, respectively. Therefore, if the convection velocity (U_c) is considered to be 0.62 of the jet velocity, convection velocities for the Mach 2.5 (Vj = 550 m/s) and Mach 1.5 (Vj = 427 m/s) are 340 and 265 m/s, respectively. Correction values ($10 \log_{10} \phi_m/\phi$) for the 80 kHz upper frequency are:

	Mach 1.5 Nozzle		Mach 2.5 Nozzle	
	Kulite	Piezatronics	Kulite	Piezatronics
$\omega R/U_c$	6.05	5.27	4.70	4.1
ϕ_m/ϕ (Fig. 9)	0.0067	0.0103	0.0124	0.0136
$10 \log_{10} \frac{\phi_m}{\phi}$	-21.74 dB	-19.87 dB	-19.06 dB	-19.87 dB

As can be seen, the finite size effect for the transducers used for the SCAT 15-F test is large.

Dynamic Range.-The sonic environment on the wing surface of the SCAT 15-F model was estimated to be within a range of 100 to 160 dB. Table 2 shows that the dynamic range of the B&K 4138 microphone is 76 to 168 dB. However, the sonic environment may have exceeded the upper limit of the dynamic range and contributed to failure of the microphone. The dynamic range of the Piezatronics and Kulite transducers is suitable for the higher intensity environment encountered in the test.

Sensitivity of the Piezatronics transducers used for the SCAT 15-F model test were considered to be marginal for the range of pressures measured. Table 2 shows the lower limit of the dynamic range to be 131 dB. Therefore, internally generated noise of the measuring system may have affected the lower intensity noise level measurements. Frequency response calibrations were not available for either the Piezatronics or Kulite transducers and means were not available for performing them. Therefore, the response was assumed to be uniform with frequency.

Frequency Response.-Model scale for the SCAT 15-F model test was considered to be 0.03. Therefore, if the model jet velocity is considered to be equal to full-size engine jet velocity, $f_a = 0.03 \times f_m$ (see Section 4.1). Measured noise levels covered the frequency range from 50 to 80,000 Hz. Consequently, the corresponding full-scale frequency range was from 1.5 to 2400 Hz. It should be noted the the frequency range of interest for structural analyses (50 to 2000 Hz) is well within limits of the measured noise levels.

Data Storage.-The FM mode was used for recording the SCAT 15-F model test data. Data were recorded at 3.048 m/sec tape speed on a 432 kHz carrier. Time expansion was accomplished by playing back the tape at 0.38 m/sec on a 54 kHz carrier. Therefore, the 80-kHz frequency was reduced to 10 kHz, and it was possible to reduce the data with a spectral analyzer that had a 10-kHz upper frequency limit.

Data Reduction.-Upper-wing surface pressure data were recorded during the SCAT 15-F test runs 46P and 47P at Mach 2.5 and runs 20P, 31P, 32P, 33P, 36P, 37P, and 92P at Mach 1.5. The test parameters for each of the conditions are given in Table 3. The locations of microphones 10, 11, and 12 relative to the several jet locations used are shown in Figure 12. The initial data-reduction included one-third-octave-band analyses from 50 Hz to 80 kHz (Figure 13) and narrowband analyses from 50 to 80 kHz (Figure 14). Later the narrowband data were plotted for 50 to 16 kHz (Figure 15) in order to better resolve the frequency content.

In the process of reducing the data, a difference of 7.2 dB was noted between the pre- and post-calibration of the Kulite transducer (Location 10). These calibrations were recorded several days apart, and it was not readily apparent when the shift occurred. Calibrations were performed each day and used to verify the operation of each microphone system prior to each day of testing. However, the calibrations were not recorded on magnetic tape each

TABLE 3. SUMMARY OF TEST CONDITIONS

Run No.	Nozzle Location	Pressure Ratio	Nozzle Mach No.	Exit Velocity Meters/Second
31P	1	3.67	1.5	427
32P	2	3.67	1.5	427
33P	3	3.67	1.5	427
20P	4	3.67	1.5	427
92P	5	3.67	1.5	427
36P	6	3.67	1.5	427
37P	7	3.67	1.5	427
46P	6	1.70	2.5	550
47P	7	1.70	2.5	550

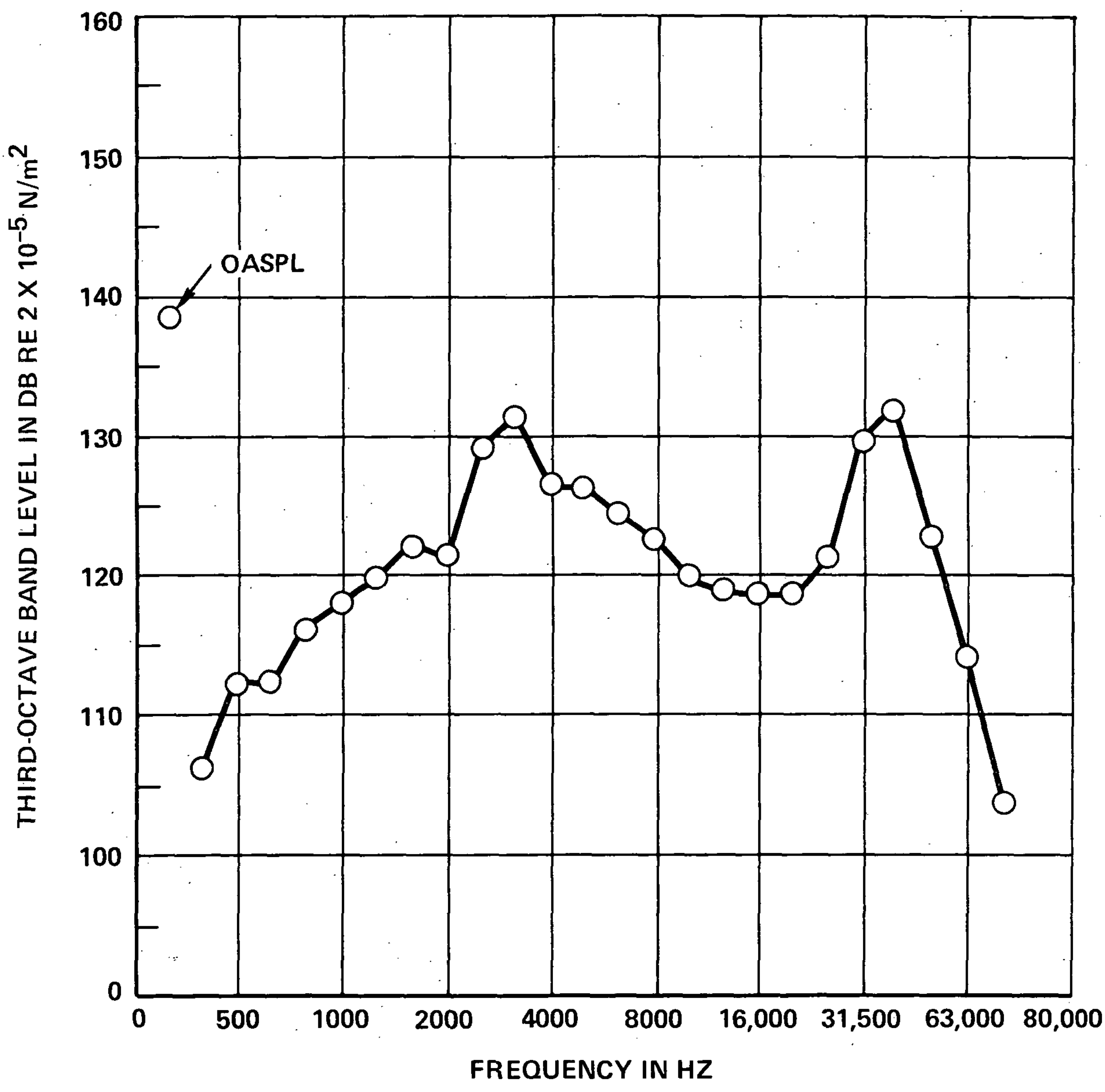

Figure 13. Typical One-Third-Octave-Band Spectrum

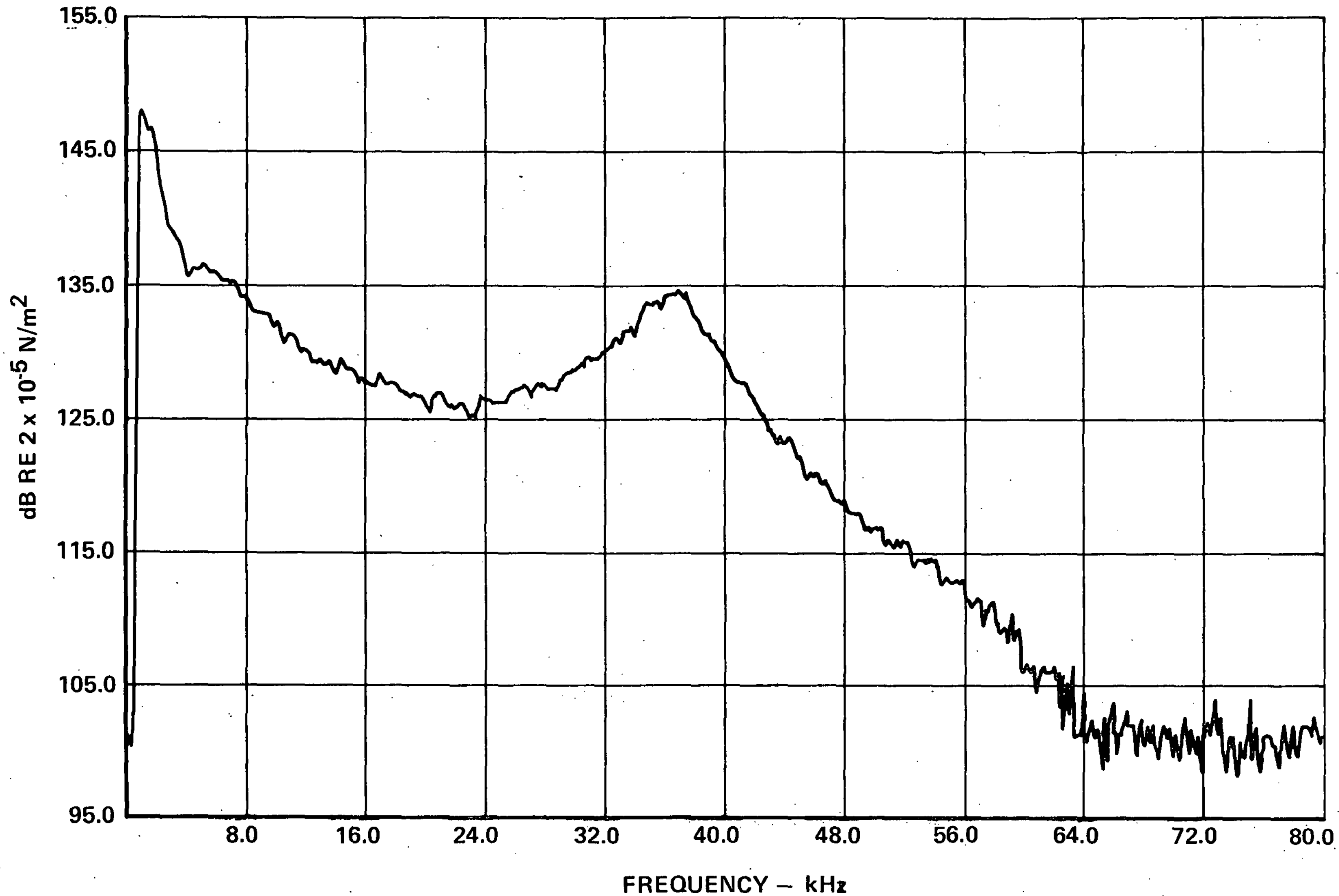

Figure 14. Typical Narrow Band Spectrum (50 to 80,000 Hz)

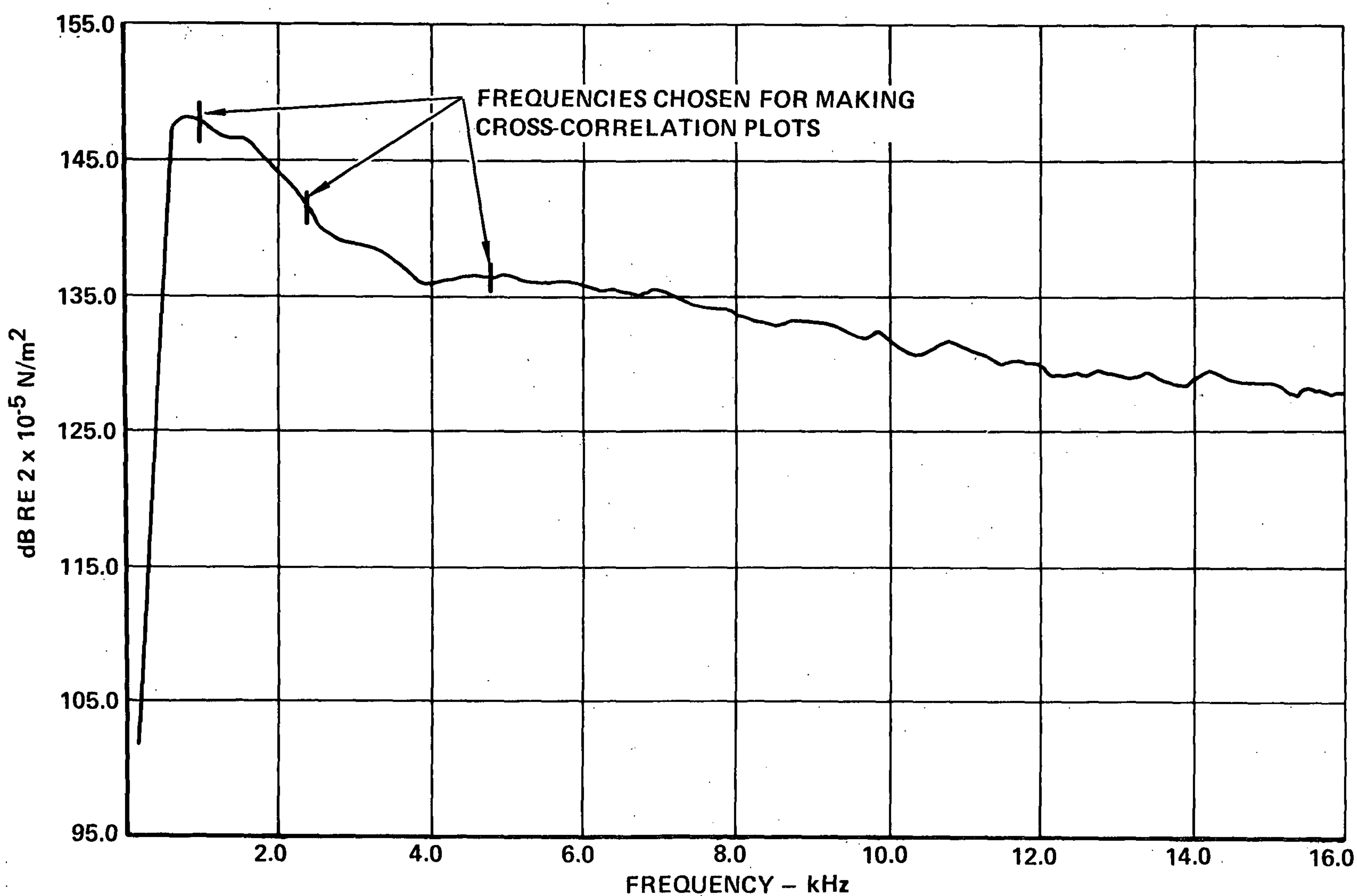

Figure 15. Typical Narrow Band Spectrum (50 to 16,000 Hz)

day, in the interest of completing all of the scheduled tests within the allotted time period. The change in calibration level was not noted until the post-calibration was recorded at completion of the test program. The calibration problem was investigated for the Mach 1.5 tests by plotting sound pressure level contours (Figure 16). First, the precalibration value was used and then the post-calibration value was used. The contours which assumed the precalibration value to be correct were disjointed, whereas, those which assumed the post-calibration value to be correct was smoother. The contours given in Figure 16 were constructed from the transducer data grid shown in Figure 17.

The narrow-band plots such as the one shown in Figure 15 were used to determine frequencies for making correlation plots. The frequencies chosen are given in Table 4. Typical autocorrelation and cross-correlation plots are shown in Figures 18 through 20. The plots are for run 31P at a 1000-Hz frequency. Figures 18 and 19 are the autocorrelation plots for transducers 11 and 12 respectively. Figure 20 is the cross-correlation plot for transducers 11 and 12. The ordinate of plots 18 through 20 are given in terms of linear dimensions that are proportional to pressure squared. Since the autocorrelation and cross-correlation curves are used only for computing normalized cross-correlation coefficients, the conversion factor for converting linear dimensions to pressure squared cancel out. Computation of the cross-correlation coefficient at the top of Figure 20 was accomplished by using the method illustrated in Figure 10. The narrow-band cross-correlation coefficients were determined for all of the frequencies defined in Table 4 in a similar manner. Tables 5 and 6 give the correlation summaries for the Mach 1.5 and 2.5 nozzles, respectively. The maximum correlation coefficient values given in column 5 are the $\rho_P(0,\eta,\tau,\omega)$ values that are used in Equation (7) to compute excitation cross-spectral density.

3.3 Methods for Improving Data Acquisition and Reduction

Improvements listed below are with reference to the SCAT 15-F model test program.

- A hot jet will better simulate a SST-type engine. Current SST engine concepts have exhaust velocities on the order of 823 m/s.
- The pressure transducers should have smaller sensing elements to improve high-frequency space resolutions.
- The transducer array should include longitudinal and lateral positions so that true convection velocities can be determined.

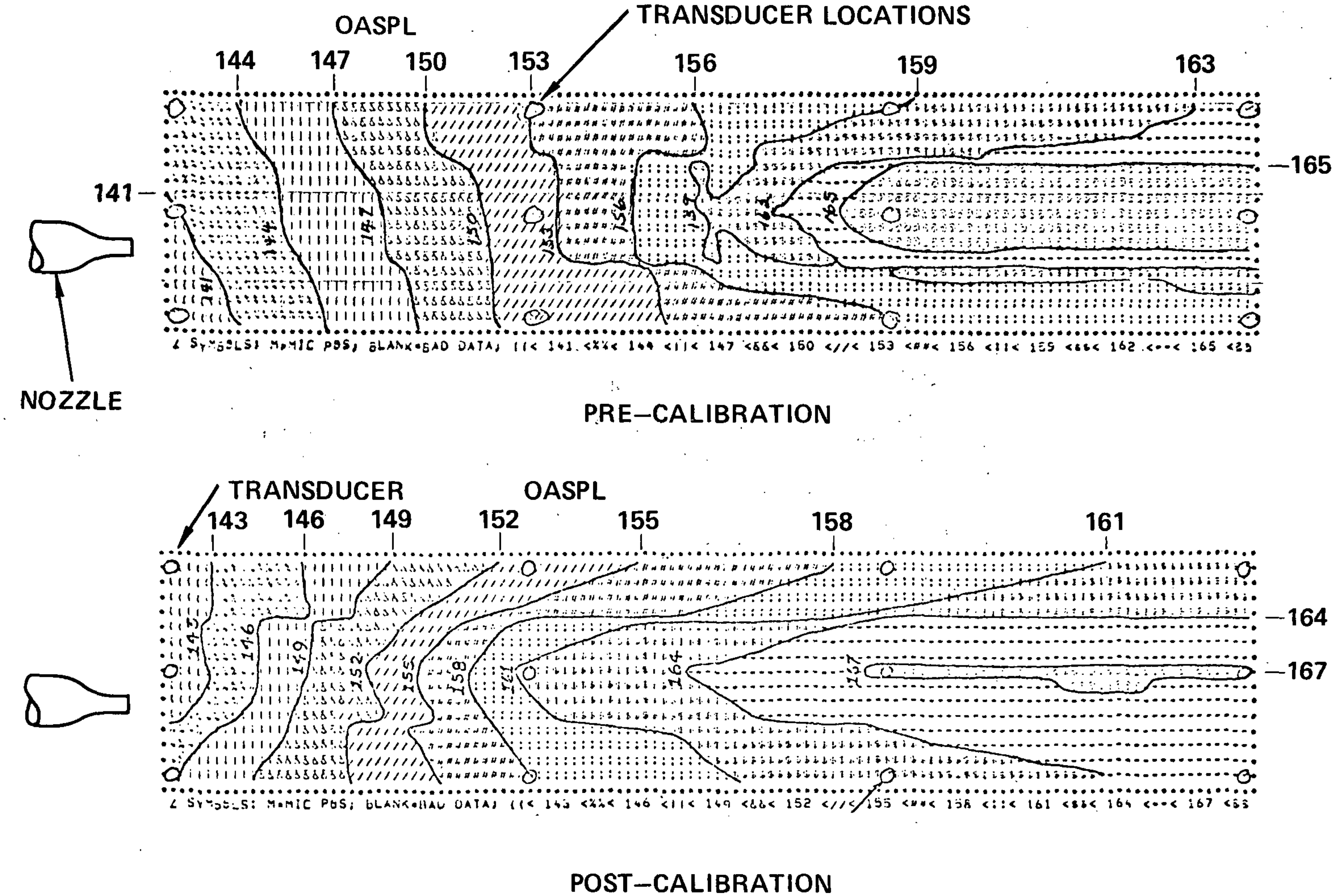

Figure 16. Comparison of Pre- and Post-Calibration OASPL Contours

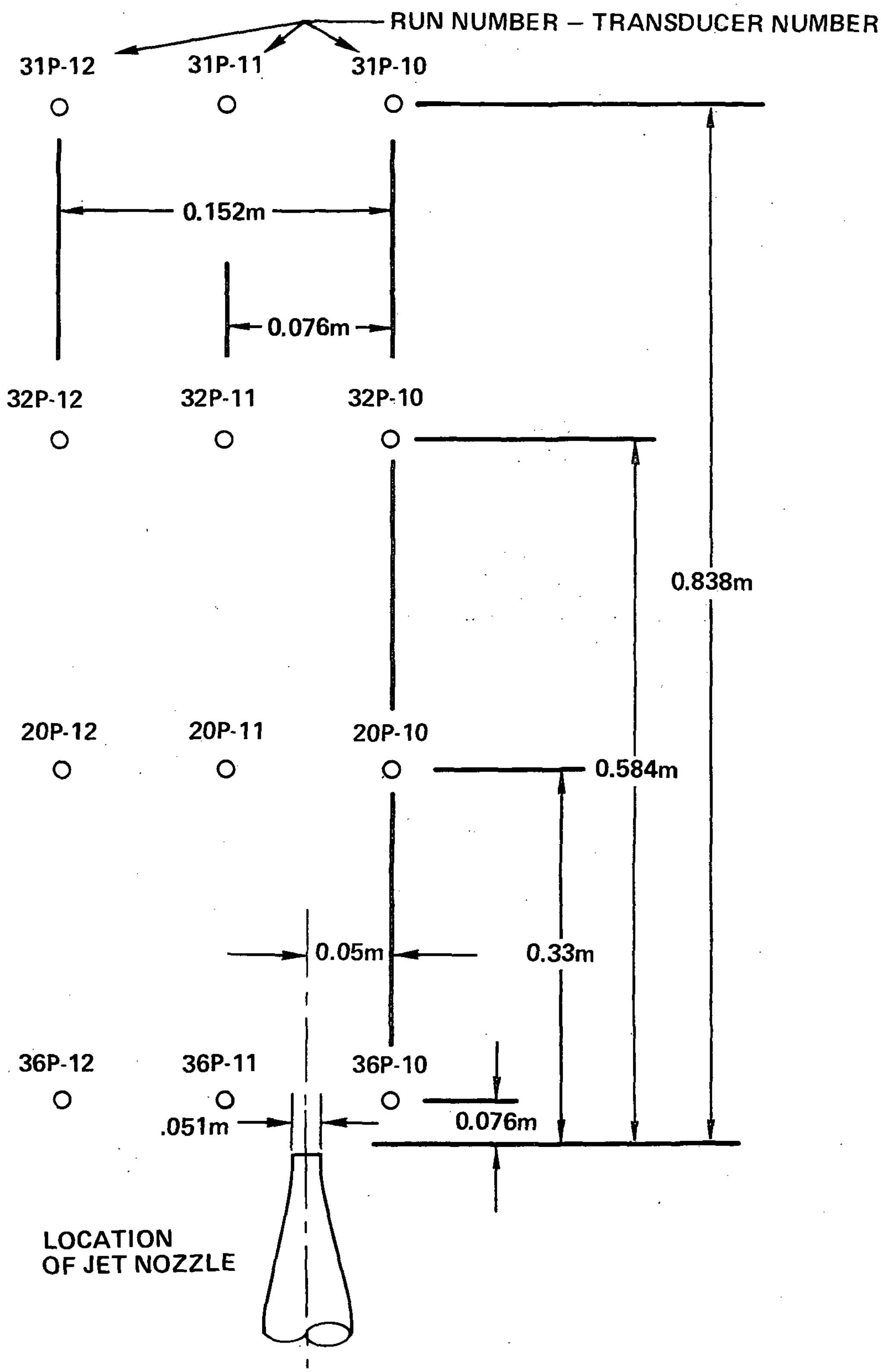

Figure 17. Contour Data Grid

TABLE 4. CORRELATION MATRIX

Run No.	Transducer A	Transducer B	Correlation Frequencies - kHz			
31P	11	12	1.0	2.4	4.8	
32P	11	12	1.0	2.4	4.8	
33P	12	10	1.0	2.4	4.8	
33P	12	11	1.0	2.4	4.8	
20P	11	12	1.0	2.4	4.8	
92P	12	11	1.0	2.4	6.6	
92P	12	10	1.0	2.4	6.6	
36P	11	12	1.5	2.4	6.6	
37P	12	11	1.0	2.4	6.6	15
37P	12	10	1.0	2.4	6.6	15
37P	11	10	1.0	2.4		
46P	11	12	1.0	6.6	9.0	15
47P	10	12	1.6	6.6	7.2	15
47P	11	12	1.6	6.6	7.2	15

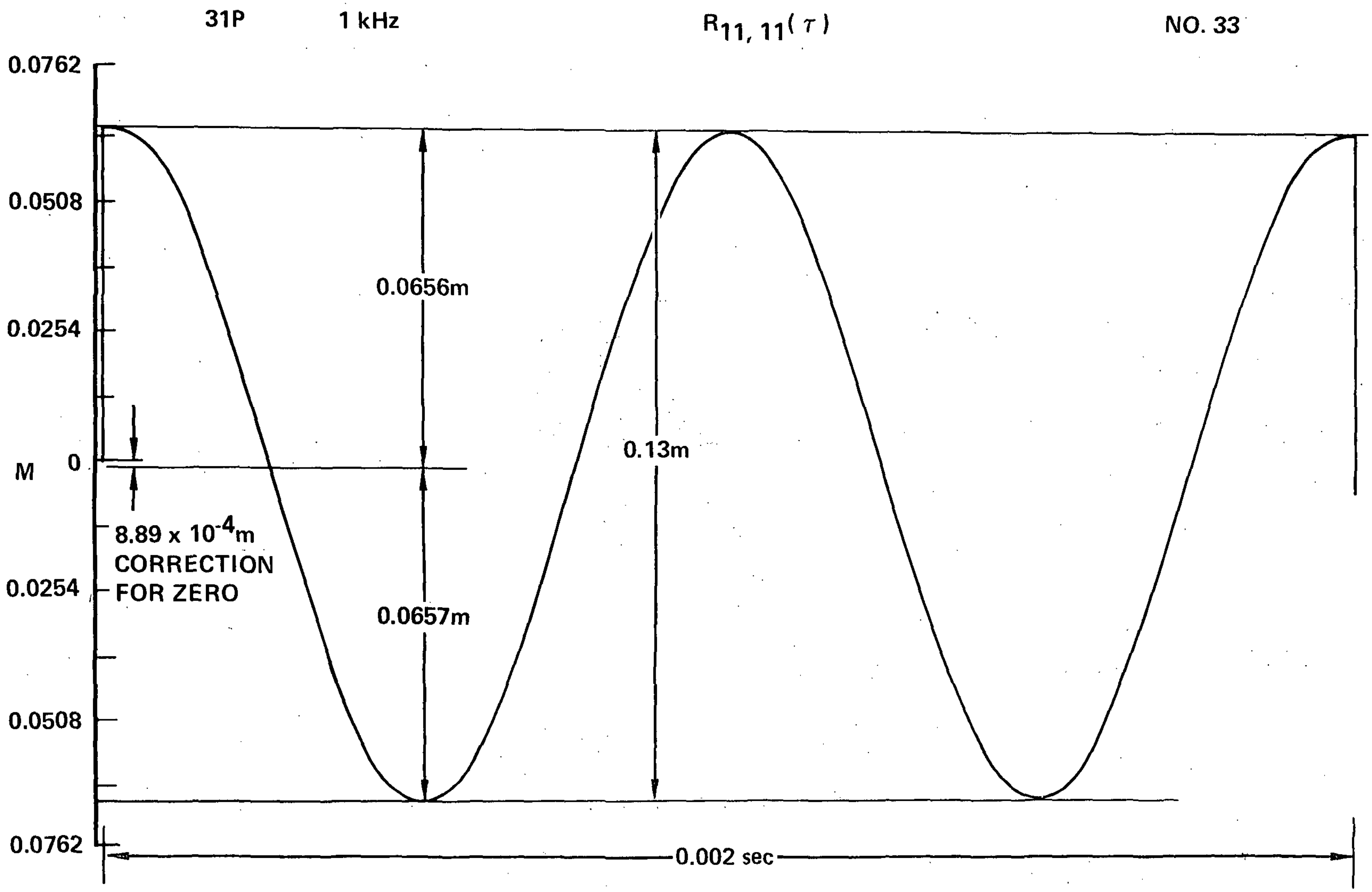

Figure 18. Autocorrelation Plot for Run 31P Transducer 11

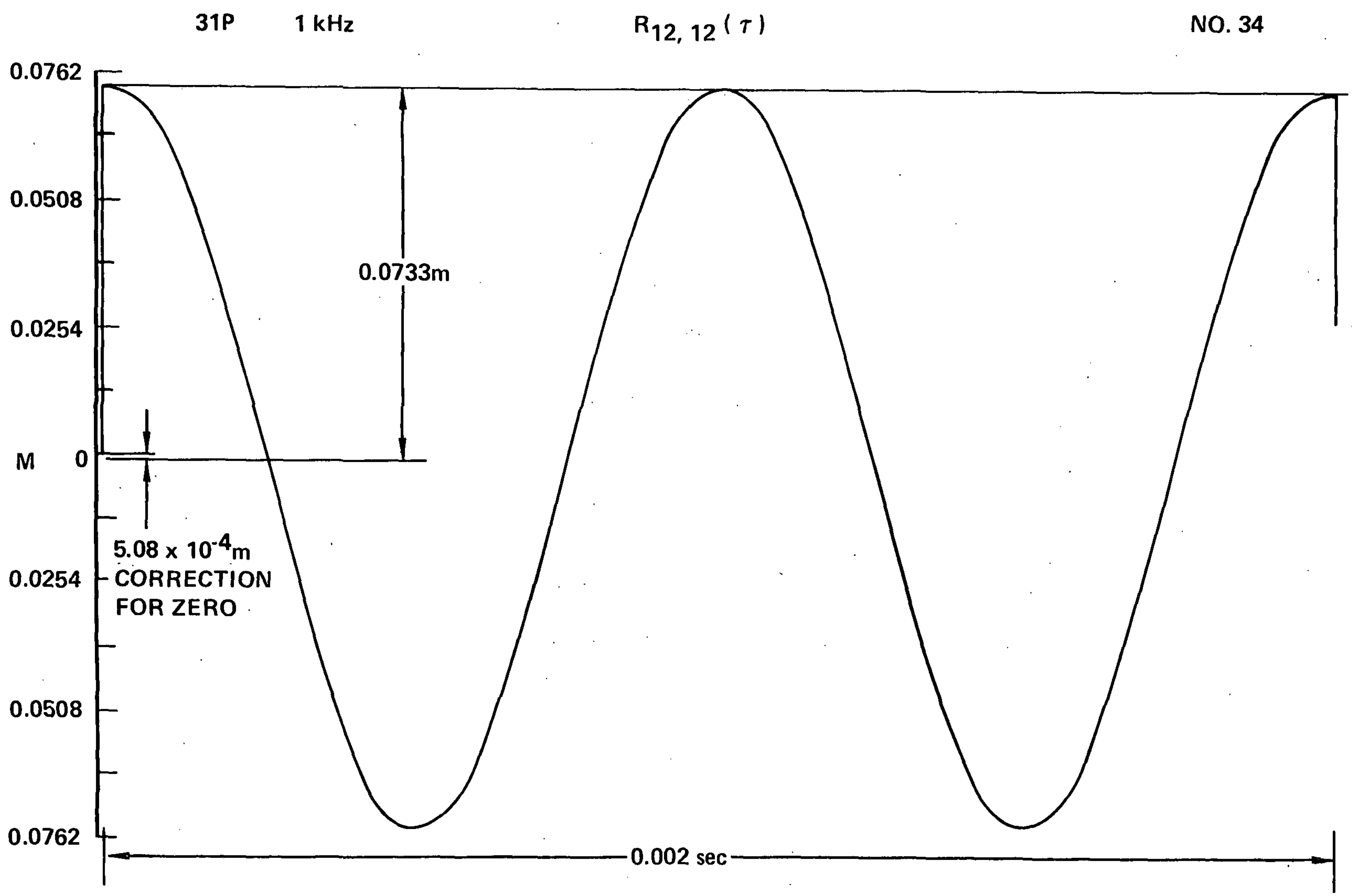

Figure 19. Autocorrelation Plot for Run 31P Transducer 12

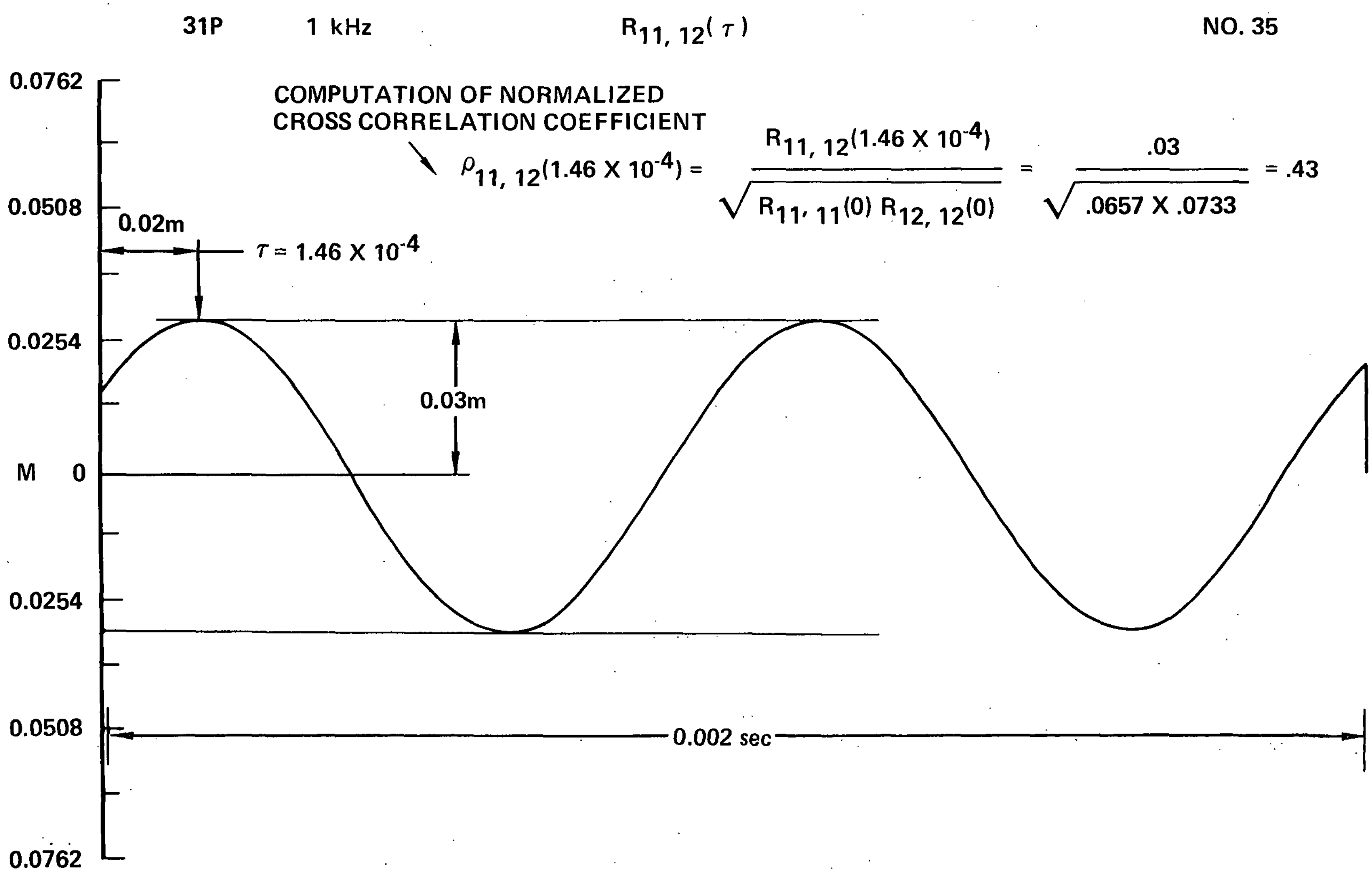

Figure 20. Cross-Correlation Plot for Run 31P Transducer 11 and 12

TABLE 5. MACH 1.5 NOZZLE CORRELATION SUMMARY

Run No.	Transducers	Correl. Freq (kHz)	Maximum Correlation Function (m)	Maximum Correlation Coefficient	Peak τ (sec)
31P	11-11	1	6.56×10^{-2}		0
	12-12		7.33×10^{-2}		0
	11-12		2.98×10^{-2}	0.43	1.46×10^{-4}
	11-11	2.4	2.71×10^{-2}		0
	12-12		3.70×10^{-2}		0
	11-12		7.49×10^{-3}	0.24	1.775×10^{-5}
	11-11	4.8	4.11×10^{-2}		0
	12-12		4.57×10^{-2}		0
	11-12		6.60×10^{-3}	0.15	1.96×10^{-4}
32P	11-11	1	7.32×10^{-2}		0
	12-12		6.86×10^{-2}		0
	11-12		3.86×10^{-2}	0.55	1.30×10^{-4}
	11-11	2.4	3.33×10^{-2}		0
	12-12		4.85×10^{-2}		0
	11-12		1.19×10^{-2}	0.30	0.65×10^{-4}
	11-11	4.8	5.51×10^{-2}		0
	12-12		8.28×10^{-2}		0
	11-12		1.22×10^{-2}	0.18	0.80×10^{-4}
33P	10-10	1	3.10×10^{-2}		0
	11-11		7.37×10^{-2}		0
	12-12		3.38×10^{-2}		0
	10-12		3.3×10^{-3}	0.10	4.2×10^{-4}
	11-12		7.37×10^{-3}	0.15	1.9×10^{-4}
	10-10	2.4	8.08×10^{-2}		0
	11-11		8.64×10^{-2}		0
	12-12		7.54×10^{-2}		0
	10-12		6.86×10^{-2}	0.09	0.65×10^{-4}
	11-12		2.21×10^{-2}	0.27	0.45×10^{-4}
	10-10	4.8	5.46×10^{-2}		0
	11-11		6.99×10^{-2}		0
	12-12		7.87×10^{-2}		0
	10-12		7.62×10^{-3}	0.12	1.9×10^{-4}
	11-12		2.54×10^{-3}	0.03	1.4×10^{-4}

TABLE 5. MACH 1.5 NOZZLE CORRELATION SUMMARY - Continued

Run No.	Transducers	Correl. Freq (kHz)	Maximum Correlation Function (m)	Maximum Correlation Coefficient	Peak τ (sec)
20P	11-11	1	6.85×10^{-2}		0
	12-12		6.46×10^{-2}		0
	11-12		2.24×10^{-2}	0.338	1.6×10^{-5}
	11-11	2.4	7.94×10^{-2}		0
	12-12		7.68×10^{-2}		0
	11-12		2.91×10^{-2}	0.372	6.9×10^{-5}
	11-11	4.8	2.92×10^{-2}		0
	12-12		3.49×10^{-2}		0
	11-12		1.27×10^{-3}	0.04	--
92P	10-10	1	3.87×10^{-2}		0
	11-11		7.94×10^{-2}		0
	12-12		6.20×10^{-2}		0
	10-12		1.07×10^{-2}	0.22	3.96×10^{-4}
	11-12		2.41×10^{-2}	0.44	--
	10-10	2.4	9.02×10^{-2}		0
	11-11		2.54×10^{-2}		0
	12-12		5.59×10^{-2}		0
	10-12		7.11×10^{-3}	0.10	1.97×10^{-4}
	11-12		4.32×10^{-3}	0.09	--
	10-10	6.6	3.86×10^{-2}		0
	11-11		5.64×10^{-2}		0
	12-12		5.08×10^{-2}		0
	10-12		2.79×10^{-3}	0.063	1.78×10^{-4}
	11-12		9.65×10^{-3}	0.18	1.83×10^{-4}
36P	11-11	1.5	4.38×10^{-2}		0
	12-12		4.85×10^{-2}		0
	11-12		1.47×10^{-2}	0.32	6.3×10^{-5}
	11-11	2.4	5.84×10^{-2}		0
	12-12		5.91×10^{-2}		0
	11-12		9.65×10^{-3}	0.16	2.82×10^{-4}
	11-11	6.6	4.94×10^{-2}		0
	12-12		2.71×10^{-2}		0
	11-12		8.89×10^{-3}	0.24	4.77×10^{-5}

TABLE 5. MACH 1.5 NOZZLE CORRELATION SUMMARY - Concluded

Run No.	Transducers	Correl. Freq (kHz)	Maximum Correlation Function (m)	Maximum Correlation Coefficient	Peak τ (sec)
37P	10-10	1.5	7.25×10^{-2}		0
	11-11		6.54×10^{-2}		0
	12-12		7.87×10^{-2}		0
	10-12		5.59×10^{-3}	0.074	0.0
	11-12		4.42×10^{-2}	0.616	0.0
	10-10	2.4	3.77×10^{-2}		0
	11-11		5.65×10^{-2}		0
	12-12		4.95×10^{-2}		0
	10-12		2.10×10^{-2}	0.485	1.66×10^{-4}
	11-12		2.92×10^{-2}	0.719	1.65×10^{-4}
	10-10	6.6	7.68×10^{-2}		0
	11-11		6.44×10^{-2}		0
	12-12		2.07×10^{-2}		
	10-12		2.79×10^{-3}	0.07	6.59×10^{-5}
	11-12		3.81×10^{-3}	0.104	8.63×10^{-5}
	10-10	15	5.84×10^{-2}		0
	11-11		7.24×10^{-2}		0
	12-12		4.76×10^{-2}		0
	10-12		1.27×10^{-3}	0.02	-
	11-12		2.54×10^{-3}	0.04	-
Repeat 37P	10-10	1.5	8.89×10^{-2}		0
	11-11		4.83×10^{-2}		0
	10-11		3.30×10^{-2}	0.54	6.12×10^{-4}
	10-10	2.4	3.45×10^{-2}		0
	11-11		4.72×10^{-2}		0
	10-11		1.52×10^{-2}	0.38	1.3×10^{-4}

TABLE 6. MACH 2.5 NOZZLE CORRELATION SUMMARY

Run No.	Transducers	Correl. Freq (kHz)	Maximum Correlation Function (m)	Maximum Correlation Coefficient	Peak τ (sec)
46P	11-11	1	8.00×10^{-2}		0
	12-12		4.60×10^{-2}		
	11-12		4.65×10^{-2}	0.77	2.5×10^{-4}
	11-11	6.6	7.11×10^{-2}		
	12-12		7.70×10^{-2}		
	11-12		4.83×10^{-2}	0.65	$.9 \times 10^{-4}$
	11-11	9	4.34×10^{-2}		
	12-12		3.05×10^{-2}		
	11-12		1.27×10^{-2}	0.35	1.02×10^{-4}
	11-11	15	7.77×10^{-2}		
	12-12		4.57×10^{-2}		
	11-12		6.25×10^{-3}	0.11	0.6×10^{-5}
47P	10-10	1.6	4.11×10^{-2}		
	11-11		1.85×10^{-2}		
	12-12		8.81×10^{-2}		
	10-12		2.41×10^{-2}	0.40	2.3×10^{-4}
	11-12		2.11×10^{-2}	0.52	1.2×10^{-4}
	10-10	6.6	1.80×10^{-2}		
	11-11		4.11×10^{-2}		
	12-12		3.84×10^{-2}		
	10-12		6.35×10^{-3}	0.24	0.6×10^{-4}
	11-12		3.30×10^{-3}	0.08	0.5×10^{-4}
	10-10	7.2	2.77×10^{-2}		
	11-11		6.60×10^{-2}		
	12-12		3.48×10^{-2}		
	10-12		3.30×10^{-3}	0.11	3.3×10^{-4}
	11-12		2.46×10^{-2}	0.51	5.6×10^{-4}
	10-10	15	3.33×10^{-2}		
	11-11		2.36×10^{-2}		
	12-12		3.89×10^{-2}		
	10-12		5.08×10^{-3}	0.14	0.4×10^{-4}
	11-12		1.09×10^{-2}	0.36	0.6×10^{-4}

- The transducer systems should be phase synchronized, and calibrations should be recorded at the beginning and end of each day's testing.
- A sufficient number of transducers should be available so that measurements can be made in and adjacent to the jet flow stream.

4. TASK III - DATA SCALING

4.1 Scaling Procedures

A literature search (Appendix B) failed to produce a procedure that appears to be more representative of current technology for scaling model data to full-scale aircraft sonic environments than the procedure discussed in the following paragraphs.

Frequency scaling is accomplished by considering the Strouhal number of the model flow field to be equal to the Strouhal number of the aircraft flow field Equation (11).

$$\frac{f_m D_m}{\left(V_j\right)_m} = \frac{f_a D_a}{\left(V_j\right)_a} \qquad (11)$$

f_m = model noise data frequency

D_m = model nozzle diameter

$\left(V_j\right)_m$ = model jet velocity

f_a = aircraft sonic environment frequency

D_a = aircraft engine nozzle diameter

$\left(V_j\right)_a$ = aircraft engine jet velocity

Equation (11) can be solved for f_a to obtain the aircraft sonic environment frequency that corresponds to a designated model noise data frequency, Equation (12).

$$f_a = f_m \left[\frac{\left(V_j\right)_a}{\left(V_j\right)_m} \times \frac{D_m}{D_a}\right] \qquad (12)$$

The ratio (D_m/D_a) is equal to the model scale. Therefore, when the model jet velocity is equal to the aircraft engine jet velocity (which is generally the case), the frequency is accomplished by a simple equation, Equation (13)

$$f_a = f_m \times \text{Model Scale} \qquad (13)$$

Amplitude scaling is easily accomplished when flow velocity and temperature of the model jet simulate the full-scale jet. Model sound pressure levels (SPL_m) need only to be corrected for pressure transducer sensing element size (Ref. 33) to obtain actual full-scale sound pressure levels (SPL_a). Therefore, scaling is accomplished by using Equation (14).

$$SPL_a = SPL_m + 10 \log_{10} \phi m/\phi \tag{14}$$

The value of ϕ_m/ϕ is determined from Figure 9. Distance from the nozzle exit to a location on the aircraft that corresponds to the model measurement location is given by Equation (15).

$$R_a = \left(\frac{D_a}{D_m}\right)(R_m) \tag{15}$$

R_a = distance from a point at the centerline of the aircraft engine nozzle exit plane to the sonic environment location of interest

D_a = diameter of aircraft nozzle

D_m = diameter of model nozzle

R_m = distance from a point at the centerline of the model nozzle exit plane to the pressure transducer location

When the model jet velocity and temperature do not simulate full-scale jet operating conditions, additional terms are required in the scaling equation. These addition terms are defined in Equation (16).

$$SPL_a = SPL_m + 10 \log_{10} \frac{\phi_m}{\phi} + K \log \frac{\left(V_j\right)_a}{\left(V_j\right)_m} + 10 \log_{10} \left(\frac{\rho_a}{\rho_m}\right) \tag{16}$$

K = Constant (80 for $V_j \leq 610$ m/sec and
30 for $V_j > 610$ m/sec)

The third and fourth terms in Equation (16) must be scrutinized. Since the sonic environment on a panel immersed in a jet flow stream is a combination of hydrodynamic and acoustic pressure fluctuations, a unified scaling equation must account for both phenomena at all points in and adjacent to the jet flow field. Such an equation has not been developed to date. Therefore, Equation (16) is a provisional equation that has been defined in order to scale the SCAT 15-F data to full-scale supersonic transport engine operating conditions. The velocity and density terms are based on methods for predicting acoustic power of free jets as defined in References 35 and 36. The basic assumption made to derive Equation (16) was that acoustic pressure fluctuations have a greater impact than hydrodynamic pressure fluctuations on the sonic environment of a panel immersed in the flow field of a high temperature supersonic jet. If the hydrodynamic flow field is considered to have a predominant impact on the sonic environment, the sound pressure levels will be a function of dynamic pressure (q). The relation normally used is SPL=20 log q + constant. Therefore, since $q=1/2\ \rho V_j^2$, the scaling equation will be in terms of velocity to the fourth power. Reference 37 shows that the sonic environment of surfaces immersed in a jet flow stream increases according to V^4. The relative importance of acoustic and hydrodynamic pressure fluctuations will not be pursued further in this report. However, a computer program has been developed (Appendix C) based on Equation (16) and is subsequently evaluated in Section 4.2.

4.2 Comparison of Scaled Model Data and Full Scale Aircraft Date

The literature search (Appendix B) did not result in finding a corresponding set of model and full-scale aircraft data that is pertinent to sonic environment in a supersonic jet flow stream. However, subsonic jet data was available for the following three aircraft.

- S-3A (Refs. 38 and 39)
- L-1011 (Refs. 39 and 40)
- V/STOL (Ref. 41)

The full-scale sonic environment data for the V/STOL aircraft were obtained from unpublished data that were provided by Langley Research Center.

To compile the model test data in a format for input to the computer program, the following information must be available.

- Model Data: scafac, ttmr, ptmi, dmi, mixm, rmi, trim fm, spℓm
- Aircraft Data: ttar, pra, wa, mixa, tria

- Atmospheric Data: psi

  scafac = model scale factor

  ttmr = total temperature of model jet - deg R

  ptmi = total pressure upstream of the nozzle - lb/in^2

  dmi = model nozzle diameter (exit) - in.

  mixm = fuel/air mixture of model jet

  rmi = distance from model nozzle exit to pressure transducer - in.

  trim = diameter of pressure transducer sensing element (model test) - in.

  fm = model frequency band center frequency - Hz

  spℓm = sound pressure levels corresponding to fm - dB

  ttar = total temperature of engine jet - deg R

  pra = engine nozzle pressure ratio

  wa = engine exhaust flow - lb/sec

  mixa = engine exhaust fuel/air ratio

  tria = diameter of pressure transducer sensing element (Full scale test) - in.

  psi = atmospheric pressure - lb/in^2

Several problems were found to exist in compiling the required input data. These included.

- Sufficient information was not reported with regard to propulsion, geometry, and instrumentation.
- Decisions had to be made regarding the relative importance of the core and bypass jet streams
- Spectra that was expressed in terms of spectral density had to be converted to third octave band data.
- Range of the frequency spectrum was too small
- Validity of test data could not be assessed.

The data compiled in Table 7 were determined to be the best available and were used for scaling the model data to full-scale conditions.

Figure 21 shows location of the pressure transducers for the S-3A. The locations were similar for the model and aircraft. Figures 22, 23 and 24 show the measured model data, measured aircraft data and scaled sonic environment for pressure transducer locations 1, 2 and 3, respectively.

Figure 25 shows the transducer location for the L-1011 tests and Figure 26 shows the comparison between scaled and measured noise.

Figures 27 and 28 give the geometrical and noise data for a V/STOL aircraft with lower surface blowing of the flaps by the jet stream.

The S-3A and L-1011 model jets simulated full-scale aircraft engine characteristics. Therefore, velocity and density terms in Equation (16) have a minimal effect on noise scaling. Consequently, scaling of the model data is accomplished according to Equations (13) and (14) for the frequency and amplitude respectively. Figures 22 through 24 and Figure 26 show that the scaled noise spectrum has approximately the same shape and magnitude as the measured model spectrum and has a frequency shift that is proportional to the model scale factor. Pressure transducers 1 and 3 on the S-3A aircraft (Figure 21) and the transducer on the L-1011 aircraft (Figure 25) are believed to be in the jet flow stream whereas the number 2 S-3A transducer is outside of and adjacent to the flow stream. Observation shows that the scaled model spectrum for the No. 2 S-3A transducer agrees reasonably well in shape and magnitude with the measured full-scale data whereas the scaled-model spectra in Figures 22, 24 and 26 are not representative of the full-scale measured spectra. Comparison of the scaled spectra with full-scale measured data does not show any specific trend regarding shape, peak frequencies or magnitude.

Scaling of the V/STOL transducer data (Figure 28) for the transducer location shown in Figure 27 involved accounting for velocity and density differences in model and full-scale jets. Figure 28 shows that the scaled model data is significantly higher than the full-scale measured data.

Discrepancies between the scaled model data and full-scale measured data may be attributed to several factors. These factors include:

- The models and full-size engines had coaxial nozzles and bypass jet parameters were used to scale the data
- Noise measurements were made by different investigators which used different types of instrumentation and had different test environments.
- The compatible model and full-size aircraft data that were available for evaluating the prediction method were for subsonic jets whereas the scaling equation was developed for supersonic jets.

TABLE 7. COMPUTER PROGRAM INPUT DATA

	S-3A						L-1011		V/STOL	
	LOC 1		LOC 2		LOC 3					
scafac			0.143				0.05		0.185	
ttmr			537				537		537	
ptmi			20.8				22.2		22.2	
dmi			4.2				2.88		6.95	
mixm			0				0		0	
rmi	8		18		30		11.5		30.5	
trim			0.25				0.25		0.218	
ttar			593				620		1,515	
pra			1.42				1.49		1.5	
wa			411				1,159.5		333.5	
mixa			0				0		0.033	
tria			0.25				0.25		0.5	
psi			14.7				14.7		14.7	
n	fm	splm	fm	splm	fm	splm	fm	splm	fm	splm
1	250	142.7		132.2		130.7	1,250	126.4	315	144.1
2	315	143.6		132.3		127.5	1,600	126.2	400	144.9
3	400	145.1		132.5		125.4	2,000	125.3	500	145.6
4	500	145.6		130.2		121.8	2,500	125.3	630	145.4
5	630	146.4		128.2		120.4	3,150	124.2	800	145.1
6	800	146.3		126.2		119.5	4,000	123.2	1,000	144.9
7	1,000	146.8		125.0		120.0	5,000	122.0	1,250	144.7
8	1,250	147.1		124.4		120.5	6,300	120.2	1,600	143.8
9	1,600	146.2		123.3		120.4	8,000	119.0	2,000	143.9
10	2,000	145.5		122.1		120.0	10,000	117.0	2,500	143.0
11	2,500	144.5		120.0		119.5	0	0	3,150	142.3
12	3,150	142.8		118.2		117.9	0	0	4,000	141.0
13	4,000	141.5		117.0		117.8	0	0	5,000	139.0
14	5,000	139.8		116.2		116.4	0	0	6,300	137.8
15	6,300	138.6		115.0		115.3	0	0	8,000	136.2
16	8,000	136.6		114.0		113.4	0	0	10,000	133.0
17	10,000	134.2		112.4		110.5	0	0	12,500	129.2
18	0	0		0		0	0	0	16,000	125.5
19	0	0		0		0	0	0	20,000	121.6
20	0	0		0		0	0	0	25,000	116.3
⋮	0	0		0		0	0	0	31,500	112.0
24	0	0		0		0	0	0	40,000	110.0

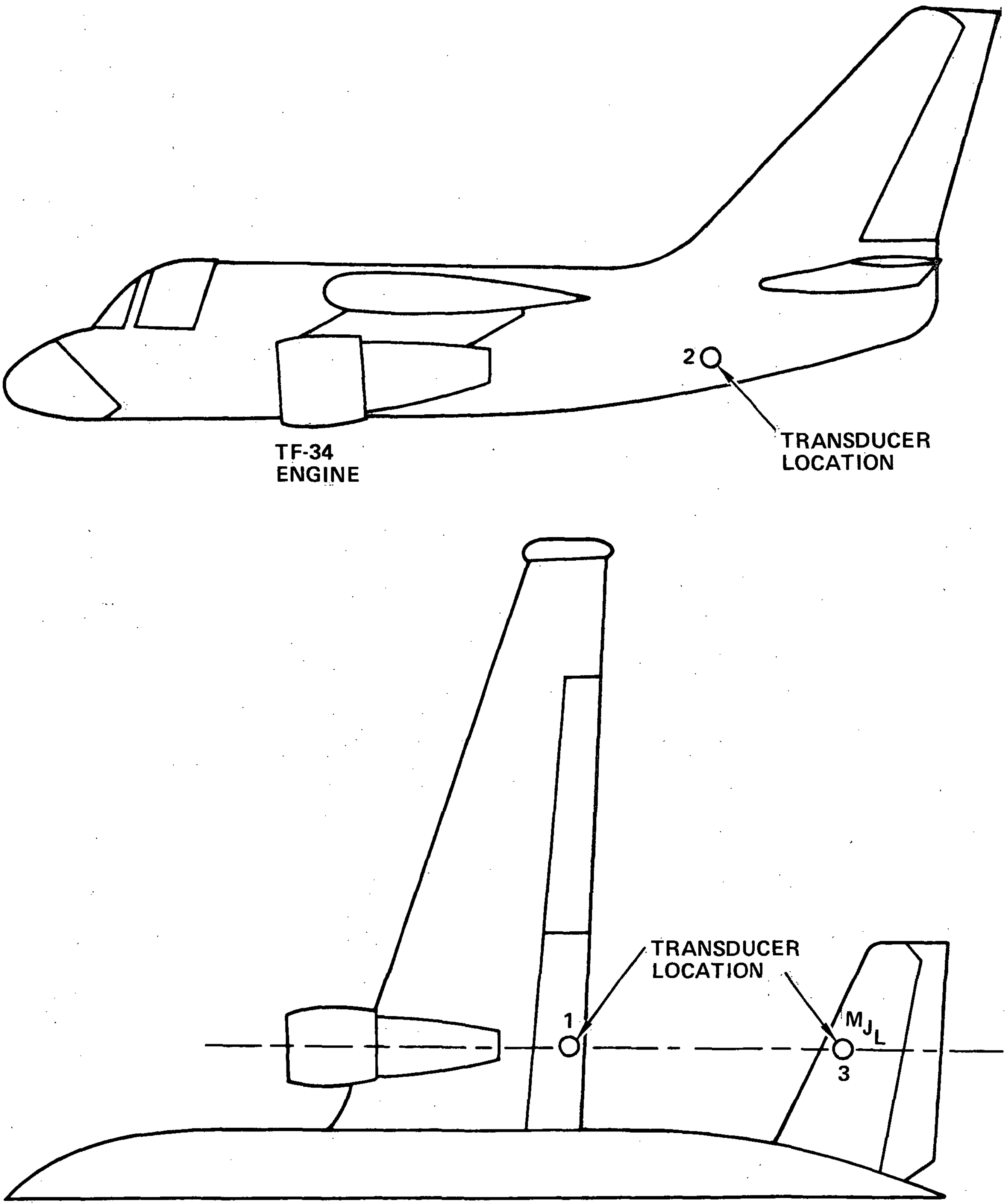

Figure 21. S-3A Measurement Locations

THE COMPUTER PRINTOUT SHOWING THE MODEL SPECTRA, FULL SCALE SPECTRA, AND SCALED SPECTRA FOR FIGURES 22, 23, 24, 26 AND 28 ARE GIVEN IN APPENDIX C.

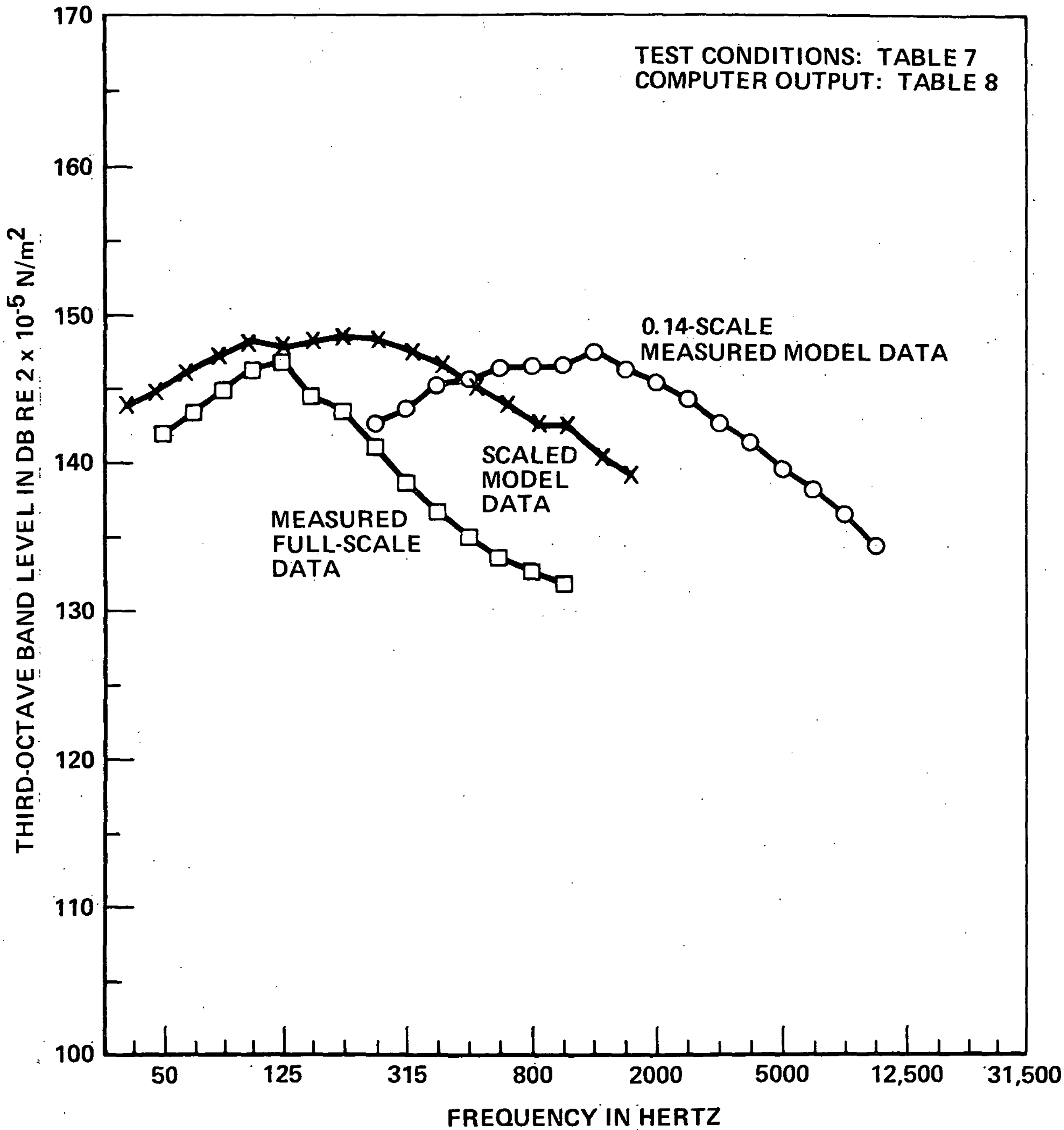

Figure 22. S-3A Spectra - Location 1

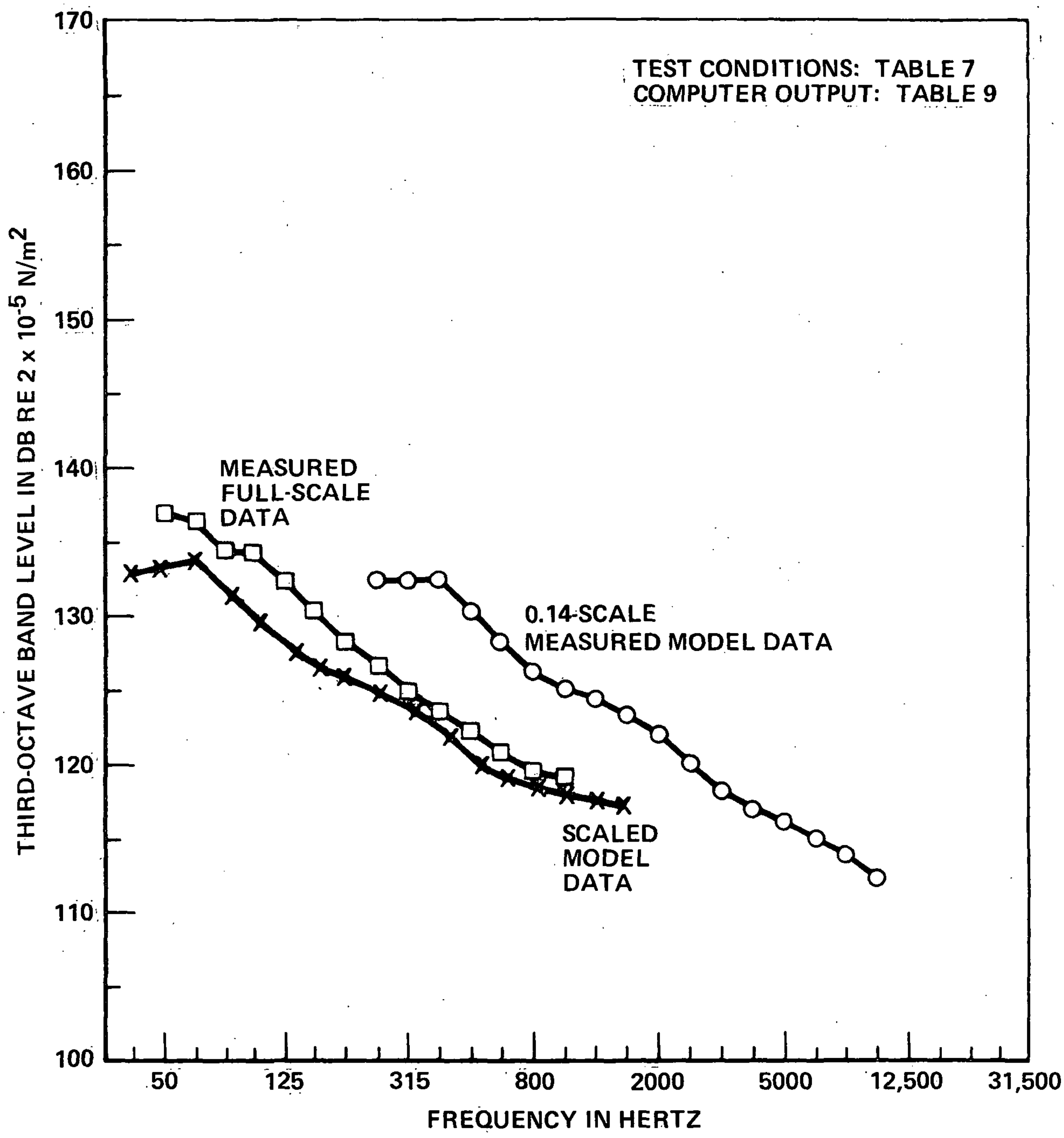

Figure 23. S-3A Spectra - Location 2

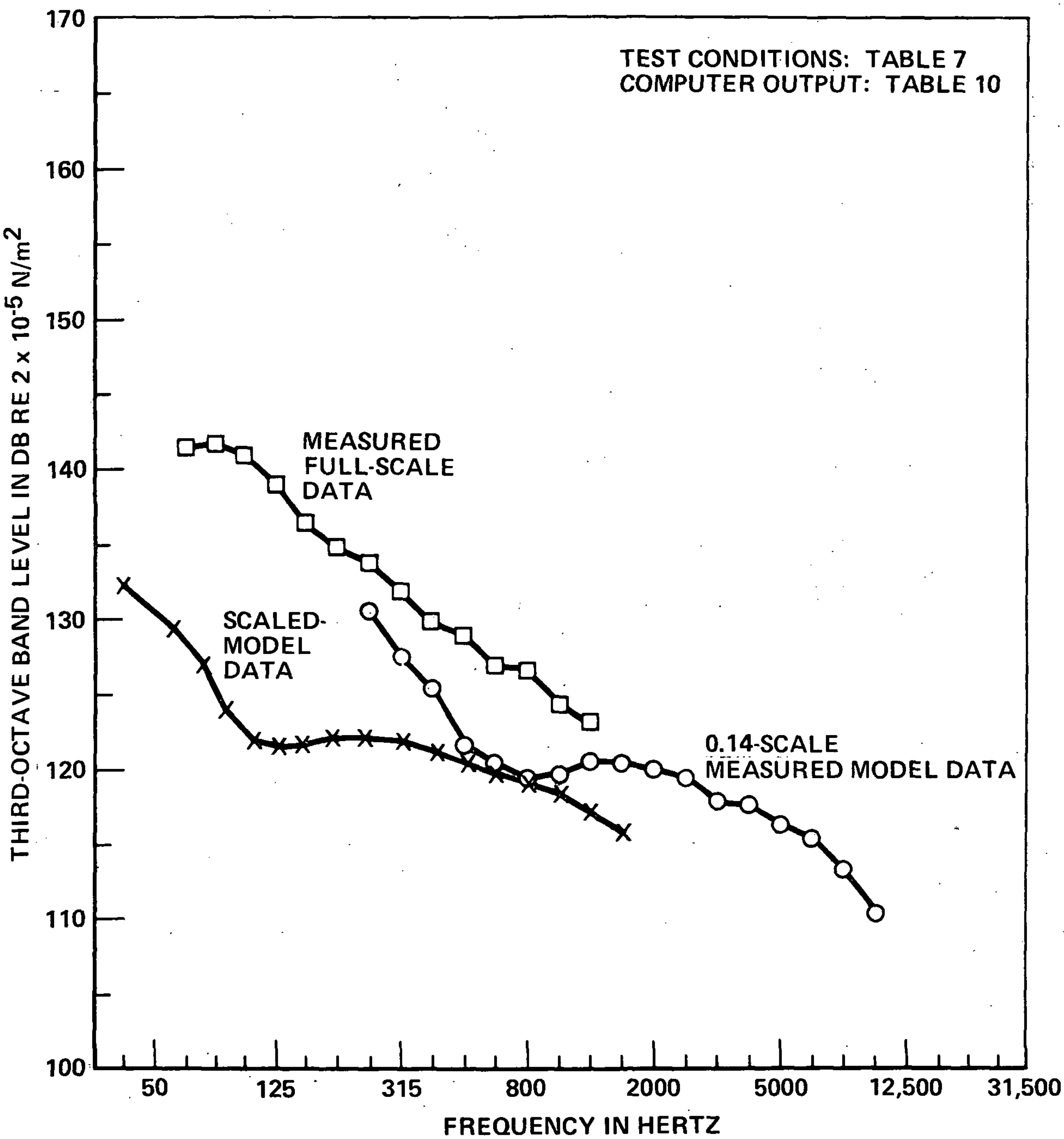

Figure 24. S-3A Spectra - Location 3

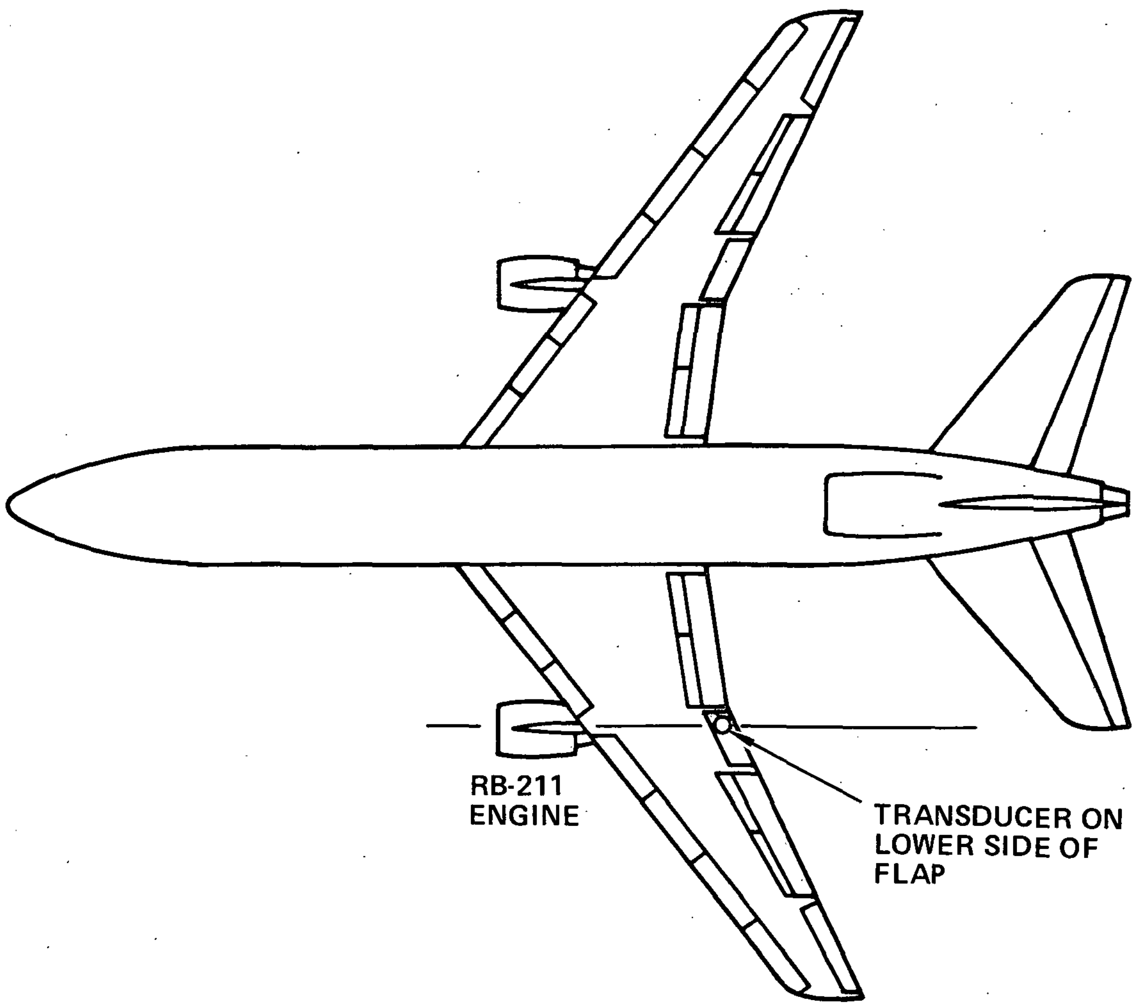

Figure 25. L-1011 Measurement Location

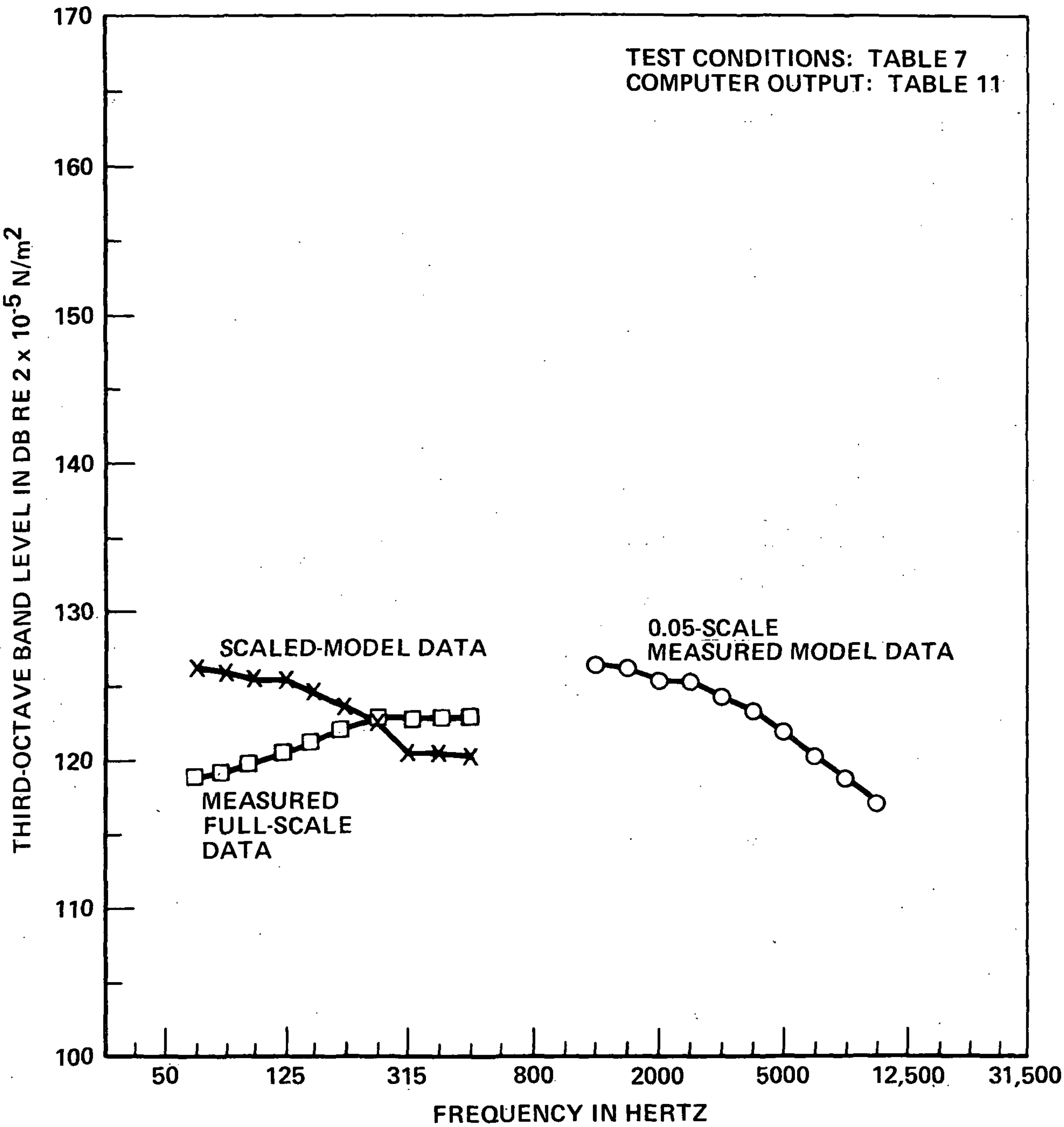

Figure 26. L-1011 Spectra

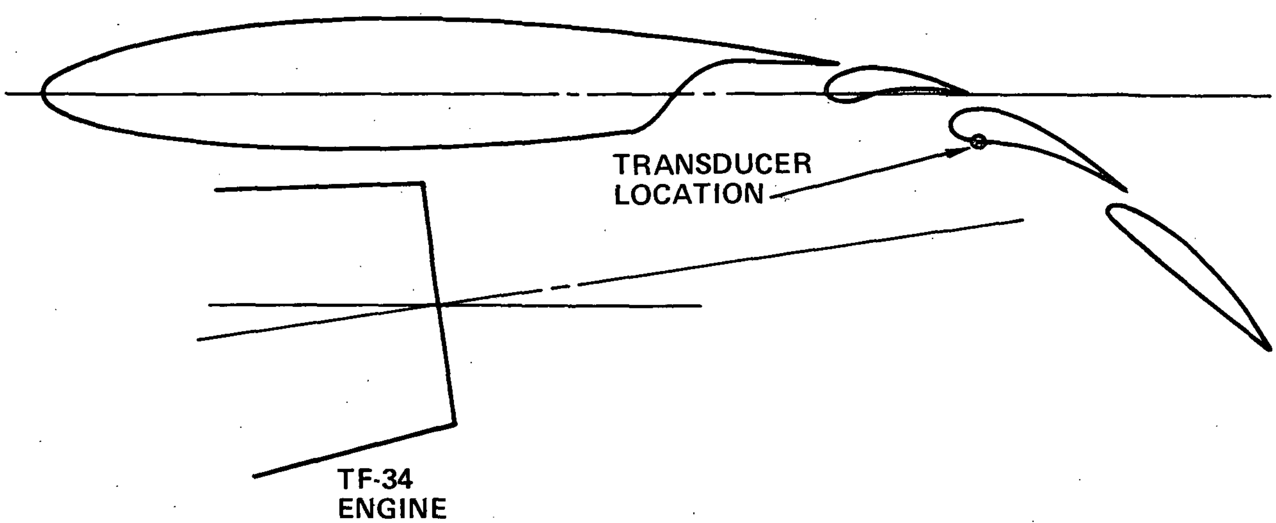

Figure 27. V/STOL Measurement Locations

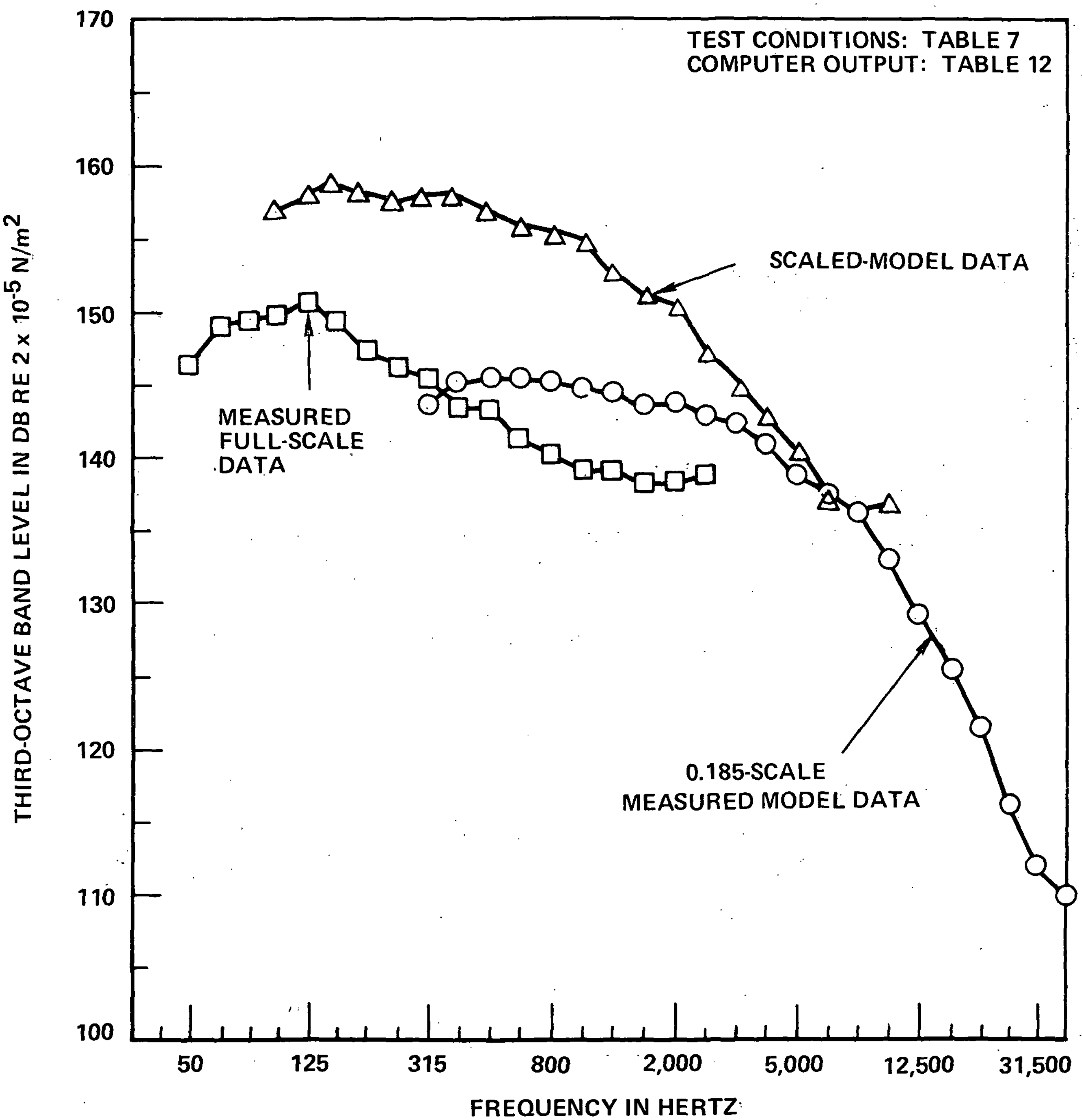

Figure 28. V/STOL Spectra

4.3 SCAT 15-F Scaled Model Data

Inability to accurately scale the data in Section 4.2 may be due to the complex confluent flow field of the coaxial jets. Therefore, even with the limitations of the SCAT 15-F model test data (see Section 3.3), scaling of the data to full size aircraft dimensions should provide some insight as to the severity of the sonic environment for a SST with over-the-wing engine installations. Figure 29 gives a comparison of SCAT 15-F measured model data with scaled spectra for a realistic SST engine. The spectra plotted are for run number 31P transducer 10. Model data and scaled spectra are given in Table 15 of Appendix D along with model and full scale engine operating characteristics. Table 15 shows model velocity and full-scale engine velocity to be 440 m/s (1450.5 ft/s) and 845 m/s (2766 ft/s), respectively. This differential velocity has a significant impact on the scaled noise level, see Equation (16). The computed value, because of decreased density for the full-scale engine jet, is shown in Table 15 to be -6.68 dB. Comparison for other run numbers and transducer locations could be made by plotting values given in Tables 16 through 30.

Figure 30 shows scaled OASPL contours on the wing surface of an arrow wing for Mach 1.5 nozzle cold jet test conditions. This is the same contour plot that is given in Figure 16. Maximum OASPL values occur approximately 22 meters downstream of the nozzle exit. Since the scaled-nozzle diameter is 1.69 meters, the ratio of downstream distance to nozzle diameter is 13.

OASPL contour plots were not made for the scaled SST engine operating conditions. However, Figure 31 gives a point-by-point comparison of scaled Mach-1.5 nozzle data and realistic SST engine OASPL values. Differences in the Mach 1.5 scaled OASPL values and realistic SST engine OASPL values range from 6 to 20 dB because of sensitivity of the scaling method to spectrum shape. The peak sonic environment level for the wing structure is shown to have an OASPL value of 181 dB.

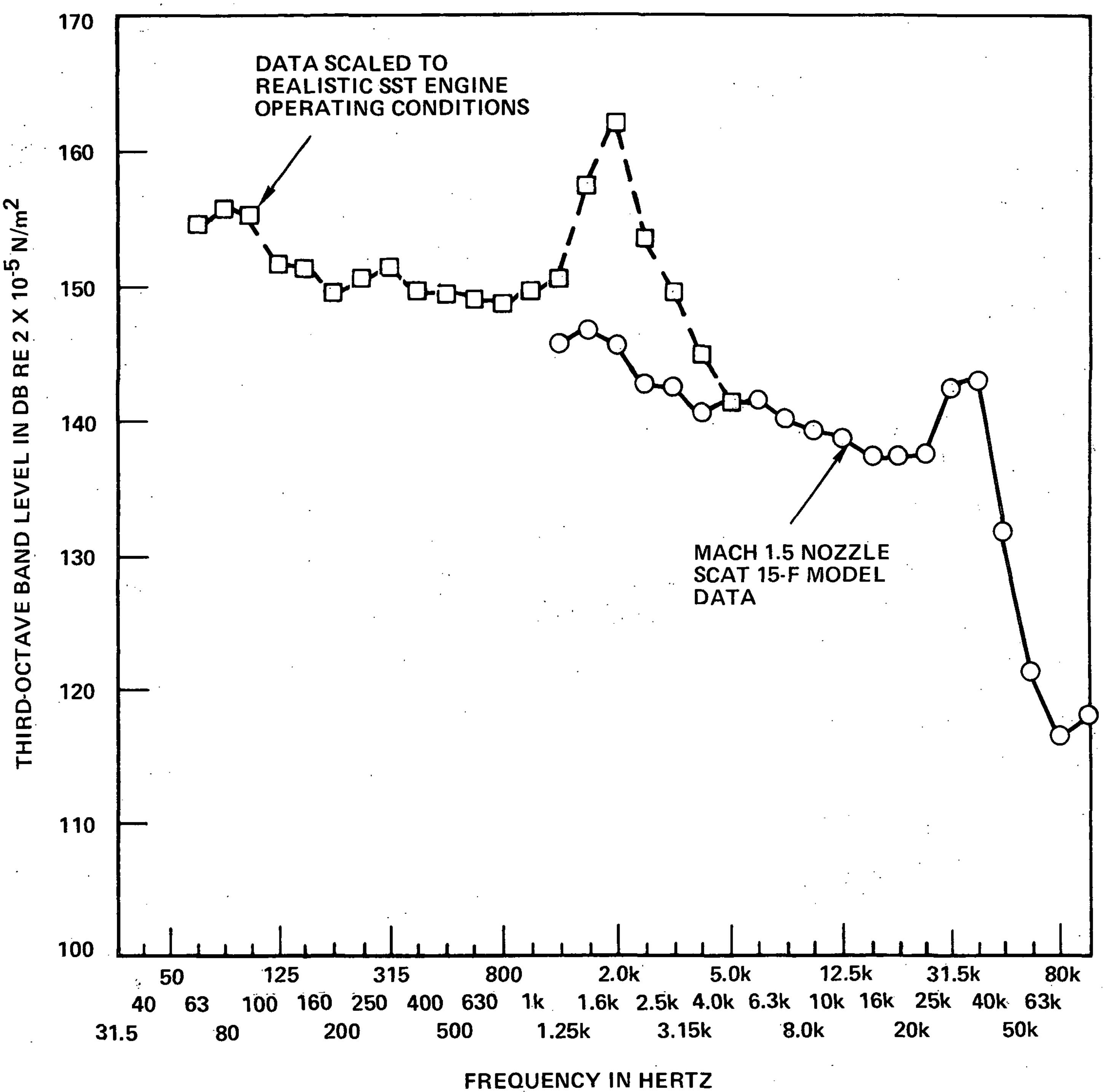

Figure 29. Comparison of SCAT 15-F Measured Model Data with Scaled Spectra for a Realistic SST Engine

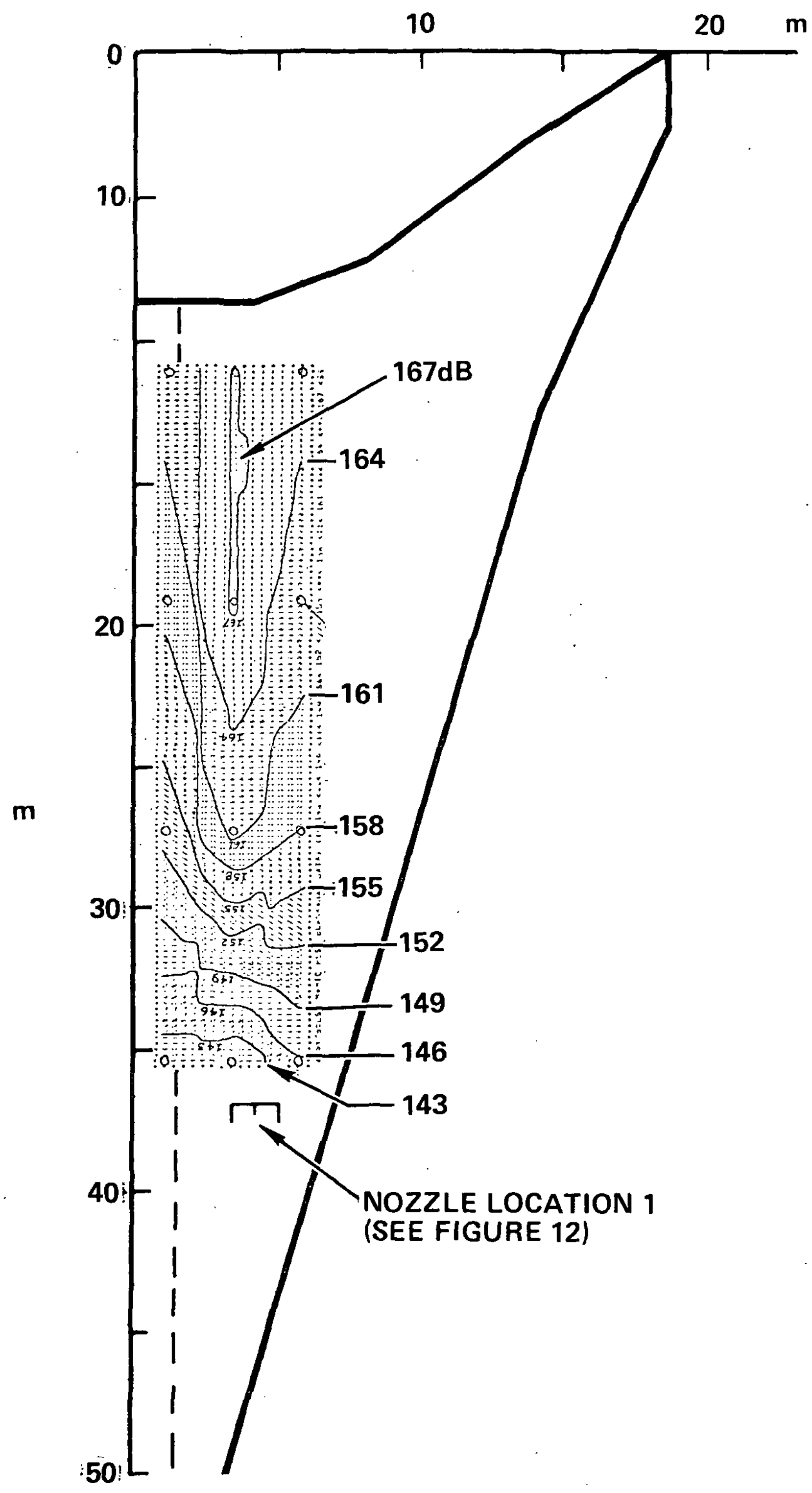

Figure 30. SCAT 15-F Mach 1.5 Nozzle Scaled OASPL Contours

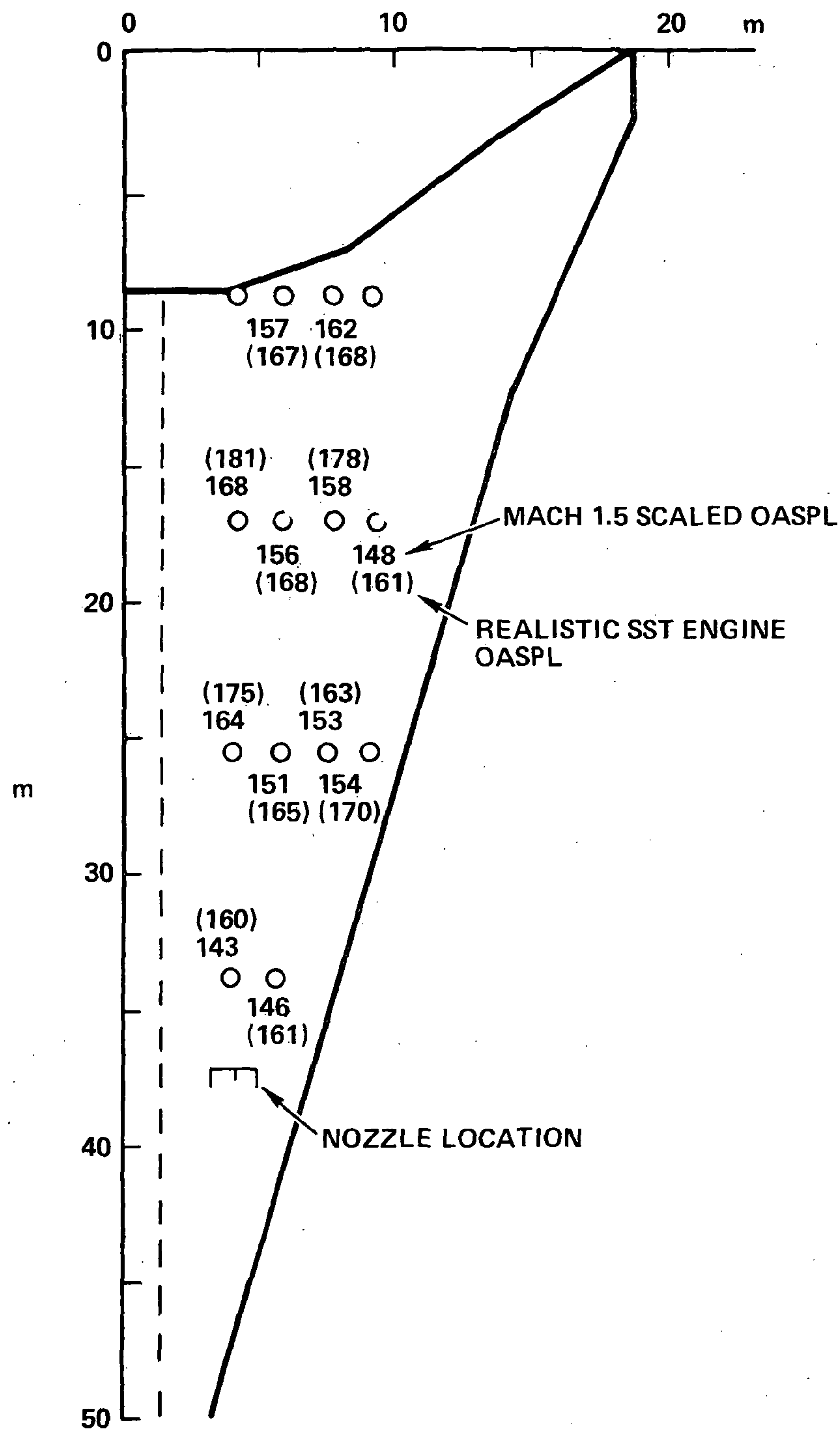

Figure 31. Point by Point Comparison of Scaled Mach 1.5 Nozzle Data and Realistic SST Engine OASPL Values

5. CONCLUSIONS

Accuracy of the prediction method used for scaling the SCAT 15-F test data to full-size supersonic transport dimensions has not been established. However, scaling of the SCAT 15-F data by considering the bypass flow conditions of an SST duct-burning turbofan engine concept, results in noise levels of up to 180 dB on a surface immersed in the jet flow stream. It is not inconceivable to believe that noise levels of this magnitude are possible for jet velocities that are on the order of 1000 m/s as are typical of duct-burning turbofan engines.

Sufficient test data pertaining to the sonic environment of a surface immersed in a supersonic jet flow stream does not exist to compile a data bank for determining validity of model scaling procedures. However, scaling of the S-3A, L-1011 and a V/STOL subsonic jet model data to full-size aircraft conditions and making comparisons with measured aircraft data show discrepancies of up to approximately 20 dB in some of the spectra one-third-octave bands. These results indicate that additional studies are needed to evaluate scaling methods and model test procedures.

The relation between sonic environments on a structure that are associated with hot and cold jet flow fields has not been determined. Hot jet flow sonic environment measurements have not been obtained because pressure transducers have not been developed that are known to provide accurate measurements in a hot jet flow stream. Therefore, significant improvements in high-temperature pressure transducers are needed.

Finite size of a transducer sensing element limits its space resolution of a pressure field. The error becomes progressively larger as the value of the quantity $\omega R/u_c$ increases. Therefore, values of the circular frequency should be as low as possible. This can be accomplished by increasing the model size so that the model frequency range required is made smaller. Also, the sensing element of the transducer should be as small as possible. The sensitivity of the transducer decreases as the sensing element becomes smaller. Consequently, a compromise must be made between sensitivity verses spatial resolution characteristics.

If narrow-band cross-correlation functions are required for making modal analyses, the transducer systems must be phase synchronized. Otherwise, an initial phase shift will result in a time shift of the entire function.

Scaling of data from coaxial jets is more complex than scaling the data for simple circular nozzles. Therefore, it appears that simple circular nozzle tests will provide a better basis than coaxial nozzle tests for investigation and refining of supersonic jet noise scaling procedures.

APPENDIX A

DERIVATION OF RESPONSE SPECTRAL DENSITY EQUATION

Determining the response of a structure that is subjected to a random excitation force consists of three major steps. They are:

- Expression of the random excitation force in terms of the excitation spectral density
- Determining the receptance of the system
- Expressing the response spectral density in terms of receptance and excitation spectral density

The computation procedure will first be developed for a simple spring mass system and then extended to the general procedure for a structure.

A.1 Simple Spring-Mass System

Figure 3.2 shows the steps required for determining the response of a simple spring-mass system. Plot a is a time history of the excitation force, Plot b is a typical excitation spectral density curve, Plot c expresses the receptance in terms of the absolute value of the receptance squared and Plot d shows the response spectral density. Computation methods for obtaining plots b, c and d are given below.

Excitation Spectral Density. - The excitation spectral density can be obtained by relating the spectral density to the autocorrelation function by use of the Fourier Transform, Equation (17).

$$S_p(\omega) = \int_{-\infty}^{\infty} R_p(\tau)E^{-i\omega\tau} \, d\tau \qquad (17)$$

$S_p(\omega)$ = Excitation spectral density

$R_p(\tau)$ = Autocorrelation function

ω = Circular frequency

τ = Delay time

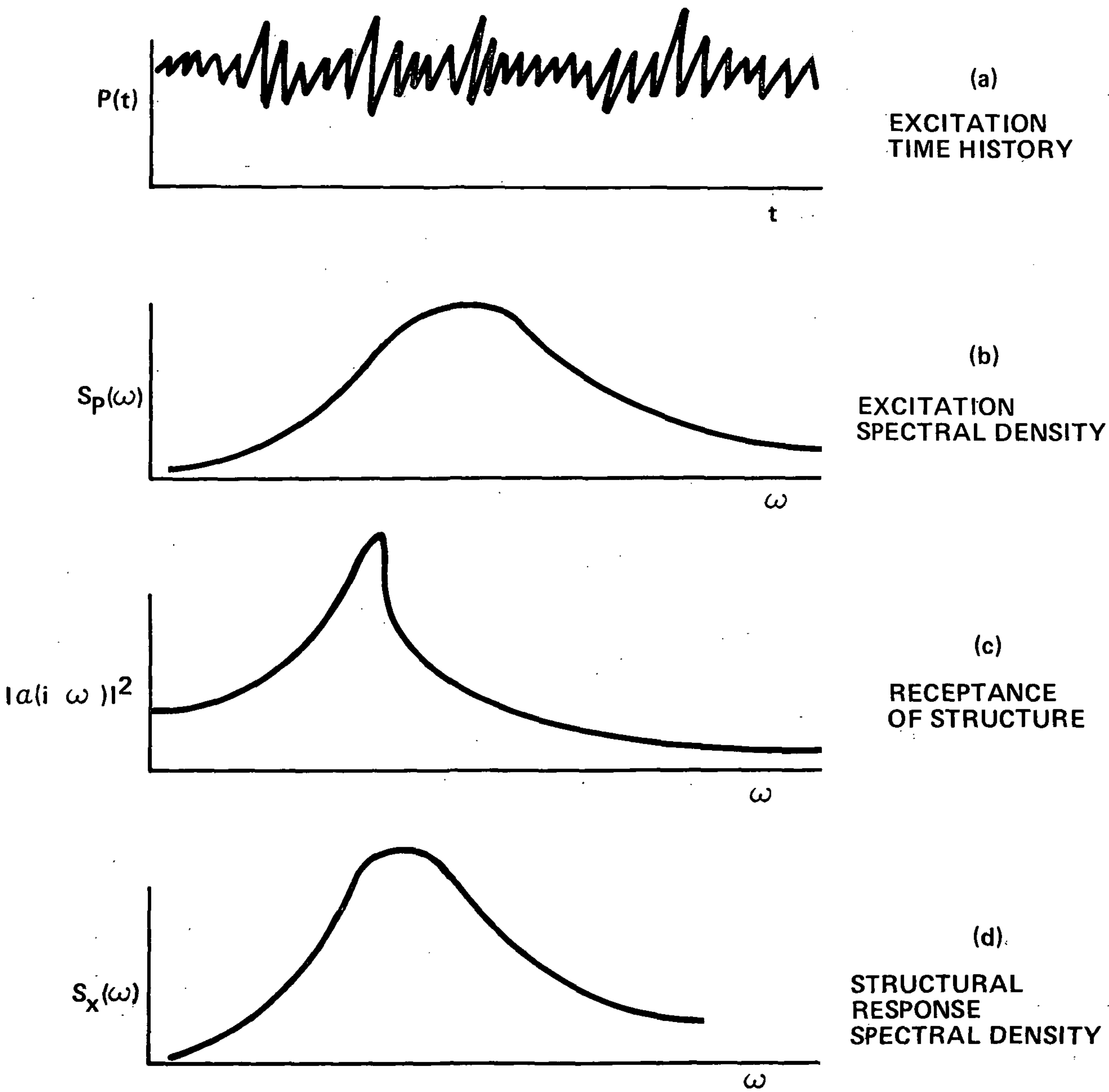

Figure 32. Steps Involved in Determining the Structural Response Caused by a Random Excitation Force

The autocorrelation function can be determined from the random excitation signal by using an autocorrelation function analyzer to determine the time average of the product of the signal at times t and $t + \tau$, Equation (18)

$$R(\tau) = \langle P(t)\, P(t + \tau) \rangle \tag{18}$$

τ = Delay time

$P(t)$ = Value of signal at time t

$P(t + \tau)$ = Value of signal at time $(t + \tau)$

Receptance of the System. - The equation of motion for a simple spring-mass system (Figure 33) is given by Equation (19).

$$m\ddot{x} + c\dot{x} + kx = P(t) \tag{19}$$

The response to a transient force can be determined from the receptance by using a Fourier integral technique, but it is usually more convenient to make use of a convolution integral which expresses the response in terms of the response to a unit impulse. An impulsive loading can be expressed mathematically by Equation (20).

$$P(t) = I\delta(t) \tag{20}$$

$P(t)$ = exciting force

I = magnitude of the impulse

$\delta(t)$ = dirac delta function

The response to the impulse loading is given by Equation (21).

$$x(t) = W(t)\, I \tag{21}$$

$x(t)$ = System response

$W(t)$ = Response to a unit impulse

The solution of the equation of motion when $P(t) = I\delta(t)$ is given by Equation (22).

$$x = \frac{I}{m\omega_d} e^{-(c/2m)t} \sin \omega_d t \tag{22}$$

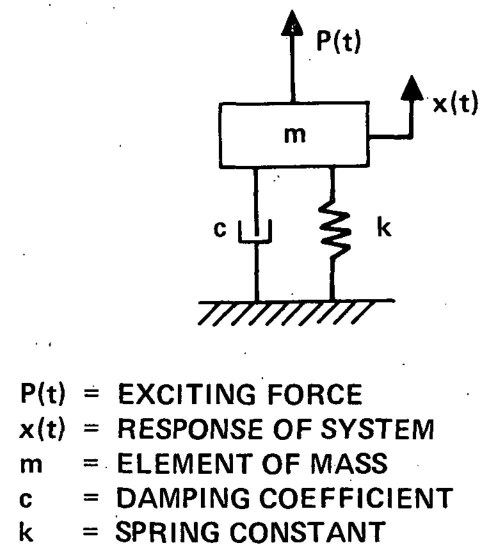

Figure 33. Simple Spring Mass System

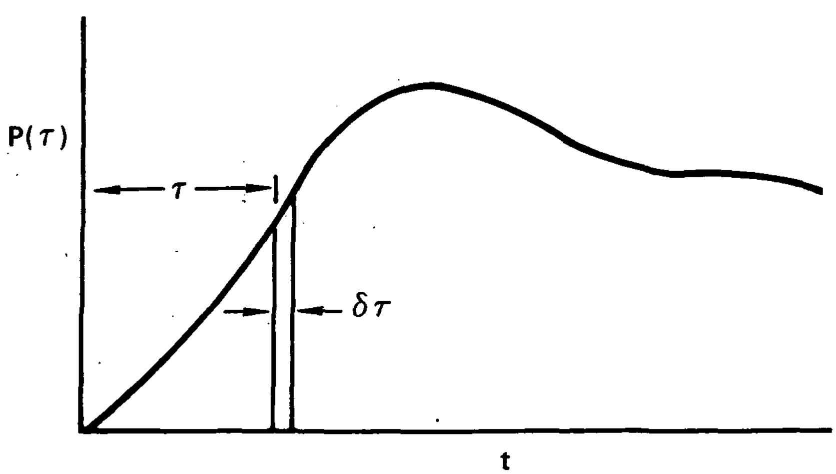

Figure 34. Continuous Pressure Loading Plot

where

$$\omega_d = \sqrt{\frac{k}{m} - \left(\frac{c}{2m}\right)^2} = \text{Damped natural frequency}$$

Substitution of Equation (22) into Equation (21) and solving for W(t) results in Equation (23).

$$W(t) = \frac{1}{m\omega_d} e^{-(c/2m)t} \sin \omega_d t \tag{23}$$

If the loading is continuous instead of a single impulse (see Figure 34), the area under the loading-time curve can be divided into impulsive loadings $P(\tau)\delta\tau$ and the response at any time t is given by the convolution integral, Equation (24).

$$x(t) = \int_{-\infty}^{\tau} W(t - \tau)\ P(\tau)\ d\tau \tag{24}$$

The value of the convolution integral is not changed by a shift in time. Therefore, the response can also be determined by Equation (25).

$$x(t) = \int_{0}^{\infty} W(\tau)\ P(t - \tau)\ d\tau \tag{25}$$

If $P(t) = P_o\ e^{i\omega t}$ the response is given by Equation (26).

$$x(t) = P_o e^{i\omega t} \int_{0}^{\infty} W(\tau) e^{-i\omega\tau}\ d\tau = P_o e^{i\omega t}\ \delta(i\omega) \tag{26}$$

where

$$\delta(i\omega) = \int_0^\infty W(\tau)e^{-i\omega\tau}\, d\tau$$

$\delta(i\omega)$ = Receptance of the system

Equation (26) will be used subsequently for determining the response spectral density. The value of the receptance can be determined by determining the particular integral of Equation (27).

$$m\ddot{x} + c\dot{x} + kx = P_o e^{i\omega t} \qquad (27)$$

Divide Equation (27) by m then let $c/m = 2\zeta\omega_n$ and $k/m = \omega_n^2$ to obtain Equation (28).

$$\ddot{x} + 2\zeta\omega_n\dot{x} + \omega_n^2 x = \frac{Po}{m} e^{i\omega t} \qquad (28)$$

The solution of Equation (28) is $x = x_o e^{i\omega t}$. Therefore, by taking the first and second time derivatives of the solution and substituting the results into Equation (28), Equation (29) is derived.

$$(-\omega^2 + i2\zeta\omega_n\omega + \omega_n^2)\, x_o = \frac{P_o}{m} \qquad (29)$$

Solving for x_o gives Equation (30).

$$x_o = \frac{P_o}{m(\omega_n^2 - \omega^2 + i\zeta\omega_n\omega)} \qquad (30)$$

The required response, Equation (31), is determined by substituting the value for x_o into the solution.

$$x = \left[\frac{1}{m(\omega_n^2 - \omega^2 + i\zeta\omega_n\omega)} \right] P_o e^{i\omega t} \tag{31}$$

The term in the brackets is the receptance of the system, Equation (32).

$$\alpha(i\omega) = \frac{1}{m(\omega_n^2 - \omega^2 + i\delta\omega_n\omega)} \tag{32}$$

The ordinate of the plot in Figure 32-c is the square of the absolute valve of the receptance.

Response Spectral Density. - The response autocorrelation function is given by Equation (33).

$$R_x(\tau) = \langle x(t)\, x(t+\tau) \rangle \tag{33}$$

Substitution x(t) from Equation (25) gives:

$$\left. \begin{aligned} x(t) &= \int_0^\infty W(\tau_1)\, P(t-\tau_1)\, d\tau \\ x(t+\tau) &= \int_0^\infty W(\tau_2)\, P\,(t+\tau-\tau_2)\, d\tau \end{aligned} \right\} \tag{34}$$

Substitution of Equation (34) into Equation (33) gives:

$$R_x(t) = \int_0^\infty W(\tau_1) \int_0^\infty W(\tau_2)\, \langle P(t-\tau_1)\, P(t+\tau-\tau_2) \rangle d\tau_2 d\tau, \tag{35}$$

By changing the origin of t:

$$R_x(t) = \int_0^\infty W(\tau_1) \int_0^\infty W(\tau_2) \ \langle P(t) \ P \ (t+\tau_1-\tau_2\tau)\rangle d\tau_2 d\tau_1 \tag{36}$$

The time average $\langle P(t) \ P \ (t + \tau_1 - \tau_2 + \tau)\rangle$ is the autocorrelation function of the exciting force. Therefore:

$$R_x(\tau) = \int_0^\infty W(\tau_1) \int_0^\infty W(\tau_2) \ R_P(\tau_1 - \tau_2 + \tau) \ d\tau_2 d\tau_1 \tag{37}$$

The relationship between the response and excitation spectral densities can be obtained from Equation (37) by making use of the Fourier transform relationship between the autocorrelation function and spectral density, Equation (38).

$$S_x(\omega) = \int_{-\infty}^\infty R_x(\tau) e^{-i\omega\tau} \ d\tau \tag{38}$$

Substitution of Equation (21) into Equation (38) gives:

$$S_x(\omega) = \int_{-\infty}^\infty \left[\int_0^\infty W(\tau_1) \int_0^\infty W(\tau_2) \ R_P \ (\tau_1-\tau_2+\tau) \ d\tau_2 d\tau_1\right] e^{-i\omega\tau} \ d\tau \tag{39}$$

$$= \int_0^\infty W(\tau_1) e^{i\omega\tau_1} \ dT_1 \int_0^\infty W(\tau_2) e^{-i\omega\tau_2} \ d\tau_2$$

$$X \int_{-\infty}^\infty R_P(\tau_1-\tau_2+\tau) e^{-i\omega(\tau_1-\tau_2+\tau)} \ d(\tau_1-\tau_2+\tau)$$

The separate factors of the above expression are $\alpha^*(i\omega)$, $\alpha(i\omega)$ and $S_P(\omega)$. $\alpha^*(i\omega)$ is the complex conjugate of the receptance and $S_P(\omega)$ is the excitation spectral density. Therefore, the response spectral density is given by Equation (40).

$$S_X(\omega) = \alpha^*(i\omega)\,\alpha(i\omega)\,S_P(\omega) = \left|\alpha(i\omega)\right|^2 S_P(\omega) \tag{40}$$

This is the plot shown in Figure 31-d.

A.2 Response of a Structure

A detailed development of the generalized structural response spectral density Equation is given in References 42 and 43. Therefore, only the basic equations will be given herein. The response spectral density of any point (x_1) will be determined for distributed pressures at points x_A and x_B for a beam of length ℓ. This development shows all the essential features for more complicated systems. The beam problem requires that the displacement at any point be expressed in terms of the normal modes and normal coordinates as given in Equation (41).

$$w(x,t) = \sum_r w_r(x)\,\xi_r(t) \tag{41}$$

$w(x,t)$ = Displacement at any point

$w_r(x)$ = Normal mode of the beam

$\xi_r(t)$ = Normal coordinate

It should be noted that the normal coordinates are obtained by transforming the generalized coordinates of a system by the normal mode matrix. When the equations of motion are expressed in terms of the normal coordinates the system is inertially and elastically uncoupled. Therefore, the equations do not have to be solved simultaneously.

For a body of any shape the position at any point is described by a position vector $\vec{P}$ and the displacement vector $w(\vec{P},t)$ is given by Equation (42).

$$w(\vec{P},t) = \sum_r w_r(\vec{P})\,\xi_r(t) \tag{42}$$

Therefore, the only difference between the beam equations given below and the equations for a body of any shape is that the coordinate x is used instead of a vector $\bar{P}$. The steps involved in determining the generalized response spectral density equation are the same as for the simple spring-mass system. However, the cross correlation functions and cross spectral densities must now be determined. Also, the receptances of the system must be defined in terms of the normal modes.

Excitation Spectral Density. - The excitation cross spectral density is obtained by relating it to the cross-correlation function by use of the Fourier Transform Equation (43).

$$S_P(x_A, x_B; \omega) = \int_{-\infty}^{\infty} R_P(x_A, x_B; \tau)e^{-i\omega\tau}\, d\tau \qquad (34)$$

The cross-correlation function is:

$$R_P(x_A, x_B; \tau) = \langle P(x_A, t)dx_A P(x_B, t+\tau)dx_B \rangle \qquad (44)$$

$S_P(x_A, x_B; \omega)$ = excitation cross spectral density at any two points x_A and x_B

$R_P(x_A, x_B, \tau)$ = cross-correlation function for points x_A and x_B

$P(x_A, t)$ = distributed pressure at point x_A at time t

$P(x_B, t+\tau)$ = distributed pressure at point x_B at time $(t + \tau)$

Receptance of the system. - The receptance of the system at point x_1 for a load at x_A in terms of the normal modes is given by Equation (45).

$$\alpha_{x_1,x_A} = \sum_r \frac{w_r(x_1)w_r(x_A)}{M_r(\omega_r^2 - \omega^2 + i\zeta\omega_r\omega)} \qquad (45)$$

The receptance at x_1 for a load at x_B is:

$$\alpha_{x_1,x_B} = \sum_s \frac{w_s(x_1)\, w_s(x_B)}{M_s(\omega_s^2 - \omega^2 + i\zeta\omega_s\omega)}$$

$w_r(x_1)$, $w_s(x_1)$ = modal deflections at x_1

$w_r(x_A)$ = modal deflection at x_A

$w_s(x_B)$ = modal deflection at x_B

$M_r = \int_o^1 w_r^2(x)\ mdx$ = generalized mass for mode r

$M_s = \int_o^1 w_s^2(x)\ mdx$ = generalized mass for mode s

ω_r, ω_s = modal frequencies

ζ = viscous damping factor

Response Spectral Density. - The spectral density at x_1 can now be expressed in terms of the receptances and excitation cross-spectral density by Equation (46).

$$S_w(x_1,\omega) = \sum_r \sum_s \frac{w_r(x_1) w_s(x_1) \int_o^{\ell} \int_o^{\ell} w_r(x_A) w_s(x_B) S_P(x_A, x_B; \omega)\ dx_A dx_B}{M_r(\omega_r^2 - \omega^2 + i\zeta\omega_r\omega)\ M_x(\omega_s^2 - \omega^2 + i\zeta\omega_s\omega)} \tag{46}$$

This equation is easily changed to Equation 6 in Section 2.3 by:

- Replacing x, with x,y
- Changing integration limits to A
- Letting $x_A = \xi$
- Letting $x_B = \eta$
- Replacing dx_A and dx_B with dA
- Representing modal values w_r and w_s by f_r and f_s respectively
- **Changing symbol for damping factor from ξ to δ to δ_r and δ_{s_k} respectively**

APPENDIX B

LITERATURE SEARCH

A search was made of the following files via DIALOG - the Lockheed-California Company on-line information retrieval system - to locate information relevant to "Acoustic Loads on a Panel immersed in a Jet Flow Stream."

- NTIS - File of Government Reports: The file contains over 400,000 abstracts of research reports from over 240 government agencies, including NASA. The file dates from 1964.
- ENGINEERING INDEX - Publications of engineering organizations: The file contains approximately 360,000 citations and abstracts from 3,500 Journals. The file dates from 1970.
- ISMEC - Mechanical engineering and engineering management data base: The file includes about 30,000 items and dates from 1973.

A search was made by the NASA Scientific and Technical Information Facility.

The search also included:

- Journal of the Acoustic Society of America Index - 1971 to present
- Lockheed California Company Central Library Catalog
- Applied Mechanics Services 1974 to Sept 1975
- Applied Science and Technology Index - 1971 to Sept 1975
- AGARD Index - 1971 thru 1973
- Shock and Vibration Digest - 1971 to Sept 1975

Test Data directly related to "Acoustic Loads on a Panel Immersed in a Jet Flow Stream" were not located. However, many publications were located which provide pertinent information for development of sonic environment analysis methods (see report references).

APPENDIX C

SCALING COMPUTER PROGRAM

A listing of the noise scaling computer program is given in the following pages. The program is written in terms of the International Business Machine (IBM) conversational program system (CPS) CPS PL/1 language. The CPS PL/1 language can be regarded as a modified subset of the full set PL/1 language.

Input to the program is:

scafac	ttmr	ptmi	mixm	dmi	rmi	trim
fm	splm	n				
ttar	pra	wa	mixa	tria		
psi						

These input symbols are defined in the program symbol list that follows the program listing. Input required is in terms of the English system of units.

NOISE SCALING COMPUTER PROGRAM

```
 1.          DECLARE fm(24) DEC(6),fa(24) DEC(6),aspla(24) DEC(6),
             splm(24) DEC(6);
 2.          DECLARE tabsc(12) DEC(6),tord(12) DEC(6),mspla(24) DE
             C(6);
 3.          DECLARE scm(24) DEC(6),tc(24) DEC(6),sca(24) DEC(6);
 4.          DECLARE  gam ENTRY  EXT KEY(wag);
 5.          GET LIST(scafac,ttmr,ptmi,mixm,dmi,rmi,trim);
 6.          GET LIST(fm,splm,n);
 7.          GET LIST(ttar,pra,wa,mixa,tria);
 8.          GET LIST(psi);
 9.          GET LIST(start);
10.          dmf=dmi/12;
11.          daf=dmf/scafac;
12.          rmf=rmi/12;
13.          raf=rmf/scafac;
14.          prm=ptmi/psi;
15.          cv,cvm,cva=.98;
16.          ami=.785*dmi**2;
17.          amf=ami/144;
18.          CALL gam(mixa,ttar,pra,gamaa,tjar);
19.          CALL gam(mixm,ttmr,prm,gamam,tjmr);
20.          vm=sqrt(64.4*(gamam/(gamam-1))*53.3*ttmr*(1-1/prm**((
             gamam-1)/gamam)));
21.          va=sqrt(64.4*(gamaa/(gamaa-1))*53.3*ttar*(1-1/pra**((
             gamaa-1)/gamaa)));
22.          rhom=psi*144/(53.3*ttmr)*prm**((gamam-1)/gamam);
23.          rhoa=psi*144/(53.3*ttar)*pra**((gamaa-1)/gamaa);
24.          wm=rhom*amf*vm*cv;
25.          aa=wa/(cv*va*rhoa);
26.          fnm=cv*(wm/32.2)*vm;
27.          fna=cv*(wa/32.2)*va;
28.          sd=10*log10(rhoa/rhom);
29.   127:   print=1;
30.          ucm=.62*vm;
31.          DO i=1 TO n;
32.            omegam=6.28*fm(i);
33.            abscm=omegam*(trim/24)/ucm;
34.            DO j=1 TO 11;
35.              IF abscm>=tabsc(j)&abscm<=tabsc(j+1) THEN GO TO 1
               15;
36.            END ;
37.   115:     phirm=(abscm-tabsc(j))/(tabsc(j+1)+tabsc(j))*(tord(
             j+1)-tord(j))+tord(j);
38.            scm(i)=-10*log10(phirm);
39.            tc(i)=scm(i)+sd;
40.            fa(i)=fm(i)*(va/vm*(dmf/daf));
41.            IF va<=2000 THEN aspla(i)=splm(i)+scm(i)+sd+80*log1
               0(va/vm); ELSE aspla(i)=splm(i)+scm(i)+sd+165.051+3
               0*log10(va)-80*log10(vm);
42.          END ;
43.          uca=.62*va;
```

```
          DO I=1 TO n;
            omegaa=6.28*fa(I);
            absca=omegaa*(tria/24)/uca;
            DO j=1 TO 11;
              IF absca>=tabsc(j)&absca<=tabsc(j+1) THEN GO TO 1
              40;
            END ;
 140:       phira=(absca-tabsc(j))/(tabsc(j+1)+tabsc(j))*(tord(
            j+1)-tord(j))+tord(j);
            sca(I)=10*log10(phira);
            IF I<=n THEN mspla(I)=aspla(I)+sca(I); ELSE mspla=0
            ;
          END ;
          PUT IMAGE(print)(110);
 110:     IMAGE;
                     SONIC ENVIRONMENT SCALING PROGRAM
          PUT LIST(lf(2));
          PUT IMAGE(print)(117);
 117:     IMAGE;
              MODEL                    AIRCRAFT
          PUT LIST(' ');
          PUT IMAGE(ttmr,ttar)(118);
 118:     IMAGE;
      tt       ----.-                 ----.-       deg R
          PUT IMAGE(tjmr,tjar)(119);
 119:     IMAGE;
      ts       ----.-                 ----.-       deg R
          PUT IMAGE(prm,pra)(125);
 125:     IMAGE;
      pr         --.-----                --.-----
          PUT IMAGE(wm,wa)(133);
 133:     IMAGE;
      w        ----.--                ----.--      lb/sec
          PUT IMAGE(mixm,mixa)(121);
 121:     IMAGE;
      mix        -.-----                 -.-----   #f/#a
          PUT IMAGE(cvm,cva)(135);
 135:     IMAGE;
      cv           .---                    .---
          PUT IMAGE(dmi,daf)(123);
 123:     IMAGE;
      dia       ---.--   in          ---.--        ft
          PUT IMAGE(ami,aa)(130);
 130:     IMAGE;
      area      ---.--   sq in       ---.--        sq ft
          PUT IMAGE(rhom,rhoa)(132);
 132:     IMAGE;
      rho        --.----                --.----    lb/sq ft
          PUT IMAGE(gamam,gamaa)(126);
 126:     IMAGE;
      gama       --.----                --.----
```

```
                PUT IMAGE(vm,va)(122);
        122:    IMAGE;
         vel    -----.-                          -----.-        ft/sec
                PUT IMAGE(ucm,uca)(136);
        136:    IMAGE;
         conv     ----.--                          ----.--      ft/sec
                PUT IMAGE(rmi,raf)(124);
        124:    IMAGE;
         dist   -----.--     in                  -----.--       ft
                PUT IMAGE(fnm,fna)(134);
        134:    IMAGE;
         Fn   -----.-                         -----.-       lbs
                PUT IMAGE(trim,tria)(138);
        138:    IMAGE;
         trdia        -.---                           -.---     in
                PUT LIST(lf(2));
                PUT IMAGE(sd)(137);
        137:    IMAGE;
         Density Correction = ---.-- dB
                PUT LIST(lf(2));
                PUT IMAGE(print)(113);
        113:    IMAGE;
       fm          splm          scm          tc          fa
aspla          sca          mspla
                PUT IMAGE(print)(139);
        139:    IMAGE;
        (Hz)        (dB)          (dB)         (dB)         (Hz)
(dB)          (dB)          (dB)
                PUT LIST(' ');
                DO I=1 TO n;
                  PUT IMAGE(fm(I),splm(I),scm(I),tc(I),fa(I),aspla(I)
                  ,sca(I),mspla(i))(114);
        114:      IMAGE;
      ------      ---.-        ---.-        ---.-       -----
---.-        ---.-        ---.-
                END ;
                s=0;
                DO I=1 TO n;
                  s=10**(mspla(I)/10)+s;
                END ;
                oaspl=10*log10(s);
                PUT LIST(lf(1));
                PUT IMAGE(oaspl)(120);
        120:    IMAGE;
       OASPL= ---.- dB
                PUT LIST(lf(15));
```

COMPUTER PROGRAM VARIABLES

			Units
aa	=	Aircraft engine fully expanded jet area	ft^2
absca	=	Abscissa of finite size correction curve (Figure 9) for aircraft noise	--
abscm	=	Abscissa of finite size correction curve (Figure 9) for model noise	--
ami	=	Area of model jet	in^2
amf	=	Area of model jet	ft^2
aspla	=	Aircraft noise overall sound pressure level	dB
cva	=	Nozzle velocity coefficient of aircraft engine nozzle	--
cvm	=	Nozzle velocity coefficient of model engine nozzle	ft/sec
daf	=	Diameter of aircraft engine nozzle exit	ft
dmf	=	Diameter of model nozzle exit	ft
dmi	=	Diameter of model nozzle exit	in.
fa	=	Aircraft noise frequency (one-third octave)	Hz
fm	=	Model noise frequency (one-third octave)	Hz
fna	=	Aircraft engine jet thrust	lb
fnm	=	Model jet thrust	lb
gam	=	Subroutine for computing values of ratio of specific heat	--
gamaa	=	Ratio of specific heat for aircraft engine fully expanded jet	--
gamam	=	Ratio of specific heat for model engine fully expanded jet	--
i	=	Do loop counter	--

			Units
j	=	Do loop counter	--
mixa	=	Fuel/air mixture of aircraft jet	lb-fuel/lb-air
mixm	=	Fuel/air mixture of model jet	lb-fuel/lb-air
mspla	=	Model noise overall sound pressure level	dB
n	=	Number of one-third octave bands	--
omegaa	=	Aircraft noise one-third octave band circular frequency	rad/sec
omegam	=	Model noise one-third octave band circular noise	rad/sec
phira	=	Transducer finite size correction for aircraft noise	dB
phirm	=	Transducer finite size correction for model noise	dB
pra	=	Aircraft engine nozzle pressure ratio	--
prm	=	Model nozzle pressure ratio	--
print	=	Dummy variable used to facilitate printout	--
psi	=	Atmospheric pressure	lb/in^2
pta	=	Total pressure of aircraft jet	lb/ft^2
ptmi	=	Total pressure of model jet	lb/in^2
raf	=	Distance from aircraft engine nozzle exit to transducer	ft
rmf	=	Distance from model nozzle exit to transducer	ft
rhoa	=	Fully expanded aircraft jet density	$slug/ft^3$
rhom	=	Fully expanded model jet density	$slug/ft^3$
rmi	=	Distance from model nozzle exit to transducer	in.
sca	=	Transducer finite size vorrection for aircraft noise	dB

COMPUTER PROGRAM VARIABLES - Concluded

			Units
scafac	=	Model scale factor	dB
scm	=	Transducer finite size corrections for model noise	dB
sd	=	Density correction	dB
spla	=	Aircraft noise one-third octave band sound pressure levels	dB
splm	=	Model noise one-third octave band sound pressure levels	dB
start	=	Dummy variable used to initiate start of analysis and output	--
tabsc	=	Abscissa values of Figure 9	--
tc	=	Sum of finite size and density corrections	dB
tjar	=	Static fully expanded aircraft jet temperature	deg R
tjmr	=	Static fully expanded model jet temperature	deg R
tord	=	Ordinate values of Figure 9	--
tria	=	Diameter of transducer sensing element (aircraft test)	in.
trim	=	Diameter of transducer sensing element (model test)	in.
ttar	=	Total temperature of aircraft engine jet	deg R
ttmr	=	Total temperature of model engine jet	deg R
uca	=	Convection velocity of aircraft engine jet	ft/sec
ucm	=	Convection velocity of model jet	ft/sec
va	=	Aircraft engine fully expanded jet velocity	ft/sec
vm	=	Model fully expanded jet velocity	ft/sec
wa	=	Aircraft engine exhaust flow	lb/sec
wm	=	Model engine exhaust flow	lb/sec

APPENDIX D

COMPUTER PROGRAM OUTPUT

Included in this appendix are the output data for:

- S-3A (Tables 8 through 10)
- L-1011 (Table 11)
- V/STOL (Table 12)
- SCAT 15-F (Tables 13 through 30)

The symbols used on the printout sheet correspond to those given in Appendix C. However for convenience the symbols for each column are defined below.

1. fm = Model frequency
2. splm = Model noise one-third octave spl
3. scm = Transducer finite size correction for model noise
4. tc = Sum of finite size and density correction
5. fa = Aircraft noise frequency
6. aspla = Actual sonic environment one-third octave spl's on aircraft structure
7. sca = Transducer finite size correction for aircraft noise
8. mspla = Measured one-third octave spl for aircraft noise

TABLE 8. COMPUTER OUTPUT: S-3A SPECTRUM - LOCATION 1

	MODEL		AIRCRAFT	
tt	537.0		593.0	deg R
ts	486.6		536.8	deg R
pr	1.41497		1.42000	
w	6.01		842.00	lb/sec
mix	0.00000		0.00000	#f/#a
cv	.980		.980	
dia	4.20	in	2.45	ft
area	13.85	sq in	14.08	sq ft
rho	0.0817		0.0740	lb/sq ft
gama	1.4018		1.4013	
vel	780.4		824.1	ft/sec
conv	483.84		510.92	ft/sec
dist	8.00	in	4.67	ft
Fn	142.7		21117.6	lbs
trdia	0.250		0.250	in

Density Correction = -0.43 dB

fm (Hz)	splm (dB)	scm (dB)	tc (dB)	fa (Hz)	aspla (dB)	sca (dB)	mspla (dB)
250	142.7	0.1	-0.3	38	144.2	-0.0	144.2
315	143.6	0.1	-0.3	48	145.2	-0.0	145.2
400	145.1	0.1	-0.3	60	146.7	-0.0	146.7
500	145.6	0.2	-0.3	75	147.2	-0.0	147.2
630	146.4	0.2	-0.2	95	148.1	-0.0	148.0
800	146.3	0.3	-0.2	121	148.0	-0.0	148.0
1000	146.8	0.3	-0.1	151	148.6	-0.0	148.6
1250	147.1	0.4	-0.0	189	149.0	-0.1	148.9
1600	146.2	0.6	0.1	241	148.2	-0.1	148.1
2000	145.5	0.7	0.3	302	147.7	-0.1	147.6
2500	144.5	0.9	0.5	377	146.9	-0.1	146.7
3150	142.8	1.1	0.7	475	145.4	-0.1	145.2
4000	141.5	1.2	0.8	603	144.2	-0.2	144.0
5000	139.8	1.4	0.9	754	142.6	-0.2	142.4
6300	138.6	2.5	2.0	950	142.5	-0.3	142.2
8000	136.6	2.6	2.2	1207	140.7	-0.4	140.3
10000	134.2	4.1	3.6	1509	139.7	-0.5	139.2

OASPL= 158.6 dB

TABLE 9. COMPUTER OUTPUT: S-3A SPECTRUM - LOCATION 2

	MODEL		AIRCRAFT	
tt	537.0		593.0	deg R
ts	486.6		536.8	deg R
pr	1.41497		1.42000	
w	6.01		842.00	lb/sec
mix	0.00000		0.00000	#f/#a
cv	.980		.980	
dia	4.20	in	2.45	ft
area	13.85	sq in	14.08	sq ft
rho	0.0817		0.0740	lb/sq ft
gama	1.4018		1.4013	
vel	780.4		824.1	ft/sec
conv	483.84		510.92	ft/sec
dist	18.00	in	10.50	ft
Fn	142.7		21117.6	lbs
trdia	0.250		0.250	in

Density Correction = -0.43 dB

fm (Hz)	splm (dB)	scm (dB)	tc (dB)	fa (Hz)	aspla (dB)	sca (dB)	mspla (dB)
250	132.2	0.1	-0.3	38	133.7	-0.0	133.7
315	132.3	0.1	-0.3	48	133.9	-0.0	133.9
400	132.5	0.1	-0.3	60	134.1	-0.0	134.1
500	130.2	0.2	-0.3	75	131.8	-0.0	131.8
630	128.2	0.2	-0.2	95	129.9	-0.0	129.8
800	126.2	0.3	-0.2	121	127.9	-0.0	127.9
1000	125.0	0.3	-0.1	151	126.8	-0.0	126.8
1250	124.4	0.4	-0.0	189	126.3	-0.1	126.2
1600	123.3	0.6	0.1	241	125.3	-0.1	125.2
2000	122.1	0.7	0.3	302	124.3	-0.1	124.2
2500	120.0	0.9	0.5	377	122.4	-0.1	122.2
3150	118.2	1.1	0.7	475	120.8	-0.1	120.6
4000	117.0	1.2	0.8	603	119.7	-0.2	119.5
5000	116.2	1.4	0.9	754	119.0	-0.2	118.8
6300	115.0	2.5	2.0	950	118.9	-0.3	118.6
8000	114.0	2.6	2.2	1207	118.1	-0.4	117.7
10000	112.4	4.1	3.6	1509	117.9	-0.5	117.4

OASPL= 141.0 dB

TABLE 10. COMPUTER OUTPUT: S-3A SPECTRUM - LOCATION 3

	MODEL		AIRCRAFT	
tt	537.0		593.0	deg R
ts	486.6		536.8	deg R
pr	1.41497		1.42000	
w	6.01		842.00	lb/sec
mix	0.00000		0.00000	#f/#a
cv	.980		.980	
dia	4.20	in	2.45	ft
area	13.85	sq in	14.08	sq ft
rho	0.0817		0.0740	lb/sq ft
gama	1.4018		1.4013	
vel	780.4		824.1	ft/sec
conv	483.84		510.92	ft/sec
dist	30.00	in	17.50	ft
Fn	142.7		21117.6	lbs
trdia	0.250		0.250	in

Density Correction = -0.43 dB

fm (Hz)	splm (dB)	scm (dB)	tc (dB)	fa (Hz)	aspla (dB)	sca (dB)	mspla (dB)
250	130.7	0.1	-0.3	38	132.2	-0.0	132.2
315	127.5	0.1	-0.3	48	129.1	-0.0	129.1
400	125.4	0.1	-0.3	60	127.0	-0.0	127.0
500	121.8	0.2	-0.3	75	123.4	-0.0	123.4
630	120.4	0.2	-0.2	95	122.1	-0.0	122.0
800	119.5	0.3	-0.2	121	121.2	-0.0	121.2
1000	120.0	0.3	-0.1	151	121.8	-0.0	121.8
1250	120.5	0.4	-0.0	189	122.4	-0.1	122.3
1600	120.4	0.6	0.1	241	122.4	-0.1	122.3
2000	120.0	0.7	0.3	302	122.2	-0.1	122.1
2500	119.5	0.9	0.5	377	121.9	-0.1	121.7
3150	117.9	1.1	0.7	475	120.5	-0.1	120.3
4000	117.8	1.2	0.8	603	120.5	-0.2	120.3
5000	116.4	1.4	0.9	754	119.2	-0.2	119.0
6300	115.3	2.5	2.0	950	119.2	-0.3	118.9
8000	113.4	2.6	2.2	1207	117.5	-0.4	117.1
10000	110.5	4.1	3.6	1509	116.0	-0.5	115.5

OASPL= 136.8 dB

TABLE 11. COMPUTER OUTPUT: L-1011 SPECTRUM

	MODEL		AIRCRAFT	
tt	537.0		620.0	deg R
ts	477.6		553.6	deg R
pr	1.51020		1.49000	
w	3.12		1159.50	lb/sec
mix	0.00000		0.00000	#f/#a
cv	.980		.980	
dia	2.88	in	4.80	ft
area	6.51	sq in	18.40	sq ft
rho	0.0832		0.0718	lb/sq ft
gama	1.4019		1.4010	
vel	846.6		895.6	ft/sec
conv	524.88		555.24	ft/sec
dist	11.50	in	19.17	ft
Fn	80.4		31603.3	lbs
trdia	0.250		0.250	in

Density Correction = -0.64 dB

fm (Hz)	splm (dB)	scm (dB)	tc (dB)	fa (Hz)	aspla (dB)	sca (dB)	mspla (dB)
1250	126.4	0.4	-0.3	66	128.1	-0.0	128.1
1600	126.2	0.5	-0.1	85	128.0	-0.0	128.0
2000	125.3	0.6	-0.0	106	127.3	-0.0	127.2
2500	125.3	0.8	0.2	132	127.4	-0.0	127.4
3150	124.2	1.1	0.4	167	126.6	-0.0	126.5
4000	123.2	1.2	0.5	212	125.7	-0.1	125.6
5000	122.0	1.3	0.7	264	124.6	-0.1	124.5
6300	120.2	1.5	0.8	333	123.0	-0.1	122.9
8000	119.0	2.6	1.9	423	122.9	-0.1	122.8
10000	117.0	4.0	3.4	529	122.3	-0.2	122.2

OASPL= 136.0 dB

TABLE 12. COMPUTER OUTPUT: V/STOL SPECTRUM

	MODEL		AIRCRAFT	
tt	537.0		1515.0	deg R
ts	477.6		1367.2	deg R
pr	1.51020		1.50000	
w	18.18		333.50	lb/sec
mix	0.00000		0.03300	#f/#a
cv	.980		.980	
dia	6.95	in	3.13	ft
area	37.92	sq in	8.28	sq ft
rho	0.0832		0.0290	lb/sq ft
gama	1.4019		1.3362	
vel	846.6		1415.8	ft/sec
conv	524.88		877.81	ft/sec
dist	30.59	in	13.78	ft
Fn	468.5		14370.6	lbs
trdia	0.218		0.500	in

Density Correction = -4.57 dB

fm (Hz)	splm (dB)	scm (dB)	tc (dB)	fa (Hz)	aspla (dB)	sca (dB)	mspla (dB)
315	144.1	0.1	-4.5	97	157.5	-0.0	157.4
400	144.9	0.1	-4.5	124	158.3	-0.0	158.3
500	145.6	0.1	-4.4	155	159.0	-0.1	159.0
630	145.4	0.2	-4.4	195	158.9	-0.1	158.8
800	145.1	0.2	-4.4	248	158.6	-0.1	158.5
1000	144.9	0.3	-4.3	309	158.5	-0.1	158.3
1250	144.7	0.3	-4.2	387	158.3	-0.1	158.2
1600	143.8	0.4	-4.1	495	157.5	-0.2	157.3
2000	143.9	0.6	-4.0	619	157.7	-0.2	157.5
2500	143.0	0.7	-3.9	773	157.0	-0.3	156.7
3150	142.3	0.9	-3.7	975	156.5	-0.4	156.1
4000	141.0	1.1	-3.5	1238	155.4	-0.5	154.9
5000	139.0	1.2	-3.4	1547	153.5	-0.6	152.9
6300	137.8	1.4	-3.2	1949	152.5	-0.8	151.7
8000	136.2	2.5	-2.1	2475	152.0	-1.0	151.0
10000	133.0	2.6	-1.9	3094	148.9	-1.1	147.8
12500	129.2	4.1	-0.5	3867	146.6	-1.3	145.3
16000	125.5	5.9	1.3	4950	144.7	-1.4	143.3
20000	121.6	8.0	3.5	6188	142.9	-2.5	140.4
25000	116.3	10.6	6.0	7735	140.2	-2.7	137.5
31500	112.0	15.3	10.7	9746	140.6	-4.1	136.5
40000	110.0	20.0	15.4	12376	143.3	-6.0	137.3

OASPL= 168.9 dB

TABLE 13. COMPUTER OUTPUT: SCAT 15-F MODEL TEST - LOCATION 31P-10

	MODEL		AIRCRAFT	
tt	540.0		2245.0	deg R
ts	364.8		1695.8	deg R
pr	3.94558		3.12100	
w	3.38		411.00	lb/sec
mix	0.00000		0.02000	#f/#a
cv	.980		.980	
dia	2.00	in	5.56	ft
area	3.14	sq in	6.48	sq ft
rho	0.1089		0.0234	lb/sq ft
gama	1.4010		1.3267	
vel	1450.5		2765.6	ft/sec
conv	899.31		1714.69	ft/sec
dist	34.00	in	94.44	ft
Fn	149.1		34594.3	lbs
trdia	0.218		0.250	in

Density Correction = -6.68 dB

fm (Hz)	splm (dB)	scm (dB)	tc (dB)	fa (Hz)	aspla (dB)	sca (dB)	mspla (dB)
1250	145.8	0.2	-6.5	72	154.7	-0.0	154.7
1600	146.9	0.2	-6.4	92	155.9	-0.0	155.8
2000	145.6	0.3	-6.4	114	154.6	-0.0	154.6
2500	142.8	0.4	-6.3	143	151.9	-0.0	151.9
3150	142.2	0.5	-6.2	180	151.4	-0.0	151.4
4000	140.1	0.7	-6.0	229	149.5	-0.0	149.4
5000	141.2	0.8	-5.8	286	150.7	-0.0	150.7
6300	141.3	1.1	-5.6	360	151.1	-0.0	151.1
8000	140.0	1.2	-5.5	458	149.9	-0.0	149.8
10000	139.1	1.3	-5.4	572	149.1	-0.1	149.1
12500	138.9	1.5	-5.2	715	149.1	-0.1	149.0
16000	137.4	2.6	-4.1	915	148.7	-0.1	148.6
20000	137.1	4.0	-2.7	1144	149.8	-0.1	149.7
25000	137.4	4.2	-2.5	1430	150.3	-0.1	150.2
31500	142.8	6.0	-0.6	1802	157.5	-0.2	157.4
40000	143.0	10.5	3.8	2288	162.2	-0.2	162.0
50000	131.6	13.1	6.4	2860	153.4	-0.3	153.2
63000	121.3	17.1	10.4	3604	147.1	-0.3	146.8
80000	116.5	20.0	13.4	4576	145.2	-0.4	144.8
100000	118.0	20.1	13.4	5720	146.8	-0.6	146.2

OASPL= 166.6 dB

TABLE 14. COMPUTER OUTPUT: SCAT 15-F MODEL TEST - LOCATION 31P-12

	MODEL		AIRCRAFT	
tt	540.0		2245.0	deg R
ts	364.8		1695.8	deg R
pr	3.94558		3.12100	
w	3.38		411.00	lb/sec
mix	0.00000		0.02000	#f/#a
cv	.980		.980	
dia	2.00	in	5.56	ft
area	3.14	sq in	6.48	sq ft
rho	0.1089		0.0234	lb/sq ft
gama	1.4010		1.3267	
vel	1450.5		2765.6	ft/sec
conv	899.31		1714.69	ft/sec
dist	34.23	in	95.08	ft
Fn	149.1		34594.3	lbs
trdia	0.218		0.250	in

Density Correction = -6.68 dB

fm (Hz)	splm (dB)	scm (dB)	tc (dB)	fa (Hz)	aspla (dB)	sca (dB)	mspla (dB)
1250	152.0	0.2	-6.5	72	160.9	-0.0	160.9
1600	149.3	0.2	-6.4	92	158.3	-0.0	158.2
2000	148.6	0.3	-6.4	114	157.6	-0.0	157.6
2500	146.1	0.4	-6.3	143	155.2	-0.0	155.2
3150	146.1	0.5	-6.2	180	155.3	-0.0	155.3
4000	143.5	0.7	-6.0	229	152.9	-0.0	152.8
5000	143.2	0.8	-5.8	286	152.7	-0.0	152.7
6300	144.0	1.1	-5.6	360	153.8	-0.0	153.8
8000	143.2	1.2	-5.5	458	153.1	-0.0	153.0
10000	142.1	1.3	-5.4	572	152.1	-0.1	152.1
12500	140.4	1.5	-5.2	715	150.6	-0.1	150.5
16000	138.7	2.6	-4.1	915	150.0	-0.1	149.9
20000	137.6	4.0	-2.7	1144	150.3	-0.1	150.2
25000	134.9	4.2	-2.5	1430	147.8	-0.1	147.7
31500	133.4	6.0	-0.6	1802	148.1	-0.2	148.0
40000	130.9	10.5	3.8	2288	150.1	-0.2	149.9
50000	129.6	13.1	6.4	2860	151.4	-0.3	151.2
63000	126.8	17.1	10.4	3604	152.6	-0.3	152.3
80000	126.8	20.0	13.4	4576	155.5	-0.4	155.1
100000	127.6	20.1	13.4	5720	156.4	-0.6	155.8

OASPL= 167.5 dB

TABLE 15. COMPUTER OUTPUT: SCAT 15-F MODEL TEST - LOCATION 32P-10

	MODEL		AIRCRAFT	
tt	540.0		2245.0	deg R
ts	364.8		1695.8	deg R
pr	3.94558		3.12100	
w	3.38		411.00	lb/sec
mix	0.00000		0.02000	#f/#a
cv	.980		.980	
dia	2.00	in	5.56	ft
area	3.14	sq in	6.48	sq ft
rho	0.1089		0.0234	lb/sq ft
gama	1.4010		1.3267	
vel	1450.5		2765.6	ft/sec
conv	899.31		1714.69	ft/sec
dist	24.08	in	66.89	ft
Fn	149.1		34594.3	lbs
trdia	0.218		0.250	in

Density Correction = -6.68 dB

fm (Hz)	splm (dB)	scm (dB)	tc (dB)	fa (Hz)	aspla (dB)	sca (dB)	mspla (dB)
1250	144.4	0.2	-6.5	72	153.3	-0.0	153.3
1600	145.2	0.2	-6.4	92	154.2	-0.0	154.1
2000	144.7	0.3	-6.4	114	153.7	-0.0	153.7
2500	141.4	0.4	-6.3	143	150.5	-0.0	150.5
3150	141.5	0.5	-6.2	180	150.7	-0.0	150.7
4000	139.2	0.7	-6.0	229	148.6	-0.0	148.5
5000	140.4	0.8	-5.8	286	149.9	-0.0	149.9
6300	140.4	1.1	-5.6	360	150.2	-0.0	150.2
8000	139.0	1.2	-5.5	458	148.9	-0.0	148.8
10000	137.7	1.3	-5.4	572	147.7	-0.1	147.7
12500	137.2	1.5	-5.2	715	147.4	-0.1	147.3
16000	136.9	2.6	-4.1	915	148.2	-0.1	148.1
20000	136.8	4.0	-2.7	1144	149.5	-0.1	149.4
25000	137.2	4.2	-2.5	1430	150.1	-0.1	150.0
31500	143.0	6.0	-0.6	1802	157.7	-0.2	157.6
40000	144.8	10.5	3.8	2288	164.0	-0.2	163.8
50000	134.6	13.1	6.4	2860	156.4	-0.3	156.2
63000	127.0	17.1	10.4	3604	152.8	-0.3	152.5
80000	126.6	20.0	13.4	4576	155.3	-0.4	154.9
100000	123.4	20.1	13.4	5720	152.2	-0.6	151.6

OASPL= 167.5 dB

TABLE 16. COMPUTER OUTPUT: SCAT 15-F MODEL TEST - LOCATION 32P-12

	MODEL		AIRCRAFT	
tt	540.0		2245.0	deg R
ts	364.8		1695.8	deg R
pr	3.94558		3.12100	
w	3.38		411.00	lb/sec
mix	0.00000		0.02000	#f/#a
cv	.980		.980	
dia	2.00	in	5.56	ft
area	3.14	sq in	6.48	sq ft
rho	0.1089		0.0234	lb/sq ft
gama	1.4010		1.3267	
vel	1450.5		2765.6	ft/sec
conv	899.31		1714.69	ft/sec
dist	24.33	in	67.58	ft
Fn	149.1		34594.3	lbs
trdia	0.218		0.250	in

Density Correction = -6.68 dB

fm (Hz)	splm (dB)	scm (dB)	tc (dB)	fa (Hz)	aspla (dB)	sca (dB)	mspla (dB)
1250	153.9	0.2	-6.5	72	162.8	-0.0	162.8
1600	155.1	0.2	-6.4	92	164.1	-0.0	164.0
2000	154.7	0.3	-6.4	114	163.7	-0.0	163.7
2500	151.7	0.4	-6.3	143	160.8	-0.0	160.8
3150	151.0	0.5	-6.2	180	160.2	-0.0	160.2
4000	148.8	0.7	-6.0	229	158.2	-0.0	158.1
5000	150.2	0.8	-5.8	286	159.7	-0.0	159.7
6300	150.1	1.1	-5.6	360	159.9	-0.0	159.9
8000	148.9	1.2	-5.5	458	158.8	-0.0	158.7
10000	147.6	1.3	-5.4	572	157.6	-0.1	157.6
12500	147.1	1.5	-5.2	715	157.3	-0.1	157.2
16000	146.8	2.6	-4.1	915	158.1	-0.1	158.0
20000	146.6	4.0	-2.7	1144	159.3	-0.1	159.2
25000	147.0	4.2	-2.5	1430	159.9	-0.1	159.8
31500	152.7	6.0	-0.6	1802	167.4	-0.2	167.3
40000	154.5	10.5	3.8	2288	173.7	-0.2	173.5
50000	144.3	13.1	6.4	2860	166.1	-0.3	165.9
63000	137.6	17.1	10.4	3604	163.4	-0.3	163.1
80000	136.1	20.0	13.4	4576	164.8	-0.4	164.4
100000	137.9	20.1	13.4	5720	166.7	-0.6	166.1

OASPL= 177.5 dB

TABLE 17. COMPUTER OUTPUT: SCAT 15-F MODEL TEST - LOCATION 33P-10

	MODEL		AIRCRAFT	
tt	540.0		2245.0	deg R
ts	364.8		1695.8	deg R
pr	3.94558		3.12100	
w	3.38		411.00	lb/sec
mix	0.00000		0.02000	#f/#a
cv	.980		.980	
dia	2.00	in	5.56	ft
area	3.14	sq in	6.48	sq ft
rho	0.1089		0.0234	lb/sq ft
gama	1.4010		1.3267	
vel	1450.5		2765.6	ft/sec
conv	899.31		1714.69	ft/sec
dist	24.73	in	68.69	ft
Fn	149.1		34594.3	lbs
trdia	0.218		0.250	in

Density Correction = -6.68 dB

fm (Hz)	splm (dB)	scm (dB)	tc (dB)	fa (Hz)	aspla (dB)	sca (dB)	mspla (dB)
1250	136.1	0.2	-6.5	72	145.0	-0.0	145.0
1600	143.4	0.2	-6.4	92	152.4	-0.0	152.3
2000	136.7	0.3	-6.4	114	145.7	-0.0	145.7
2500	131.3	0.4	-6.3	143	140.4	-0.0	140.4
3150	129.8	0.5	-6.2	180	139.0	-0.0	139.0
4000	127.0	0.7	-6.0	229	136.4	-0.0	136.3
5000	130.8	0.8	-5.8	286	140.3	-0.0	140.3
6300	130.8	1.1	-5.6	360	140.6	-0.0	140.6
8000	129.2	1.2	-5.5	458	139.1	-0.0	139.0
10000	128.8	1.3	-5.4	572	138.8	-0.1	138.8
12500	129.2	1.5	-5.2	715	139.4	-0.1	139.3
16000	129.5	2.6	-4.1	915	140.8	-0.1	140.7
20000	129.1	4.0	-2.7	1144	141.8	-0.1	141.7
25000	129.4	4.2	-2.5	1430	142.3	-0.1	142.2
31500	136.7	6.0	-0.6	1802	151.4	-0.2	151.3
40000	138.1	10.5	3.8	2288	157.3	-0.2	157.1
50000	127.3	13.1	6.4	2860	149.1	-0.3	148.9
63000	118.8	17.1	10.4	3604	144.6	-0.3	144.3
80000	116.7	20.0	13.4	4576	145.4	-0.4	145.0
100000	113.5	20.1	13.4	5720	142.3	-0.6	141.7

OASPL= 160.6 dB

TABLE 18. COMPUTER OUTPUT: SCAT 15-F MODEL TEST - LOCATION 33P-12

	MODEL		AIRCRAFT	
tt	540.0		2245.0	deg R
ts	364.8		1695.8	deg R
pr	3.94558		3.12100	
w	3.38		411.00	lb/sec
mix	0.00000		0.02000	#f/#a
cv	.980		.980	
dia	2.00	in	5.56	ft
area	3.14	sq in	6.48	sq ft
rho	0.1089		0.0234	lb/sq ft
gama	1.4010		1.3267	
vel	1450.5		2765.6	ft/sec
conv	899.31		1714.69	ft/sec
dist	24.00	in	66.67	ft
Fn	149.1		34594.3	lbs
trdia	0.218		0.250	in

Density Correction = -6.68 dB

fm (Hz)	splm (dB)	scm (dB)	tc (dB)	fa (Hz)	aspla (dB)	sca (dB)	mspla (dB)
1250	157.2	0.2	-6.5	72	166.1	-0.0	166.1
1600	159.2	0.2	-6.4	92	168.2	-0.0	168.1
2000	161.9	0.3	-6.4	114	170.9	-0.0	170.9
2500	158.4	0.4	-6.3	143	167.5	-0.0	167.5
3150	158.0	0.5	-6.2	180	167.2	-0.0	167.2
4000	155.8	0.7	-6.0	229	165.2	-0.0	165.1
5000	154.8	0.8	-5.8	286	164.3	-0.0	164.3
6300	154.2	1.1	-5.6	360	164.0	-0.0	164.0
8000	152.9	1.2	-5.5	458	162.8	-0.0	162.7
10000	152.0	1.3	-5.4	572	162.0	-0.1	162.0
12500	151.2	1.5	-5.2	715	161.4	-0.1	161.3
16000	149.7	2.6	-4.1	915	161.0	-0.1	160.9
20000	147.9	4.0	-2.7	1144	160.6	-0.1	160.5
25000	145.9	4.2	-2.5	1430	158.8	-0.1	158.7
31500	144.1	6.0	-0.6	1802	158.8	-0.2	158.7
40000	143.1	10.5	3.8	2288	162.3	-0.2	162.1
50000	142.7	13.1	6.4	2860	164.5	-0.3	164.3
63000	143.3	17.1	10.4	3604	169.1	-0.3	168.8
80000	145.1	20.0	13.4	4576	173.8	-0.4	173.4
100000	146.9	20.1	13.4	5720	175.7	-0.6	175.1

OASPL= 180.7 dB

TABLE 19. COMPUTER OUTPUT: SCAT 15-F MODEL TEST - LOCATION 20P-10

	MODEL		AIRCRAFT	
tt	540.0		2245.0	deg R
ts	364.8		1695.8	deg R
pr	3.94558		3.12100	
w	3.38		411.00	lb/sec
mix	0.00000		0.02000	#f/#a
cv	.980		.980	
dia	2.00	in	5.56	ft
area	3.14	sq in	6.48	sq ft
rho	0.1089		0.0234	lb/sq ft
gama	1.4010		1.3267	
vel	1450.5		2765.6	ft/sec
conv	899.31		1714.69	ft/sec
dist	14.14	in	39.28	ft
Fn	149.1		34594.3	lbs
trdia	0.218		0.250	in

Density Correction = -6.68 dB

fm (Hz)	splm (dB)	scm (dB)	tc (dB)	fa (Hz)	aspla (dB)	sca (dB)	mspla (dB)
1250	136.2	0.2	-6.5	72	145.1	-0.0	145.1
1600	138.2	0.2	-6.4	92	147.2	-0.0	147.1
2000	139.5	0.3	-6.4	114	148.5	-0.0	148.5
2500	136.4	0.4	-6.3	143	145.5	-0.0	145.5
3150	137.6	0.5	-6.2	180	146.8	-0.0	146.8
4000	136.0	0.7	-6.0	229	145.4	-0.0	145.3
5000	137.6	0.8	-5.8	286	147.1	-0.0	147.1
6300	135.8	1.1	-5.6	360	145.6	-0.0	145.6
8000	133.8	1.2	-5.5	458	143.7	-0.0	143.6
10000	133.5	1.3	-5.4	572	143.5	-0.1	143.5
12500	133.5	1.5	-5.2	715	143.7	-0.1	143.6
16000	133.5	2.6	-4.1	915	144.8	-0.1	144.7
20000	133.6	4.0	-2.7	1144	146.3	-0.1	146.2
25000	134.3	4.2	-2.5	1430	147.2	-0.1	147.1
31500	142.5	6.0	-0.6	1802	157.2	-0.2	157.1
40000	143.7	10.5	3.8	2288	162.9	-0.2	162.7
50000	133.0	13.1	6.4	2860	154.8	-0.3	154.6
63000	123.3	17.1	10.4	3604	149.1	-0.3	148.8
80000	109.7	20.0	13.4	4576	138.4	-0.4	138.0
100000	110.2	20.1	13.4	5720	139.0	-0.6	138.4

OASPL= 165.2 dB

TABLE 20. COMPUTER OUTPUT: SCAT 15-F MODEL TEST - LOCATION 20P-12

	MODEL		AIRCRAFT	
tt	540.0		2245.0	deg R
ts	364.8		1695.8	deg R
pr	3.94558		3.12100	
w	3.38		411.00	lb/sec
mix	0.00000		0.02000	#f/#a
cv	.980		.980	
dia	2.00	in	5.56	ft
area	3.14	sq in	6.48	sq ft
rho	0.1089		0.0234	lb/sq ft
gama	1.4010		1.3267	
vel	1450.5		2765.6	ft/sec
conv	899.31		1714.69	ft/sec
dist	14.56	in	40.44	ft
Fn	149.1		34594.3	lbs
trdia	0.218		0.250	in

Density Correction = -6.68 dB

fm (Hz)	splm (dB)	scm (dB)	tc (dB)	fa (Hz)	aspla (dB)	sca (dB)	mspla (dB)
1250	136.5	0.2	-6.5	72	145.4	-0.0	145.4
1600	137.8	0.2	-6.4	92	146.8	-0.0	146.7
2000	139.0	0.3	-6.4	114	148.0	-0.0	148.0
2500	139.3	0.4	-6.3	143	148.4	-0.0	148.4
3150	140.2	0.5	-6.2	180	149.4	-0.0	149.4
4000	139.3	0.7	-6.0	229	148.7	-0.0	148.6
5000	137.9	0.8	-5.8	286	147.4	-0.0	147.4
6300	138.9	1.1	-5.6	360	148.7	-0.0	148.7
8000	139.7	1.2	-5.5	458	149.6	-0.0	149.5
10000	139.6	1.3	-5.4	572	149.6	-0.1	149.6
12500	139.5	1.5	-5.2	715	149.7	-0.1	149.6
16000	138.8	2.6	-4.1	915	150.1	-0.1	150.0
20000	137.7	4.0	-2.7	1144	150.4	-0.1	150.3
25000	136.2	4.2	-2.5	1430	149.1	-0.1	149.0
31500	135.4	6.0	-0.6	1802	150.1	-0.2	150.0
40000	133.5	10.5	3.8	2288	152.7	-0.2	152.5
50000	129.5	13.1	6.4	2860	151.3	-0.3	151.1
63000	126.4	17.1	10.4	3604	152.2	-0.3	151.9
80000	123.0	20.0	13.4	4576	151.7	-0.4	151.3
100000	120.6	20.1	13.4	5720	149.4	-0.6	148.8

OASPL= 162.6 dB

TABLE 21. COMPUTER OUTPUT: SCAT 15-F MODEL TEST - LOCATION 92P-10

	MODEL		AIRCRAFT	
tt	540.0		2245.0	deg R
ts	364.8		1695.8	deg R
pr	3.94558		3.12100	
w	3.38		411.00	lb/sec
mix	0.00000		0.02000	#f/#a
cv	.980		.980	
dia	2.00	in	5.56	ft
area	3.14	sq in	6.48	sq ft
rho	0.1089		0.0234	lb/sq ft
gama	1.4010		1.3267	
vel	1450.5		2765.6	ft/sec
conv	899.31		1714.69	ft/sec
dist	15.23	in	42.31	ft
Fn	149.1		34594.3	lbs
trdia	0.218		0.250	in

Density Correction = -6.68 dB

fm (Hz)	splm (dB)	scm (dB)	tc (dB)	fa (Hz)	aspla (dB)	sca (dB)	mspla (dB)
1250	139.6	0.2	-6.5	72	148.5	-0.0	148.5
1600	145.3	0.2	-6.4	92	154.3	-0.0	154.2
2000	141.9	0.3	-6.4	114	150.9	-0.0	150.9
2500	138.4	0.4	-6.3	143	147.5	-0.0	147.5
3150	138.7	0.5	-6.2	180	147.9	-0.0	147.9
4000	137.9	0.7	-6.0	229	147.3	-0.0	147.2
5000	139.6	0.8	-5.8	286	149.1	-0.0	149.1
6300	135.2	1.1	-5.6	360	145.0	-0.0	145.0
8000	136.5	1.2	-5.5	458	146.4	-0.0	146.3
10000	136.8	1.3	-5.4	572	146.8	-0.1	146.8
12500	137.2	1.5	-5.2	715	147.4	-0.1	147.3
16000	138.7	2.6	-4.1	915	150.0	-0.1	149.9
20000	138.9	4.0	-2.7	1144	151.6	-0.1	151.5
25000	139.9	4.2	-2.5	1430	152.8	-0.1	152.7
31500	147.5	6.0	-0.6	1802	162.2	-0.2	162.1
40000	148.1	10.5	3.8	2288	167.3	-0.2	167.1
50000	136.9	13.1	6.4	2860	158.7	-0.3	158.5
63000	126.8	17.1	10.4	3604	152.6	-0.3	152.3
80000	116.1	20.0	13.4	4576	144.8	-0.4	144.4
100000	117.1	20.1	13.4	5720	145.9	-0.6	145.3

OASPL= 169.5 dB

TABLE 22. COMPUTER OUTPUT: SCAT 15-F MODEL TEST - LOCATION 92P-12

	MODEL		AIRCRAFT	
tt	540.0		2245.0	deg R
ts	364.8		1695.8	deg R
pr	3.94558		3.12100	
w	3.38		411.00	lb/sec
mix	0.00000		0.02000	#f/#a
cv	.980		.980	
dia	2.00	in	5.56	ft
area	3.14	sq in	6.48	sq ft
rho	0.1089		0.0234	lb/sq ft
gama	1.4010		1.3267	
vel	1450.5		2765.6	ft/sec
conv	899.31		1714.69	ft/sec
dist	14.00	in	38.89	ft
Fn	149.1		34594.3	lbs
trdia	0.218		0.250	in

Density Correction = -6.68 dB

fm (Hz)	splm (dB)	scm (dB)	tc (dB)	fa (Hz)	aspla (dB)	sca (dB)	mspla (dB)
1250	150.1	0.2	-6.5	72	159.0	-0.0	159.0
1600	151.0	0.2	-6.4	92	160.0	-0.0	159.9
2000	151.7	0.3	-6.4	114	160.7	-0.0	160.7
2500	152.8	0.4	-6.3	143	161.9	-0.0	161.9
3150	154.1	0.5	-6.2	180	163.3	-0.0	163.3
4000	155.5	0.7	-6.0	229	164.9	-0.0	164.8
5000	155.0	0.8	-5.8	286	164.5	-0.0	164.5
6300	154.0	1.1	-5.6	360	163.8	-0.0	163.8
8000	152.4	1.2	-5.5	458	162.3	-0.0	162.2
10000	152.0	1.3	-5.4	572	162.0	-0.1	162.0
12500	151.3	1.5	-5.2	715	161.5	-0.1	161.4
16000	150.6	2.6	-4.1	915	161.9	-0.1	161.8
20000	148.6	4.0	-2.7	1144	161.3	-0.1	161.2
25000	146.2	4.2	-2.5	1430	159.1	-0.1	159.0
31500	143.5	6.0	-0.6	1802	158.2	-0.2	158.1
40000	141.1	10.5	3.8	2288	160.3	-0.2	160.1
50000	139.1	13.1	6.4	2860	160.9	-0.3	160.7
63000	137.9	17.1	10.4	3604	163.7	-0.3	163.4
80000	136.8	20.0	13.4	4576	165.5	-0.4	165.1
100000	135.1	20.1	13.4	5720	163.9	-0.6	163.3

OASPL= 175.3 dB

TABLE 23. COMPUTER OUTPUT: SCAT 15-F MODEL TEST - LOCATION 36P-10

	MODEL		AIRCRAFT	
tt	540.0		2245.0	deg R
ts	364.8		1695.8	deg R
pr	3.94558		3.12100	
w	3.38		411.00	lb/sec
mix	0.00000		0.02000	#f/#a
cv	.980		.980	
dia	2.00	in	5.56	ft
area	3.14	sq in	6.48	sq ft
rho	0.1089		0.0234	lb/sq ft
gama	1.4010		1.3267	
vel	1450.5		2765.6	ft/sec
conv	899.31		1714.69	ft/sec
dist	4.47	in	12.42	ft
Fn	149.1		34594.3	lbs
trdia	0.218		0.250	in

Density Correction = -6.68 dB

fm (Hz)	splm (dB)	scm (dB)	tc (dB)	fa (Hz)	aspla (dB)	sca (dB)	mspla (dB)
1250	127.2	0.2	-6.5	72	136.1	-0.0	136.1
1600	129.7	0.2	-6.4	92	138.7	-0.0	138.6
2000	128.9	0.3	-6.4	114	137.9	-0.0	137.9
2500	137.8	0.4	-6.3	143	146.9	-0.0	146.9
3150	139.6	0.5	-6.2	180	148.8	-0.0	148.8
4000	133.7	0.7	-6.0	229	143.1	-0.0	143.0
5000	133.9	0.8	-5.8	286	143.4	-0.0	143.4
6300	131.4	1.1	-5.6	360	141.2	-0.0	141.2
8000	130.0	1.2	-5.5	458	139.9	-0.0	139.8
10000	127.2	1.3	-5.4	572	137.2	-0.1	137.2
12500	126.3	1.5	-5.2	715	136.5	-0.1	136.4
16000	126.5	2.6	-4.1	915	137.8	-0.1	137.7
20000	126.9	4.0	-2.7	1144	139.6	-0.1	139.5
25000	128.0	4.2	-2.5	1430	140.9	-0.1	140.8
31500	136.9	6.0	-0.6	1802	151.6	-0.2	151.5
40000	139.1	10.5	3.8	2288	158.3	-0.2	158.1
50000	129.3	13.1	6.4	2860	151.1	-0.3	150.9
63000	120.4	17.1	10.4	3604	146.2	-0.3	145.9
80000	111.4	20.0	13.4	4576	140.1	-0.4	139.7
100000	111.4	20.1	13.4	5720	140.2	-0.6	139.6

OASPL= 160.8 dB

TABLE 24. COMPUTER OUTPUT: SCAT 15-F MODEL TEST - LOCATION 36P-12

	MODEL		AIRCRAFT	
tt	540.0		2245.0	deg R
ts	364.8		1695.8	deg R
pr	3.94558		3.12100	
w	3.38		411.00	lb/sec
mix	0.00000		0.02000	#f/#a
cv	.980		.980	
dia	2.00	in	5.56	ft
area	3.14	sq in	6.48	sq ft
rho	0.1089		0.0234	lb/sq ft
gama	1.4010		1.3267	
vel	1450.5		2765.6	ft/sec
conv	899.31		1714.69	ft/sec
dist	5.66	in	15.72	ft
Fn	149.1		34594.3	lbs
trdia	0.218		0.250	in

Density Correction = -6.68 dB

fm (Hz)	splm (dB)	scm (dB)	tc (dB)	fa (Hz)	aspla (dB)	sca (dB)	mspla (dB)
1250	127.2	0.2	-6.5	72	136.1	-0.0	136.1
1600	129.9	0.2	-6.4	92	138.9	-0.0	138.8
2000	129.6	0.3	-6.4	114	138.6	-0.0	138.6
2500	132.0	0.4	-6.3	143	141.1	-0.0	141.1
3150	133.9	0.5	-6.2	180	143.1	-0.0	143.1
4000	132.0	0.7	-6.0	229	141.4	-0.0	141.3
5000	129.8	0.8	-5.8	286	139.3	-0.0	139.3
6300	130.6	1.1	-5.6	360	140.4	-0.0	140.4
8000	127.3	1.2	-5.5	458	137.2	-0.0	137.1
10000	126.1	1.3	-5.4	572	136.1	-0.1	136.1
12500	125.9	1.5	-5.2	715	136.1	-0.1	136.0
16000	125.8	2.6	-4.1	915	137.1	-0.1	137.0
20000	125.2	4.0	-2.7	1144	137.9	-0.1	137.8
25000	124.3	4.2	-2.5	1430	137.2	-0.1	137.1
31500	124.4	6.0	-0.6	1802	139.1	-0.2	139.0
40000	123.5	10.5	3.8	2288	142.7	-0.2	142.5
50000	121.2	13.1	6.4	2860	143.0	-0.3	142.8
63000	119.2	17.1	10.4	3604	145.0	-0.3	144.7
80000	118.0	20.0	13.4	4576	146.7	-0.4	146.3
100000	116.8	20.1	13.4	5720	145.6	-0.6	145.0

OASPL= 154.2 dB

TABLE 25. COMPUTER OUTPUT: SCAT 15-F MODEL TEST - LOCATION 37P-10

	MODEL		AIRCRAFT	
tt	540.0		2245.0	deg R
ts	364.8		1695.8	deg R
pr	3.94558		3.12100	
w	3.38		411.00	lb/sec
mix	0.00000		0.02000	#f/#a
cv	.980		(.980	
dia	2.00	in	5.56	ft
area	3.14	sq in	6.48	sq ft
rho	0.1089		0.0234	lb/sq ft
gama	1.4010		1.3267	
vel	1450.5		2765.6	ft/sec
conv	899.31		1714.69	ft/sec
dist	7.21	in	20.03	ft
Fn	149.1		34594.3	lbs
trdia	0.218		0.250	in

Density Correction = -6.68 dB

fm (Hz)	splm (dB)	scm (dB)	tc (dB)	fa (Hz)	aspla (dB)	sca (dB)	mspla (dB)
1250	150.1	0.2	-6.5	72	159.0	-0.0	159.0
1600	155.7	0.2	-6.4	92	164.7	-0.0	164.6
2000	150.0	0.3	-6.4	114	159.0	-0.0	159.0
2500	153.7	0.4	-6.3	143	162.8	-0.0	162.8
3150	157.2	0.5	-6.2	180	166.4	-0.0	166.4
4000	152.7	0.7	-6.0	229	162.1	-0.0	162.0
5000	151.4	0.8	-5.8	286	160.9	-0.0	160.9
6300	151.4	1.1	-5.6	360	161.2	-0.0	161.2
8000	149.6	1.2	-5.5	458	159.5	-0.0	159.4
10000	147.3	1.3	-5.4	572	157.3	-0.1	157.3
12500	146.7	1.5	-5.2	715	156.9	-0.1	156.8
16000	147.0	2.6	-4.1	915	158.3	-0.1	158.2
20000	146.9	4.0	-2.7	1144	159.6	-0.1	159.5
25000	147.7	4.2	-2.5	1430	160.6	-0.1	160.5
31500	155.6	6.0	-0.6	1802	170.3	-0.2	170.2
40000	157.3	10.5	3.8	2288	176.5	-0.2	176.3
50000	147.1	13.1	6.4	2860	168.9	-0.3	168.7
63000	138.0	17.1	10.4	3604	163.8	-0.3	163.5
80000	131.1	20.0	13.4	4576	159.8	-0.4	159.4
100000	131.1	20.1	13.4	5720	159.9	-0.6	159.3

OASPL= 179.2 dB

TABLE 26. COMPUTER OUTPUT: SCAT 15-F MODEL TEST - LOCATION 37P-12

	MODEL		AIRCRAFT	
tt	540.0		2245.0	deg R
ts	364.8		1695.8	deg R
pr	3.94558		3.12100	
w	3.38		411.00	lb/sec
mix	0.00000		0.02000	#f/#a
cv	.980		.980	
dia	2.00	in	5.56	ft
area	3.14	sq in	6.48	sq ft
rho	0.1089		0.0234	lb/sq ft
gama	1.4010		1.3267	
vel	1450.5		2765.6	ft/sec
conv	899.31		1714.69	ft/sec
dist	4.00	in	11.11	ft
Fn	149.1		34594.3	lbs
trdia	0.218		0.250	in

Density Correction = -6.68 dB

fm (Hz)	splm (dB)	scm (dB)	tc (dB)	fa (Hz)	aspla (dB)	sca (dB)	mspla (dB)
1250	130.7	0.2	-6.5	72	139.6	-0.0	139.6
1600	132.7	0.2	-6.4	92	141.7	-0.0	141.6
2000	130.7	0.3	-6.4	114	139.7	-0.0	139.7
2500	132.6	0.4	-6.3	143	141.7	-0.0	141.7
3150	132.6	0.5	-6.2	180	141.8	-0.0	141.8
4000	131.6	0.7	-6.0	229	141.0	-0.0	140.9
5000	132.2	0.8	-5.8	286	141.7	-0.0	141.7
6300	126.8	1.1	-5.6	360	136.6	-0.0	136.6
8000	125.2	1.2	-5.5	458	135.1	-0.0	135.0
10000	125.7	1.3	-5.4	572	135.7	-0.1	135.7
12500	125.1	1.5	-5.2	715	135.3	-0.1	135.2
16000	125.8	2.6	-4.1	915	137.1	-0.1	137.0
20000	125.6	4.0	-2.7	1144	138.3	-0.1	138.2
25000	125.1	4.2	-2.5	1430	138.0	-0.1	137.9
31500	126.5	6.0	-0.6	1802	141.2	-0.2	141.1
40000	127.4	10.5	3.8	2288	146.6	-0.2	146.4
50000	128.0	13.1	6.4	2860	149.8	-0.3	149.6
63000	127.8	17.1	10.4	3604	153.6	-0.3	153.3
80000	127.4	20.0	13.4	4576	156.1	-0.4	155.7
100000	125.5	20.1	13.4	5720	154.3	-0.6	153.7

OASPL= 160.4 dB

TABLE 27. COMPUTER OUTPUT: SCAT 15-F MODEL TEST - LOCATION 46P-10

	MODEL		AIRCRAFT	
tt	560.0		2245.0	deg R
ts	250.6		1695.8	deg R
pr	17.00680		3.12100	
w	6.56		411.00	lb/sec
mix	0.00000		0.02000	#f/#a
cv	.980		.980	
dia	2.00	in	5.56	ft
area	3.14	sq in	6.48	sq ft
rho	0.1587		0.0234	lb/sq ft
gama	1.3971		1.3267	
vel	1934.0		2765.6	ft/sec
conv	1199.10		1714.69	ft/sec
dist	4.47	in	12.42	ft
Fn	386.0		34594.3	lbs
trdia	0.218		0.250	in

Density Correction = -8.31 dB

fm (Hz)	splm (dB)	scm (dB)	tc (dB)	fa (Hz)	aspla (dB)	sca (dB)	mspla (dB)
1250	125.3	0.1	-8.2	54	122.5	-0.0	122.5
1600	132.6	0.2	-8.1	69	129.9	-0.0	129.9
2000	128.7	0.2	-8.1	86	126.0	-0.0	126.0
2500	126.5	0.3	-8.0	107	123.9	-0.0	123.9
3150	124.3	0.4	-7.9	135	121.8	-0.0	121.7
4000	123.4	0.5	-7.8	172	121.0	-0.0	120.9
5000	122.9	0.6	-7.7	214	120.6	-0.0	120.6
6300	122.4	0.8	-7.5	270	120.3	-0.0	120.2
8000	119.1	1.0	-7.3	343	117.2	-0.0	117.2
10000	119.3	1.2	-7.2	429	117.5	-0.0	117.5
12500	119.1	1.3	-7.0	536	117.4	-0.0	117.4
16000	121.0	1.4	-6.9	686	119.5	-0.1	119.5
20000	124.7	2.5	-5.8	858	124.3	-0.1	124.2
25000	127.6	2.7	-5.6	1072	127.4	-0.1	127.3
31500	135.3	4.1	-4.2	1351	136.5	-0.1	136.4
40000	138.6	6.0	-2.3	1716	141.7	-0.2	141.5
50000	128.8	8.1	-0.2	2145	134.0	-0.2	133.8
63000	120.5	13.1	4.8	2703	130.6	-0.3	130.4
80000	108.7	17.0	8.7	3432	122.8	-0.3	122.5
100000	110.1	20.0	11.7	4290	127.2	-0.4	126.8

OASPL= 144.2 dB

TABLE 28. COMPUTER OUTPUT: SCAT 15-F MODEL TEST - LOCATION 46P-12

	MODEL		AIRCRAFT	
tt	560.0		2245.0	deg R
ts	250.6		1695.8	deg R
pr	17.00680		3.12100	
w	6.56		411.00	lb/sec
mix	0.00000		0.02000	#f/#a
cv	.980		.980	
dia	2.00	in	5.56	ft
area	3.14	sq in	6.48	sq ft
rho	0.1587		0.0234	lb/sq ft
gama	1.3971		1.3267	
vel	1934.0		2765.6	ft/sec
conv	1199.10		1714.69	ft/sec
dist	5.66	in	15.72	ft
Fn	386.0		34594.3	lbs
trdia	0.218		0.250	in

Density Correction = -8.31 dB

fm (Hz)	splm (dB)	scm (dB)	tc (dB)	fa (Hz)	aspla (dB)	sca (dB)	mspla (dB)
1250	139.3	0.1	-8.2	54	136.5	-0.0	136.5
1600	144.5	0.2	-8.1	69	141.8	-0.0	141.8
2000	142.5	0.2	-8.1	86	139.8	-0.0	139.8
2500	134.9	0.3	-8.0	107	132.3	-0.0	132.3
3150	134.7	0.4	-7.9	135	132.2	-0.0	132.1
4000	131.7	0.5	-7.8	172	129.3	-0.0	129.2
5000	133.0	0.6	-7.7	214	130.7	-0.0	130.7
6300	135.6	0.8	-7.5	270	133.5	-0.0	133.4
8000	133.1	1.0	-7.3	343	131.2	-0.0	131.2
10000	131.6	1.2	-7.2	429	129.8	-0.0	129.8
12500	129.7	1.3	-7.0	536	128.0	-0.0	128.0
16000	129.5	1.4	-6.9	686	128.0	-0.1	128.0
20000	130.2	2.5	-5.8	858	129.8	-0.1	129.7
25000	129.8	2.7	-5.6	1072	129.6	-0.1	129.5
31500	129.6	4.1	-4.2	1351	130.8	-0.1	130.7
40000	128.4	6.0	-2.3	1716	131.5	-0.2	131.3
50000	125.9	8.1	-0.2	2145	131.1	-0.2	130.9
63000	124.3	13.1	4.8	2703	134.4	-0.3	134.2
80000	122.5	17.0	8.7	3432	136.6	-0.3	136.3
100000	121.0	20.0	11.7	4290	138.1	-0.4	137.7

OASPL= 147.7 dB

TABLE 29. COMPUTER OUTPUT: SCAT 15-F MODEL TEST - LOCATION 47P-10

	MODEL		AIRCRAFT	
tt	560.0		2245.0	deg R
ts	250.6		1695.8	deg R
pr	17.00680		3.12100	
w	6.56		411.00	lb/sec
mix	0.00000		0.02000	#f/#a
cv	.980		.980	
dia	2.00	in	5.56	ft
area	3.14	sq in	6.48	sq ft
rho	0.1587		0.0234	lb/sq ft
gama	1.3971		1.3267	
vel	1934.0		2765.6	ft/sec
conv	1199.10		1714.69	ft/sec
dist	7.21	in	20.03	ft
Fn	386.0		34594.3	lbs
trdia	0.218		0.250	in

Density Correction = -8.31 dB

fm (Hz)	splm (dB)	scm (dB)	tc (dB)	fa (Hz)	aspla (dB)	sca (dB)	mspla (dB)
1250	125.9	0.1	-8.2	54	123.1	-0.0	123.1
1600	133.0	0.2	-8.1	69	130.3	-0.0	130.3
2000	131.1	0.2	-8.1	86	128.4	-0.0	128.4
2500	128.9	0.3	-8.0	107	126.3	-0.0	126.3
3150	125.6	0.4	-7.9	135	123.1	-0.0	123.0
4000	125.7	0.5	-7.8	172	123.3	-0.0	123.2
5000	122.9	0.6	-7.7	214	120.6	-0.0	120.6
6300	121.5	0.8	-7.5	270	119.4	-0.0	119.3
8000	120.1	1.0	-7.3	343	118.2	-0.0	118.2
10000	119.2	1.2	-7.2	429	117.4	-0.0	117.4
12500	118.9	1.3	-7.0	536	117.2	-0.0	117.2
16000	120.2	1.4	-6.9	686	118.7	-0.1	118.7
20000	122.0	2.5	-5.8	858	121.6	-0.1	121.5
25000	123.2	2.7	-5.6	1072	123.0	-0.1	122.9
31500	131.7	4.1	-4.2	1351	132.9	-0.1	132.8
40000	135.3	6.0	-2.3	1716	138.4	-0.2	138.2
50000	125.3	8.1	-0.2	2145	130.5	-0.2	130.3
63000	116.1	13.1	4.8	2703	126.2	-0.3	126.0
80000	105.8	17.0	8.7	3432	119.9	-0.3	119.6
100000	105.4	20.0	11.7	4290	122.5	-0.4	122.1

OASPL= 141.4 dB

TABLE 30. COMPUTER OUTPUT: SCAT 15-F MODEL TEST - LOCATION 47P-12

	MODEL		AIRCRAFT	
tt	560.0		2245.0	deg R
ts	250.6		1695.8	deg R
pr	17.00680		3.12100	
w	6.56		411.00	lb/sec
mix	0.00000		0.02000	#f/#a
cv	.980		.980	
dia	2.00	in	5.56	ft
area	3.14	sq in	6.48	sq ft
rho	0.1587		0.0234	lb/sq ft
gama	1.3971		1.3267	
vel	1934.0		2765.6	ft/sec
conv	1199.10		1714.69	ft/sec
dist	4.00	in	11.11	ft
Fn	386.0		34594.3	lbs
trdia	0.218		0.250	in

Density Correction = -8.31 dB

fm (Hz)	splm (dB)	scm (dB)	tc (dB)	fa (Hz)	aspla (dB)	sca (dB)	mspla (dB)
1250	135.7	0.1	-8.2	54	132.9	-0.0	132.9
1600	141.5	0.2	-8.1	69	138.8	-0.0	138.8
2000	142.8	0.2	-8.1	86	140.1	-0.0	140.1
2500	136.5	0.3	-8.0	107	133.9	-0.0	133.9
3150	136.2	0.4	-7.9	135	133.7	-0.0	133.6
4000	132.3	0.5	-7.8	172	129.9	-0.0	129.8
5000	134.5	0.6	-7.7	214	132.2	-0.0	132.2
6300	136.3	0.8	-7.5	270	134.2	-0.0	134.1
8000	135.2	1.0	-7.3	343	133.3	-0.0	133.3
10000	133.6	1.2	-7.2	429	131.8	-0.0	131.8
12500	135.6	1.3	-7.0	536	133.9	-0.0	133.9
16000	136.9	1.4	-6.9	686	135.4	-0.1	135.4
20000	138.5	2.5	-5.8	858	138.1	-0.1	138.0
25000	139.5	2.7	-5.6	1072	139.3	-0.1	139.2
31500	141.5	4.1	-4.2	1351	142.7	-0.1	142.6
40000	141.9	6.0	-2.3	1716	145.0	-0.2	144.8
50000	142.7	8.1	-0.2	2145	147.9	-0.2	147.7
63000	142.9	13.1	4.8	2703	153.0	-0.3	152.8
80000	140.7	17.0	8.7	3432	154.8	-0.3	154.5
100000	139.2	20.0	11.7	4290	156.3	-0.4	155.9

OASPL= 160.1 dB

REFERENCES

1. Rudder, F.F., and Plumblee, H.E., "Sonic Fatigue Guide for Military Aircraft," AFFDL-TR-74-112, May 1975.

2. Schneider, C.W., "Acoustic Fatigue of Aircraft Structures at Elevated Temperatures," AFFDL-TR-73-155, Parts 4 and 2, December 1973.

3. Jacobson, M.J., Finwall, P.E., "Effects of Structural Heating on the Sonic Fatigue of Aerospace Vehicle Structures," AFFDL-TR-73-56, January 1974.

4. Baird, E.F., Bernstein, H., Arcas, N., "Sonic Fatigue Failure Mechanisms in Potential Space Shuttle Orbiter Designs," AIAA/ASME/SAE 15th Structures, Structural Dynamics and Materials Conference, April 1974.

5. Sakata, E.F. and Davis, G.W., "Arrow-Wing Supersonic Cruise Aircraft Structural Design Concepts Evaluation," NASA CR-132575, October 1975.

6. Love, E.S., "Advanced Technology and Space Shuttle," Aeronautics and Astronautics, February 1973.

7. Powell, A., "The Noise of Choked Jets," Jour. Acous. Soc. Am., Vol. 25, May 1953.

8. Lassiter, L.W., Hubbard, H.H., "The Near Noise Field of Static Jets and Some Model Studies of Devices for Noise Reduction," NACA TN 3187, 1954.

9. Hay, J.A., "Shock-Cell Noise; Aircraft Measurements," A Conference on Current Developments in Sonic Fatigue, Southhampton, England, July 1970.

10. Harper-Bourne, M., Fisher, M.J., "The Noise From Shock Waves in Supersonic Jets," AGARD-CP-131, March 1974.

11. Grosche, F.R., "Distribution of Sound Source Intensities in Subsonic and Supersonic Jets," AGARD-CP-131, March 1974.

12. Hoch, R., Hawkins, R., "Recent Studies Into Concorde Noise Reduction," AGARD-CP-13, March 1974.

13. Ffowcs-Williams, J.E., "Impulsive Source of Aerodynamic Noise," AGARD-CP-131, March 1974.

REFERENCES (Continued)

14. Lansing, D.L., Drishler, J.A., Brown, T.J. and Mixson, J.S., "Dynamic Loading of Aircraft Surfaces Due to Jet Exhaust Impingement," AGARD-CP-113, May 1973.

15. Westly, R., Wooley, J.H., Brosseau, P., "Surface Pressure Fluctuations from Jet Impingement on an Inclined Flat Plate," AGARD-CP-113, May 1973.

16. Speaker, W.V., Ailman, C.M., "Spectra and Space Time Correlations of the Fluctuating Pressures Beneath a Supersonic Turbulent Boundary Layer Perturbed by Steps and Shock Waves," NASA-CR-486, May 1966.

17. Coe, C.F., Chuy, W.J., "Pressure - Fluctuation Inputs and Response of Panels Underlying Attached and Separated Supersonic Turbulent Boundary Layers," AGARD-CP-113, May 1973.

18. LaBarge, W.L., "Experimental Evaluation of the Sonic Fatigue Resistance of Structure of a Modified C-141 Airplane Structure," NASA AMES Contract NAS2-7644, October 1973.

19. Willmarth, W.W., Wooldridge, C.E., "Measurement of the Fluctuating Pressure at the Wall Beneath a Thick Turbulent Boundary Layer," J. Fluid Mech. 14, Pt. 2, 1962.

20. Wilby, J.F., "The Response of Simple Panels to Turbulent Boundary Layer Excitation," AFFDL-TR-67-70, October 1967.

21. Maistrello, L., "Measurement and Analysis of the Response Field of Turbulent Boundary Layer Excited Panels," J. Sound and Vib., 2(3), 1965.

22. Cockburn, J.A., Jolly, A.C., "Structural-Acoustic Response, Noise Transmission Losses and Interior Noise Levels of an Aircraft Fuselage Excited by Random Pressure Fields," AFFDL-TR-68-2, August 1968.

23. Powell, A., "On the Fatigue Failure of Structures Due to Vibrations Excited by Random Pressure Fields," J.A.S.A., Vol. 30, December 1958.

24. Byrnes, K.P., "Fatigue Crack Propagation at the Boundaries of Acoustically Excited Panels," Ph. D. Thesis, Southampton University, England, October 1973.

25. Miles, J.W., "On Structural Fatigue Undue Random Loading," J. Aero. Sc., Vol. 21, 1954.

26. Clarkson, B.L., "Stresses in Skin Panels Subject to Random Acoustic Loading," AFML-TR-67-199, June 1967.

REFERENCES (Continued)

27. Holehouse, I., "Sonic Fatigue of Aircraft Structures Due to Jet Engine Fan Noise," Conference on Current Developments in Sonic Fatigue, Southampton, England, July 1970.

28. Mahaffey, P.T., and Smith, K.W., "A Method for Predicting Environmental Vibration Levels in Jet-Powered Vehicles," Shock and Vibration Bulletin No. 2B, Part IV, August, 1960.

29. Schneider, C.W., "Acoustic, Sonic Fatigue, and Vibration Development," Lockheed Georgia Report ER-9599-I, November 1967.

30. Wilby, J.F., and Gloyna, F.L., "Vibration Measurements of an Airplane Fuselage Structure. II. Jet Noise Excitation," J. Sound Vib. 23(4), 1972.

31. Mead, D.J., and Richards, E.J., Noise and Acoustic Fatigue in Aeronautics, John Wiley and Sons, Ltd.

32. Lewis, T.L. and Dods, Jules B. Jr., "Wind Tunnel Measurements of Surface-Pressure-Fluctuations at Mach Numbers of 1.6, 2.0 and 2.5 Using 12 Different Transducers," Rough Draft of Proposed Technical Note, October 1971.

33. Corcos, G.M., "Resolution of Pressure in Turbulence," Journal Acoust Soc of Am, Vol 35, No. 2 pp 192-199, February 1963.

34. Guinn, W.A., Balena, F.J., Clark, L.R., and Willis, C.M., "Task IV-1; Reduction of Supersonic Jet Noise by Over-the-Wing Engine Installation," NASA CR-132619, April 1975.

35. Sutherland, L.C. and Brown, D., "Prediction Methods for Near Field Noise Environments of VTOL Aircraft," AFFDL-TR-71-80, May 1972.

36. Plumblee, H.E., Wynne, G.A., and Zinn, B.T., "Effects of Jet Temperature on Jet and Pure Tone Noise Radiation," NASA CR-1472, 1969.

37. Mixon, J.S., Schoenster, J.A., and Willis, C.M., "Fluctuating Pressures on Aircraft Wing and Flap Surfaces Associated with Powered-Left Systems," AIAA Paper 75-472, March 1975.

38. Hayward, J., "Near Field Noise Survey of a Model S-3A Aircraft," Lockheed Report LR-24142, December 1970.

39. Prydz, R.A., "Evaluation of Scale Models for Prediction of Full-Scale Jet Engine Noise," Lockheed Report LR-26233, December 1973.

40. Balena, F.J., "L-1011 Near-Field Jet Noise Measurements," Lockheed Report LR-23872, September 1971.

REFERENCES (Continued)

41. Pennock, A.P., Swift, G. and Marbert, J.A., "Static and Wind Tunnel Model Tests for the Development of Externally Blown Flap Noise Reduction Techniques."

42. Robson, J.D., Random Vibration, Robert Cunningham and Sons Ltd., Alva Scotland, 1963.

43. Meirovitch, L., Analytical Methods in Vibrations, Macmillan Co., New York, 1967.